

# **MODELING OF THE ISOBUTYLENE POLYMERIZATION PROCESS IN AGITATED REACTORS**

by

**Yongtai Li**

Bachelor of Automation, Beijing University of Chemical Technology, 2007

Master of Process Control, Beijing University of Chemical Technology, 2010

Submitted to the Graduate Faculty of

Swanson School of Engineering in partial fulfillment

of the requirements for the degree of

Master of Science in Petroleum Engineering

University of Pittsburgh

2016

UNIVERSITY OF PITTSBURGH  
SWANSON SCHOOL OF ENGINEERING

This thesis was presented

by

Yongtai Li

It was defended on

July 26, 2016

and approved by

George E. Klinzing, PhD, Professor, Department of Chemical and Petroleum Engineering

Robert M. Enick, PhD, Professor, Department of Chemical and Petroleum Engineering

Thesis Advisor: Badie Morsi, PhD, Professor, Department of Chemical and Petroleum  
Engineering

Copyright © by Yongtai Li

2016

# **MODELING OF THE ISOBUTYLENE POLYMERIZATION PROCESS IN AGITATED REACTORS**

Yongtai Li, M.S.

University of Pittsburgh, 2016

In this study, a comprehensive model for the IBP process in agitated reactors was developed based on the reaction mechanism by Vasilenko et al. 2010, and takes into account the reaction rate kinetics for initiation, propagation, chain transfer, and chain termination steps as well as the mixing effects. The model coupled the mass balance equations for each reaction step with those of the segregated zones model for micro- and macro-mixing effects by Villermaux 1989, and was numerically solved by Matlab. The model was then used to predict the effect of various operating variables on the IBP process performance, in terms of the three main metrics: monomer conversion ( $X$ ), number average molecular weight ( $M_n$ ) and polydispersity index (PDI).

In the absence of mixing, our model was used to carry out sensitivity analyses to quantify the effects of the reaction rate constants of the initiation ( $k_i$ ), propagation ( $k_p$ ), chain-transfer ( $k_{tr}$ ) and chain termination ( $k_t$ ) steps on the three main performance metrics. The model predictions led to: (1) Increasing  $k_i$  was found to have negligible effect on the three main IBP process performance metrics; (2) Increasing  $k_p$  increased  $X$  and  $M_n$  and decreased PDI; (3) increasing  $k_{tr}$  the increased  $X$ , but decreased  $M_n$  and PDI; and (4) Increasing  $k_t$  decreased  $X$  and  $M_n$ , and increased PDI.

In the presence of mixing, and at given kinetic rate constant, the model was used to conduct a parametric study to determine the effect of mixing on the IBP process performance. Eight different cases, four poor and four good mixing conditions, reactor type, and impeller type as well as design, were considered, and their effects on the three main IBP process performance metrics were investigated. The model predictions led to: (1) Mixing controls the IBP process performance due to its inherently fast reaction kinetics; (2) Mixing time and impeller type significantly affected the required mixing speed; (3) all model predictions underscored the importance of good mixing in the cationic IBP process; and (4) our model was able to predict the IBP process performance metrics and the required mixing speed in agitated reactors provided with different impellers.

## TABLE OF CONTENTS

ACKNOWLEDGEMENT .....	XII
NOMENCLATURE.....	XIII
1.0 INTRODUCTION AND BACKGROUND.....	1
1.1 INTRODUCTION.....	1
1.2 CATIONIC POLYMERIZATION .....	4
1.2.1 Initiation step.....	6
1.2.2 Propagation step.....	8
1.2.3 Chain transfer step .....	9
1.2.4 Chain termination step .....	10
1.3 LITERATURE STUDIES ON ISOBUTYLENE POLYMERIZATION REACTION KINETICS.....	10
1.4 LITERATURE STUDIES ON ISOBUTYLENE POLYMERIZATION REACTION MECHANISMS .....	22
1.5 COMMERCIAL ISOBUTYLENE POLYMERIZATION PROCESSES.....	29
1.5.1 Monomer purification .....	32
1.5.2 Polymerization.....	33
1.6 EFFECT OF MIXING.....	34
1.7 NUMBER AVERAGE MOLECULAR WEIGHT ( $M_N$ ), WEIGHT AVERAGE MOLECULAR WEIGHT ( $M_w$ ), AND POLYDISPERSITY INDEX (PDI).....	39
1.8 MODELING ISOBUTYLENE POLYMERIZATION USING ASPENPLUS ....	40

<b>2.0</b>	<b>RESEARCH OBJECTIVE .....</b>	<b>42</b>
<b>3.0</b>	<b>RESEARCH APPROACH.....</b>	<b>44</b>
<b>3.1</b>	<b>KINETIC MODEL AND NOTATIONS.....</b>	<b>44</b>
<b>3.2</b>	<b>ASSUMPTIONS.....</b>	<b>45</b>
<b>3.3</b>	<b>MASS BALANCE .....</b>	<b>46</b>
<b>3.4</b>	<b>MIXING INCORPORATION INTO THE MODEL .....</b>	<b>47</b>
<b>3.5</b>	<b>NORMALIZATION OF THE MODEL EQUATIONS .....</b>	<b>54</b>
<b>4.0</b>	<b>RESULTS AND DISCUSSIONS .....</b>	<b>57</b>
<b>4.1</b>	<b>EFFECTS OF REACTION RATE CONSTANTS ON THE MODEL PREDICTIONS IN THE ABSENCE OF MIXING .....</b>	<b>57</b>
<b>4.1.1</b>	<b>Effect of the initiation rate constant (<math>k_i</math>) .....</b>	<b>59</b>
<b>4.1.2</b>	<b>Effect of the propagation rate constant (<math>k_p</math>) .....</b>	<b>61</b>
<b>4.1.3</b>	<b>Effect of the chain transfer rate constant (<math>k_{tr}</math>) .....</b>	<b>63</b>
<b>4.1.4</b>	<b>Effect of the termination rate constant (<math>k_t</math>) .....</b>	<b>66</b>
<b>4.2</b>	<b>EFFECT OF MIXING.....</b>	<b>68</b>
<b>4.3</b>	<b>MODEL PREDICTION OF THE OVERALL REACTOR PERFORMANCE..</b>	<b>73</b>
<b>5.0</b>	<b>CONCLUSIONS .....</b>	<b>83</b>
	<b>APPENDIX A .....</b>	<b>85</b>
	<b>MODELING ISOBUTYLENE POLYMERIZATION IN ASPEN PLUS .....</b>	<b>85</b>
	<b>APPENDIX B .....</b>	<b>93</b>
	<b>EFFECT OF REACTOR TYPE AND IMPELLER TYPE/SIZE ON THE MIXIN SPEED.....</b>	<b>93</b>
	<b>BIBLIOGRAPHY .....</b>	<b>97</b>

## LIST OF TABLES

Table 1-1. Some physical properties of PIBs.....	1
Table 1-2. Cationic Polymerization of Isobutylene with $\text{H}_2\text{O}/\text{AlCl}_3\text{OBu}_2$ Initiators in Different Solvents at - 20 °C [10].....	4
Table 1-3. Isobutylene polymerization reactions.....	6
Table 1-4. Initiators/co-initiators and solvents of isobutylene polymerization reported under different system temperatures [9, 10, 12-17].....	7
Table 1-5. Reported propagation rate constants of isobutylene polymerization [9, 10, 12-17] .....	9
Table 1-6. Literature review of the isobutylene polymerization kinetics .....	14
Table 1-7. Proposed mechanisms for isobutylene polymerization [3-5, 19, 23, 26-29].....	23
Table 1-8. Empirical coefficients for Equation (12) for different impeller types [51] .....	37
Table 3-1. Notations used in the model .....	44
Table 3-2. Mass balance equations for the different reaction steps.....	46
Table 3-3. Species concentration variables in this model.....	54
Table 4-1. Model parameters used in Matlab to investigate the effects of reaction rate constants .....	58
Table 4-2. Summary of Mixing effects for all mixing time constants.....	69
Table 4-3. Summary of sensitivity analysis cases .....	73
Table A-1. Kinetic parameters for each reaction step used in the model [67].....	86
Table B-2. Effect of reactor type and impeller type/size on the mixing speed.....	93



## LIST OF FIGURES

Figure 1-1. Molecular Structures of PIB.....	2
Figure 1-2. Carbon cation ionic bond categories .....	5
Figure 1-3. Isobutylene polymerization processes reaction mechanism [5].....	22
Figure 1-4. Schematic of the high molecular weight (butyl rubber) IB polymerization process [3, 5] .....	30
Figure 1-5. Schematic of the BASF low molecular weight IB polymerization process [8] .....	30
Figure 1-6. Schematic of the halogenation process [3, 5].....	31
Figure 1-7. Schematic of the different impeller types shown in Table 1-8 .....	37
Figure 1-8. Effect of mixing speed on the mixing time constant for different impellers at $H_r/D_r = 1$ .....	38
Figure 2-1. Interplay among the equation parameters required for the reactor model .....	43
Figure 3-1. Scheme of mixing model with segregation zones.....	50
Figure 4-1. Effect of $k_i$ on Monomer Conversion.....	59
Figure 4-2. Effect of $k_i$ on the Number Average Molecular Weight .....	60
Figure 4-3. Effect of $k_i$ on the Polydispersity Index .....	60
Figure 4-4. Effect of $k_p$ on the Monomer Conversion .....	62
Figure 4-5. Effect of $k_p$ on the Number Average Molecular Weight.....	62
Figure 4-6. Effect of $k_p$ on the Polydispersity Index .....	63
Figure 4-7. Effect of $k_{tr}$ on the Monomer Conversion.....	64
Figure 4-8. Effect of $k_{tr}$ on the Number Average Molecular Weight .....	65

Figure 4-9. Effect of $k_{tr}$ on the Polydispersity Index .....	65
Figure 4-10. Effect of $k_t$ on the Monomer Conversion.....	66
Figure 4-11. Effect of $k_t$ on the Number Average Molecular Weight .....	67
Figure 4-12. Effect of varying $k_t$ on the Polydispersity Index .....	67
Figure 4-13. Effect of dimensionless mixing time on the monomer conversion (Cases 1-5) .....	70
Figure 4-14. Effect of dimensionless mixing time on the monomer conversion (Cases 6-7) .....	71
Figure 4-15. Effect of dimensionless mixing time on the $M_n$ (Cases 1-5).....	71
Figure 4-16. Effect of dimensionless mixing time on the $M_n$ (Cases 6-7).....	72
Figure 4-17. Effect of dimensionless mixing time on the Polydispersity index (Cases 1-5).....	72
Figure 4-18. Effect of dimensionless mixing time on the Polydispersity index (Cases 6-7).....	73
Figure 4-19. Effect of dimensionless mixing time on the monomer conversion.....	75
Figure 4-20. Effect of dimensionless mixing time on the monomer conversion.....	76
Figure 4-21. Effect of dimensionless mixing time on the $M_n$ .....	76
Figure 4-22. Effect of dimensionless mixing time on the $M_n$ .....	77
Figure 4-23. Effect of dimensionless mixing time on the Polydispersity Index.....	77
Figure 4-24. Effect of dimensionless mixing time on the Polydispersity Index.....	78
Figure 4-25. Effect of reactor type and impeller type/size on the mixing speed .....	79
Figure 4-26. Effect of reactor type and impeller type/size on the mixing speed .....	80
Figure 4-27. Effect of reactor type and impeller type/size on the mixing speed .....	81
Figure 4-28. Effect of reactor type and impeller type/size on the mixing speed .....	82
Figure A-1. Compositions of Isobutylene, Polyisobutylene and $AlCl_3$ Initiator during IBP .....	88
Figure A-2. Weight average and Number average molecular weights during IBP .....	89
Figure A-3. Weight average and number average during IBP .....	89
Figure A-4. Effect if temperature on the conversion and polydispersity index of the IBP process .....	90

Figure A-5. Effect of initiator concentration on isobutylene conversion .....	90
Figure A-6. Model predictions of the IB concentration experimental data by Zhao et al. [53, 54] .....	91
Figure A-7. Model predictions of the weight average molecular weight experimental data by Zhao et al. [53, 54].....	92
Figure A-8. Model validation of the number average molecular weight against the experimental data by Zhao et al. [53, 54] .....	92

## **ACKNOWLEDGEMENT**

I would like to take this opportunity to thank my advisor Dr. Morsi. He sets high academic standards for himself and our lab members. I feel fortunate working on this topic under his mentoring. I am also grateful to PhD candidate Omar Basha for his thorough guide during the composing of this thesis.

Besides, I would also like to thank my families for their support. It is impossible to complete this research only on my own but the contribution from my wife, parents, and friends.

## NOMENCLATURE

$C$	Concentration ( $\text{mol/m}^3$ )
$C_o$	Reference concentration ( $\text{mol/m}^3$ )
$\hat{C}_j$	Dimensionless concentration
$E_a$	Activation energy ( $\text{J/kmol}$ )
$F$	Mass transfer rate between different mixing zones ( $\text{mol/s}$ )
$k_i$	Initiation reaction rate constant ( $[\text{mol/m}^3]^{-1}\text{s}^{-1}$ )
$k_p$	Propagation reaction rate constant ( $[\text{mol/m}^3]^{-1}\text{s}^{-1}$ )
$k_{tr}$	Chain transfer reaction rate constant ( $[\text{mol/m}^3]^{-1}\text{s}^{-1}$ )
$k_t$	Termination reaction rate constant ( $\text{s}^{-1}$ )
$k_o$	Pre-exponential factor ( $\text{s}^{-1}$ )
$m_o$	Molecular weight of monomer unit ( $\text{kg/mol}$ )
$M_i$	Molecular weight of monomers of class $i$
$M_n$	Number average molecular weight
$M_w$	Weight average molecular weight ( $\text{kg/mol}$ )
$n_n$	Number averaged degree of polymerization
$n_w$	Weight averaged degree of polymerization
$N_i$	Number of monomers of class $i$
$PDI$	Polydispersity Index

$Q$	Volumetric flow rate ( $\text{m}^3/\text{s}$ )
$\hat{Q}$	Dimensionless volumetric flow rate
$R_i$	Reaction rate ( $\text{mol}/\text{m}^3\cdot\text{s}$ )
$\hat{R}_j$	Dimensionless reaction rate
$T_o$	Reference time (s)
$t_M$	Characteristic time constant for mixing (s)
$t_X$	Characteristic time constant for diffusion (s)
$T$	Temperature (K)
$V$	Volume ( $\text{m}^3$ )
$V_o$	Reference volume ( $\text{m}^3$ )
$\hat{V}$	Dimensionless volume
$\theta$	Dimensionless time
$\theta_M$	Dimensionless mixing time constant
$\theta_X$	Dimensionless diffusion time constant
$[A]$	Active monomer concentration ( $\text{mol}/\text{m}^3$ )
$[C]$	Polymer chain concentration ( $\text{mol}/\text{m}^3$ )
$[E1]$	Concentration of polymer undergoing chain transfer ( $\text{mol}/\text{m}^3$ )
$[E2]$	Concentration of polymer undergoing chain termination ( $\text{mol}/\text{m}^3$ )
$[I]$	Initiator Concentration ( $\text{mol}/\text{m}^3$ )
$[M]$	Monomer Concentration ( $\text{mol}/\text{m}^3$ )

## 1.0 INTRODUCTION AND BACKGROUND

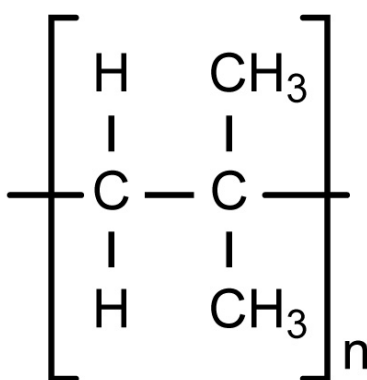
### 1.1 INTRODUCTION

Polymers and co-polymers derived from isobutylene, known as polyisobutylenes (PIBs), have been produced in a wide range of molecular weights and used in numerous important applications. Low molecular weight PIBs are extensively used in the preparation of additives for lubricants and fuels; medium molecular weight PIBs are used as viscosity-index modifiers for lubricants; and high molecular weight PIBs are used in the production of uncured rubbery compounds and as an impact additive for thermoplastics [1-5]. Table 1-1 summarizes some physical properties of PIBs.

**Table 1-1.** Some physical properties of PIBs

Density at 20 °C	0.92 g/cm <sup>3</sup>
Glass transition temperature, T <sub>g</sub> ( at differential scanning calorimetry)	- 62 °C
Specific heat, c <sub>p</sub>	2 kJ·kg <sup>-1</sup> ·K <sup>-1</sup>
Thermal coefficient of expansion at 23 °C	6.3 × 10 <sup>-4</sup> K <sup>-1</sup>
Thermal conductivity, k	0.19 W·K <sup>-1</sup> ·m <sup>-1</sup>
Coefficient of permeability to water vapor	2.5 × 10 <sup>-7</sup> g·m <sup>-1</sup> h <sup>-1</sup> mbar <sup>-1</sup>
Specific resistivity	1.016 ohm·cm

The low molecular weight PIBs ( $M_w = 500\text{-}5000 \text{ g/mol}$ ) are conventionally produced by isobutylene polymerization in the presence of either  $\text{AlCl}_3$  or  $\text{BF}_3$  as an initiator [6, 7]. The low molecular weight PIBs produced using the  $\text{AlCl}_3$  catalyst is known as conventional PIBs as shown in Figure 1-1. It should be mentioned that the PIB-based additives are made by reacting the double-bond-terminated PIBs with a maleic anhydride, which is the acid anhydride of maleic acid with the formula  $\text{C}_2\text{H}_2(\text{CO})_2\text{O}$  [6].



**Figure 1-1.** Molecular Structures of PIB

Since the internal tri-substituted or tetra-substituted double bonds have low reactivity to maleic anhydride, the PIB must first be converted to the corresponding diene using a chlorination/dehydro-chlorination process before it reacts with maleic anhydride, leading to the production of significant amounts of chlorine-containing wastes [7].

On the other hand, the low molecular weight PIBs produced using the  $\text{BF}_3$  initiator have high content of vinylidene end groups (exo-olefin end groups). These vinylidene end groups, in contrast with the internal tri-substituted or tetra-substituted double bonds, are able to react with maleic anhydride at sufficiently high rates. These types of PIBs, containing 75-85% of exo-



olefin end groups, are called highly reactive PIBs, and are being commercially produced by BASF [8].

The chemistry of the isobutylene polymerization has been extensively investigated; and kinetic and mechanistic models covering different operating conditions have been developed.

The carbocationic polymerization of isobutylene and its co-polymerization with co-monomers, such as isoprene and p-methylstyrene, are mechanistically complex. In this type of polymerization, an initiator and a common Lewis acid co-initiator, such as  $\text{AlCl}_3$ ,  $(\text{alkyl})\text{AlCl}_2$ ,  $\text{BF}_3$ ,  $\text{SnCl}_4$ ,  $\text{TiCl}_4$ , etc., are used. More recently, an initiator and uncommon Lewis acid co-initiators, such as methylaluminoxane (MAO) or specifically designed weakly coordinating Lewis acids, such as  $\text{B}(\text{C}_6\text{F}_5)_3$ , were used [9]. Examples of the initiators commonly used include Brønsted acids ( $\text{HCl}$ ,  $\text{RCOOH}$ );  $\text{H}_2\text{O}$ ; alkyl halides ( $(\text{CH}_3)_3\text{CCl}$ ,  $\text{C}_6\text{H}_5(\text{CH}_3)_2\text{Cl}$ ); esters; ethers; peroxides; and epoxides.

However, even though the kinetics of the isobutylene polymerization process have been widely investigated, due to its complex mechanisms, efforts towards developing comprehensive reactor models, which can be used to describe and optimize the IBP process are very scanty.

In 1931, PIB process was first developed by the BASF Chemical Company using a boron trifluoride ( $\text{BF}_3$ ) initiator at low temperatures. The soft, resin-like polymers produced in this process, appeared to have interesting properties, including low permeability to gas and moisture, good oxidative resistance and good chemical stability. The low molecular weight PIB ( $M_w$  500 ~ 5,000 g/mol) is widely used as raw materials for adhesives, sealants, lubricants, coatings and chewing gum [5]. The medium and high molecular weight PIBs ( $M_w \geq 10,000$  g/mol), on the other hand, are usually used to produce rubbery compound; and the vinyl polymer has many properties, which are potentially useful for many applications.

## 1.2 CATIONIC POLYMERIZATION

Monomers having carbon-carbon double bonds usually tend to undergo radical polymerization, whereas some monomers, which have electron-releasing substituents are likely to be polymerized through cationic reaction. These substituents are known as alkoxy, phenyl, vinyl, and 1-1-dialkyl. Due to the high sensitivity and strict selectivity of the cationic polymerization, it is difficult to stabilize the conditions for the propagation step, which requires rigorous and complex control of the process parameters. For example, most of the inorganic initiators are heterogeneous and must have high purity so that the initiated active species will not be poisoned. It was reported that the whole reaction takes only few minutes to convert most of the monomer to long chains, as shown in Table 1-2.

**Table 1-2.** Cationic Polymerization of Isobutylene with  $\text{H}_2\text{O}/\text{AlCl}_3\text{OBu}_2$  Initiators in Different Solvents at - 20 °C [10]

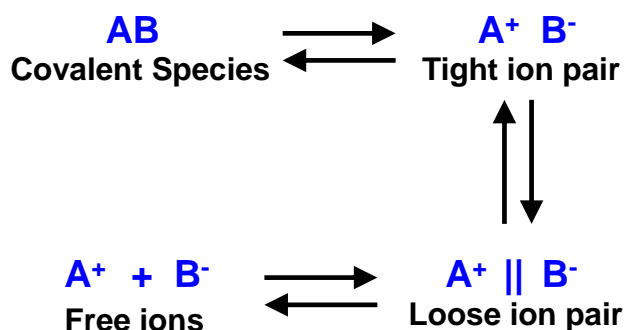
Solvent	Time(min)	Conversion (%)	Mn (g/mol)	Mw/Mn
$\text{CH}_2\text{Cl}_2$	30	64	1,330	1.26
TFT(Trifluorotoluene)	30	52	1,690	1.64
Toluene	30	79	3,770	3.80
n-Hexane	30	35	1,990	3.53

In this table, Mn and Mw are the average molecular number and the average molecular weight, respectively.

The rate of the cationic polymerization reaction is highly sensitive to several factors, such as nucleophilic ions concentration, life time of the active species and the solvent polarity. The

formed carbon cation should be sufficiently nucleophilic to allow chain growth. Moreover, the solvent polarity plays an important role in controlling the activity of the reacting species. A polarized solvent enhances the species activity, however, the solvent should be too polar to avoid negatively interfering with the reaction. Another factor is the temperature, which affects the product quality, since the propagation reaction rate constant is sensitive to high temperatures.

Figure 1-2 gives a broad classification of the carbon cations in terms of their ionic bond as: (1) completely covalent species; (2) tight ion pairs; (3) loose ion pairs (separated by solvent); and (4) free ions (completely solvated).



**Figure 1-2.** Carbon cation ionic bond categories

The formation of tight and loose ion pairs is common in the polymerization of isobutylene initiated with  $AlCl_3$  in hexane as a solvent. They result in a moderate polarity, where the unsaturated isobutylene chain has enough affinity to drag the isobutylene monomers into the propagating chain.

The cationic polymerization of isobutylene can be divided into four steps: (1) initiation, (2) propagation, (3) chain transfer and (4) chain termination. The reaction schemes are shown in Table 1-3 with different reaction rate constants  $k$ , representing each reaction step. Experimental results [11] indicated that the rate constant of the initiation step is greater than that of the

propagation step ( $k_i > k_p$ ). It should be emphasized that the rate constants for the initiation, propagation, chain-transfer, and chain termination steps in the polymerization process are difficult to measure because of the rapid rate of reaction.

**Table 1-3.** Isobutylene polymerization reactions

Step	Reaction	Rate constant
Initiation	$Initiator + M \rightarrow A_1^*$	$k_i$
Propagation	$A_1^* + M \rightarrow A_2^*$ $A_{n-1}^* + M \rightarrow A_n^*$	$k_p$
Chain transfer	$A_n^* + M \rightarrow A_1^* + P$	$k_{tr}$
Chain Termination	$A_n^* \rightarrow P$	$k_t$

Polymerizations in either hydrocarbon or halogenated hydrocarbon solvents at low temperature indicated high polymerization rates since experimental tests indicated that low temperature appeared to promote the polymer yields [3-5]. The four steps of the cationic polymerization of isobutylene are detailed below.

### 1.2.1 Initiation step

During the initiation step, isobutylene monomers react with Lewis acid co-initiator to produce carbenium ions which are paired ionized monomer and metal halide. These reactions are fast and highly exothermic. The initiation component is typically composed of two elements: an initiator and a Lewis acid co-initiator. The widely used initiators are Brønsted acids, such as HCl, RCOOH, H<sub>2</sub>O, alkyl halides, (CH<sub>3</sub>)<sub>3</sub>CCl, C<sub>6</sub>H<sub>5</sub>(CH<sub>3</sub>)<sub>2</sub>Cl, esters, ethers, peroxides, and epoxides. Recently, transition-metal complexes, such as metallocenes; and other single-site catalysts when activated with weakly coordinating Lewis acids or Lewis acid salts, have been used as initiators

for isobutylene polymerization. Lewis acid co-initiator includes  $\text{AlCl}_3$ ,  $(\text{alkyl})\text{AlCl}_2$ ,  $\text{BF}_3$ ,  $\text{SnCl}_4$ , and  $\text{TiCl}_4$ . Other Lewis acids, such as methylaluminoxane (MAO) and weakly coordinating Lewis acids, such as  $\text{B}(\text{C}_6\text{F}_5)_3$  are used as co-initiator for the isobutylene polymerization. The initiation step in cationic polymerization in various pathways occurs at a very fast rate due to the property of the ionic bond interaction. Table 1-4 shows the initiators/co-initiators and solvents reported under different system temperatures [9, 10, 12-17].

**Table 1-4.** Initiators/co-initiators and solvents of isobutylene polymerization reported under different system temperatures [9, 10, 12-17]

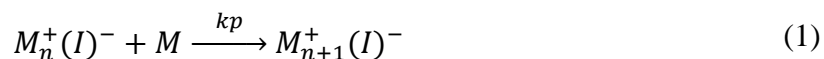
Initiating system	Solvent	T (°C)
$\text{HClO}_4$	$\text{CH}_2\text{Cl}_2$	-80
Triflic acid $\text{TMPCl}/\text{TiCl}_4/\text{DPE}/$	$\text{CH}_2\text{Cl}_2$	-65 to -10
$\text{Ti}(\text{OR})_4/\text{SnBr}_4$	$\text{Hx}/\text{CH}_3\text{Cl}$	-60 to -80
$\text{RCl}/\text{TiCl}_4$	$\text{CH}_2\text{Cl}_2/\text{CHCl}_3$	-75
$\text{TMSCl}/\text{BCl}_3$	$\text{CH}_2\text{Cl}_2$	-70
$\text{CumCl}/\text{SnCl}_4$	$\text{CH}_2\text{Cl}_2$	-40
$\text{CumCl}/\text{TiCl}_4$	$\text{CH}_2\text{Cl}_2$	-40
$\text{TmeStCl}/\text{BCl}_3$	$\text{CH}_2\text{Cl}_2$	-70
$\text{RCl}/\text{SnCl}_4$	$\text{CH}_2\text{Cl}_2$	-15
$\text{RCl}/\text{TiCl}_4$	$\text{CH}_2\text{Cl}_2$	-80 to -15
$\text{AlBr}_3/\text{TiCl}_4$	Heptane	-14
$\text{Light}/\text{VCl}_4$	Heptane	-20
$\text{Et}_2\text{AlCl}/\text{Cl}_2$	$\text{CH}_3\text{Cl}$	-45
$\text{IB n-mer}/\text{TiCl}_4$	$\text{Hx}/\text{CH}_3\text{Cl}$	-80
$\text{TMPCl}/\text{TiCl}_4$	$\text{Hx}/\text{CH}_3\text{Cl}$	-80 to -50

In some cases, the concentrations of the initiator and co-initiator can determine the maximum polymerization rate. Typically, increasing the initiator/co-initiator concentration ratio, the polymerization rate increases till it reaches a maximum. However, after reaching the maximum, it starts to decrease and then levels off at a low value [18, 19]. One possible explanation for this

behavior is that when the initiator concentration reaches a particular value, it takes over the monomer to produce an oxonium salt, which exhibits ineffectiveness in protonating the olefins. It should be remembered that there are many factors which affect the balance between the competing initiation and inactivation, including the type of monomer, the type of solvent and the system temperature.

### 1.2.2 Propagation step

In the propagation step, the carbocation and the paired counter-ion formed in the initiation step continue to add monomers as a growing chain, where a monomer M is added to the propagating chain of length n.



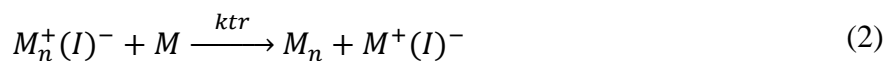
The added monomer units are strongly affected by the solvent polarity, concentration of counter ions and the system temperature. Table 1-5 lists different propagation rate constants obtained under various initiators, solvents and temperatures [9, 10, 12-17]; and as can be observed, the type of initiator, solvent and system temperature all contributes to the variation of  $k_p$  value which ranges from 6 to  $1.7 \times 10^6 \text{ m}^3/(\text{mol.s})$ . The propagation rate constant ( $k_p$ ) was reported to be stable at an abundance of monomer concentrations which is essentially diffusion-limited [3, 7].

**Table 1-5.** Reported propagation rate constants of isobutylene polymerization [9, 10, 12-17]

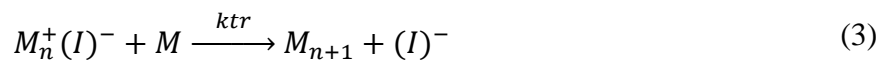
Initiator	Solvent	Temperature (°C)	$k_p$ ( $m^3/mol \cdot s$ )	Reference
AlBr <sub>3</sub> /TiCl <sub>4</sub>	Heptane	- 14	6	[9]
Light/ VCl <sub>4</sub>	In bulk	- 20	$7.9 \times 10^2$	[12]
Et <sub>2</sub> AlCl/Cl <sub>2</sub>	CH <sub>3</sub> Cl	- 48	12	[13]
Ionizing radiation	CH <sub>2</sub> Cl <sub>2</sub>	- 78	9.1	[20]
Ionizing radiation	In bulk	- 78	$1.5 \times 10^5$	[11]
R-Cl/TiCl <sub>4</sub>	CH <sub>2</sub> Cl <sub>2</sub>	- 78	$6 \times 10^5$	[15]
IB n-mer/TiCl <sub>4</sub>	Hexanes/CH <sub>3</sub> Cl	- 80	$7 \times 10^5$	[16]
TMP-Cl/TiCl <sub>4</sub>	Hexanes/CH <sub>3</sub> Cl	- 80 to - 40	$4.7 \times 10^5$	[17]
TMP-Cl/TiCl <sub>4</sub>	Hexanes/CH <sub>3</sub> Cl	- 80 to - 40	$1.7 \times 10^6$	[10]

### 1.2.3 Chain transfer step

The chain transfer step occurs when the cationic chain end reacts with isobutylene, isoprene, or a species with an unshared electron pair, i.e., solvents, counter-ion, or olefins. The reactions breaking the chain propagation terminate the growth of the macromolecule and inactivate the highly reactive chain end. The chain transfer is the main termination mechanism in the isobutylene polymerization reaction as shown below:



The chain termination may occur spontaneously to stops chain growth, and in this case, it is known as spontaneous termination:



### 1.2.4 Chain termination step

The termination reaction in terms of deionization with combination of halide ions commonly leads to the termination step. In the polymerization of isobutylene with  $\text{AlCl}_3/\text{water}$  as initiator/co-initiator system, when the end of a propagating chain combines with a counter-ion ( $\text{Cl}^-$ ), the unsaturated carbon-carbon double bond will be replaced with a saturated carbon-chloride bond and the reaction is terminated:



It should be emphasized that in this latter case, the kinetics of the propagation step will be affected because of the decreased initiator concentration.

## 1.3 LITERATURE STUDIES ON ISOBUTYLENE POLYMERIZATION REACTION KINETICS

The overall reaction kinetic rates of isobutylene (IB) polymerization vary significantly based on the type and concentrations of the imitator/co-initiator, the solvent type and system temperature. Generally, the rates of initiation, propagation, chain transfer termination and chain termination can be written as:

$$\text{Initiation: } R_i = k_i[I][M] \quad (5)$$

$$\text{Propagation: } R_p = k_p[M_n^+(I)^-][M] \quad (6)$$

$$\text{Chain Transfer Termination: } R_{tr} = k_{tr}[YM^+(IZ)^-][M] \quad (7)$$



$$\text{Spontaneous Termination: } R_t = k_t[M_n^+(I)^-] \quad (8)$$

$R_i$  is the initiation kinetic rate expression, which includes the initiation reaction rate constant  $k_i$ . It was reported to be a first order with respect to the initiator/co-initiator  $[I]$  and with respect to the monomer  $[M]$  [18, 19, 21].

$R_p$  is the propagation kinetic rate expression, which includes the propagation reaction rate constant  $k_p$ . It is a first order with respect to the monomer  $[M]$  and the first order with respect to the propagating species  $[M_n^+(I)^-]$  [18, 19, 21].

$R_t$  is the spontaneous termination rate constant, which includes the rate of chain termination reaction  $k_t$  and it is a first order with respect to of propagating species  $[M_n^+(I)^-]$  [18, 19, 21].

$R_{tr}$  the chain transfer expression, which includes the chain transfer coefficient  $k_{tr}$ . It is first order with respect to the monomer  $[M]$  and the active center continuously adding monomers to increase chain growth [18, 19, 21].

Considerable research has been conducted on investigating new initiators for the synthesis of highly reactive PIBs. Ivan et al. [22] proposed a two-step process for the preparation of mono- or di-functional exo-olefin-terminated PIB (95-98% of exo-olefin groups), which involved the synthesis of tertchloride-terminated PIB at - 78 °C via controlled cationic polymerization followed by dehydrochlorination of isolated polymer with excess of potassium tert-butoxide in refluxing tetrahydrofuran for 24 hours. Telechelic polyisobutylene with 100% of exo-olefin groups can also be obtained by the reaction of tertchloride-terminated PIB with isobutenyltrimethylsilane in the presence of  $TiCl_4$  at - 78 °C. Quantitative formation of exo-olefin-terminated PIB (95-100%) by endquenching  $TiCl_4$ -coinitiated living isobutylene polymerization with such hindered bases as 2, 5-dimethylpyrrole or 1,2,2,6,6-

pentamethylpiperidine at - 40 to - 60 °C was recently described by Storey et al. [19, 21, 23]. The same authors reported an alternative towards polyisobutylene with exo-olefin terminal bond (69-97%), consisting of the formation of adduct between the sulfide and living polyisobutylene at - 60 °C followed by adduct decomposition by excess of nucleophile (methanol, triethylamine, 2, 6-di-tert-butylpyridine) [1, 24, 25].

The main drawbacks of the abovementioned processes are (i) low reaction temperatures, (ii) use of expensive reagents, and (iii) use of multistep procedures. Recently, it has been shown that solvent-ligated complexes of the general formula  $[M(NCCH_3)_6](A)_2$  ( $M = Mn, Mo, Cu$ , and  $A =$  non-coordinating borate anions) [3-5, 19, 23, 26-29] can polymerize isobutylene in the temperature range 20 to 60 °C to produce highly reactive polyisobutylenes (60-95% of exo-olefin groups) with molecular weight between 300 and 13,000 g/mol and reasonable molecular weight distribution  $Mw/Mn = 1.4-3.0$ . However, these complexes are currently too expensive to be of significant interest to the industry. Also, heteropolyacids of the formula  $(NH_4)_{2.5}H_{0.5}PW_{12}O_{40}$  have been recently shown to polymerize isobutylene at -5 °C into highly reactive PIBs (70-85% of exo-olefin groups) with  $Mw = 1000-3500$  g/mol, but with very broad molecular weight distribution ( $Mw/Mn = 5-25$ ) [3-5, 19, 23, 26-29]. In addition, an interesting and simple initiator, tert-butyl chloride/ $EtZnCl$ , has been used in the synthesis of molecular weight PIBs ( $Mw = 10,000-29,000$  g/mol) with exo-olefin terminal groups at 20 °C. However, a high content of vinylidene end groups (85-92%) has been observed only at low conversions (< 30%); and only 60% of exo-olefin terminal groups was detected at about 95% of monomer conversion.

Recent studies of the living cationic polymerization of isobutylene and copolymerization with isoprene have just begun; and so far, living copolymerization of isobutylene and isoprene has produced a random copolymer with narrow molecular weight distribution and a well-defined

structure [3, 7]. For instance, the  $\text{BCl}_3$ /cumyl acetate polymerization in methyl chloride or methylene chloride at  $-30\text{ }^\circ\text{C}$  produces copolymers with 1 - 8 mol% trans-1, 4-isoprene units having a molecular weight between 2000 and 12,000 g/mol with  $M_w/M_n$  under 1.8.

The advent of the living polymerization of isobutylene has led to the preparation of a large number of new isobutylene-based materials. High molecular weight copolymers of isobutylene and isoprene have been prepared at temperatures  $40\text{-}50\text{ }^\circ\text{C}$  greater than that is commercially practiced using metallocenes and single-site initiators. Newer Lewis acids, such as methylaluminoxane and weakly coordinating anions or their salts, such as  $\text{B}(\text{C}_6\text{F}_5)_3$  or  $\text{R}^+[\text{B}(\text{C}_6\text{F}_5)_4]^-$  have also been used to produce high molecular weight copolymers at high temperatures. Table 1-6 highlights several kinetic rate expressions available in the literature.

**Table 1-6.** Literature review of the isobutylene polymerization kinetics

Initiator	Conditions	Kinetic Investigation	Reference
Stannic Chloride	Carbocationic polymerization in ethyl chloride at -78.5 °C.	$r_p = k_p[R^+][M]^\alpha$	Norrish and Russell (1951) [30]
TiCl <sub>4</sub>	Carbocationic polymerization in hexane over the temperature range 0 to -30 °C.	$r_p = k_p[TiCl_4]_0[M]$	Wichterle et al. (1961) [25]
AlBr <sub>3</sub> in the presence of some Friedel-Crafts halogenides (TiCl <sub>4</sub> , TiBr <sub>4</sub> , and SnCl <sub>4</sub> )	Carbocationic polymerization in heptane over the temperature range -12 to -14 °C. The rate of polymerization of isobutylene catalyzed by AlBr <sub>3</sub> in the presence of some Friedel-Crafts halogenides (TiCl <sub>4</sub> , TiBr <sub>4</sub> , and SnCl <sub>4</sub> ) in nonpolar medium and in the absence of H <sub>2</sub> O is much higher than in polymerization catalyzed by AlBr <sub>3</sub> alone. The catalytic activity increment decreases in the order TiCl <sub>4</sub> , SnCl <sub>4</sub> , and TiBr <sub>4</sub> . In the system AlBr <sub>3</sub> -TiCl <sub>4</sub> , the conversion is dependent only on the concentration of AlBr <sub>3</sub> .	No kinetics investigation	Marek and Chmelir (1968) [9]
ZnO	Radiation-induced polymerization of isobutylene under anhydrous conditions at -78 to -140 °C.	$R_p = \left(\frac{R_i}{k_t}\right)^{1/2} k_p[M]$	Taylor and Williams (1969) [11]

Initiator	Conditions	Kinetic Investigation	Reference
Table 1-6 (continued)			
Lewis acids (VCl <sub>4</sub> , TiCl <sub>4</sub> , TiBr <sub>4</sub> , SnCl <sub>4</sub> , and AlBr <sub>3</sub> ) and their mixtures	<p>Polymerization of isobutylene with Lewis acids in n-heptane solution in the dark and under irradiation at 400-480 nm at -80 to -150 °C.</p> <p>Radical-cation initiation by visible light was observed during the polymerization of isobutylene by VCl<sub>4</sub>, TiCl<sub>4</sub>, and TiBr<sub>4</sub>, and by Electron Spin Resonance (ESR) spectra. The inhibiting effect of oxygen in photochemically initiated polymerization of isobutylene was observed.</p>	No kinetics investigation	Marek et al. (1976) [12]
C <sub>6</sub> H <sub>5</sub> C(CH <sub>3</sub> ) <sub>2</sub> Cl/BCl <sub>3</sub> initiating system	<p>Investigated the effect of 2,6-di-tertbutylpyridine (DtBP) on the polymerization of isobutylene at -50 °C.</p> <p>It was found that in the absence of DtBP, initiation by cumulation, chain transfer to monomer is absent, and termination is by chlorination.</p> <p>Whereas, in the presence of DtBP, conversions and molecular weights decrease as a function of DtBP concentration, indicating that while DtBP does not interfere with non-protic initiation by the C<sub>6</sub>H<sub>5</sub>C<sup>+</sup>(CH<sub>3</sub>)<sub>2</sub> carbocation, it functions as a terminating agent.</p>	$\frac{1}{\overline{DP}_n} = \frac{[M]}{[M]_0} \left( \frac{k_{ter,Cl} + k_{ter,DtBP}}{k_p} \right)$ $\frac{k_{ter}}{k_p} = 1.28 \times 10^{-2} \text{ and } 5 \times 10^{-4}$ <p>with and without DtBP respectively</p>	Guhaniyogi et al. (1982) [31]
1,4-bis(1-chloro-1-methylethyl)benzene (DiCumCl)/BCl	Living polymerization of isobutylene (IB) in CH <sub>3</sub> Cl, CH <sub>2</sub> Cl <sub>2</sub> , and C <sub>2</sub> H <sub>5</sub> Cl solvents and a 90:10 v/v CH <sub>3</sub> Cl/n-hexane mixture at -75 °C.	$\frac{k_{ter}}{k_p} = 0.96 \text{ in } CH_3Cl$ $= 0.49 \text{ in } CH_2Cl_2$	Ivan and Kennedy (1990) [22]

Initiator	Conditions	Kinetic Investigation	Reference
Table 1-6 (continued)			
1,4-bis( 1-chloro-1-methylethyl)benzene	Living Polymerization carried out at -75 °C.	No kinetic investigation	Ivan and Kennedy (1990) [22]
Blocked Bifunctional Initiators in the Presence of Di-tert-butylpyridine as a Proton Trap	Living carbocationic polymerization in hexane at -80 °C.	$r_p = k_p[R^+][M]$	Gyor et al. (1991) [32]
1,4-dicumyl alcohol and boron trichloride (BCl <sub>3</sub> )	Living carbocationic polymerization in CH <sub>3</sub> Cl <sub>2</sub> at -65 °C, with trimethylamine used as an electron donor. The addition of an electron donor was found to effectively reduce the molecular weight (narrowing effect) of the resulting polymers. Moreover, the addition of trimethylamine resulted in the suppression of cyclo-alkylation and the total elimination of initiation due to protic impurities.	No kinetic investigation	Pratap et al. (1992) [33]
<i>tert</i> -amyl alcohol/BCl <sub>3</sub> /1-methyl-2-pyrrolidinone	Living carbocationic polymerization in CH <sub>3</sub> Cl <sub>2</sub> at -40 °C. Able to synthesize low molecular weight, living (near monodisperse) polyisobutylenes carrying “ethyl” head group and “tert-chloro” end group (asymmetric telechelic polyisobutylenes).	No kinetic investigation	Pratap et al. (1992) [34]

Initiator	Conditions	Kinetic Investigation	Reference
Table 1-6 (continued)			
BCl <sub>3</sub> and CH <sub>3</sub> Cl	Investigated Isobutylene polymerization using both haloboration and self-ionization initiation mechanisms at -25 to -60 °C.	$\ln \left( \frac{[M]_o}{[M]} \right) = \frac{k_p}{K_2} [PCL][BCl_3]t$ $\left( \frac{k_p}{K_2} \right)_{CH_3Cl} = 9.4 \times 10^{-2} s^{-1}$ $\left( \frac{k_p}{K_2} \right)_{BCl_3} = 8.8 \times 10^{-3} s^{-1}$	Balogh et al. (1994) [35]
(η <sup>5</sup> -C <sub>5</sub> Me <sub>5</sub> )TiMe <sub>3</sub> and B(C <sub>6</sub> F <sub>5</sub> )	Cationic polymerization in toluene carried out at -78 °C, resulting in a isobutylene homopolymer with a high weight average molecular mass of -5 x 10 <sup>5</sup> and a narrow polydispersity, or an isobutylene-isoprene copolymer.	No kinetic investigation	Barsan and Baird (1995) [36]
Diisobutylene hydrochloride or triisobutylene hydrochloride in the presence of BCl <sub>3</sub> and benzyltriethylammonium tetrachloroborate	Living polymerization in CH <sub>2</sub> Cl <sub>2</sub> at -78 °C. The reactions followed second-order kinetics, first-order with respect to initiator (diisobutylene or triisobutylene hydrochloride), first-order with respect to BCl <sub>3</sub> , and zeroth-order with respect to isobutylene.	$\frac{-d[R - Cl]}{dt} = Kk_p[R - Cl][BCl_3][C_4H_8]$	Roth et al. (1997) [37]

Initiator	Conditions	Kinetic Investigation	Reference
Table 1-6 (continued)			
Metallocene and non-metallocene ( $\text{Ph}_3\text{C}^+$ , $\text{R}_3\text{C}^+$ , $\text{H}^+$ , $\text{Li}^+$ , $\text{R}_3\text{Si}^+$ ) initiator-catalysts that contain the non-coordinating anions (NCA), $\text{B}(\text{C}_6\text{F}_6)_4^-$ and $\text{RB}(\text{C}_6\text{F}_5)_3^-$	Carbocationic polymerization in hexane, methyl cyclohexane and toluene at -20 °C. The presence of a proton trap can eliminate proton initiation and confine initiation to that stemming from the metal cation. Similar results can be achieved when water concentration is kept below $1 \times 10^{-4}$ mol/L in the solvents. Initiation from the metal cation is very inefficient. However, once initiated, isobutylene polymerization follows and usually goes to reasonable conversions.	No kinetic investigation	Shaffer and Ashbaugh (1997) [38]
t-Bu-m-DCC/TiCl <sub>4</sub> /2,4-DMP	Living cationic polymerization carried out over the temperature range -50 to -80 °C.	$r_p = k_p [\text{R}^+][\text{M}]$ Where $[\text{R}^+]$ is the concentration of instantaneously active growing chains	Storey and Choate (1997) [23]
Cumyl chloride/TiCl <sub>4</sub> /2,4-dimethylpyridine system	Carbocationic polymerization in 60/40 hexane/MeCl at -80 °C.	$\ln \left( \frac{[\text{P} - \text{tCl}]_o}{[\text{P} - \text{tCl}]} \right) = K t k_r$ $\frac{k_p}{k_r} = \left( \frac{k_{app}}{k_{r-app} [\text{P} - \text{tCl}]_o} \right)$ [P-tCl] is the tert-chloride chain [P-tCl] <sub>o</sub> is the total number of polymer chains	Storey et al.(1998) [21]



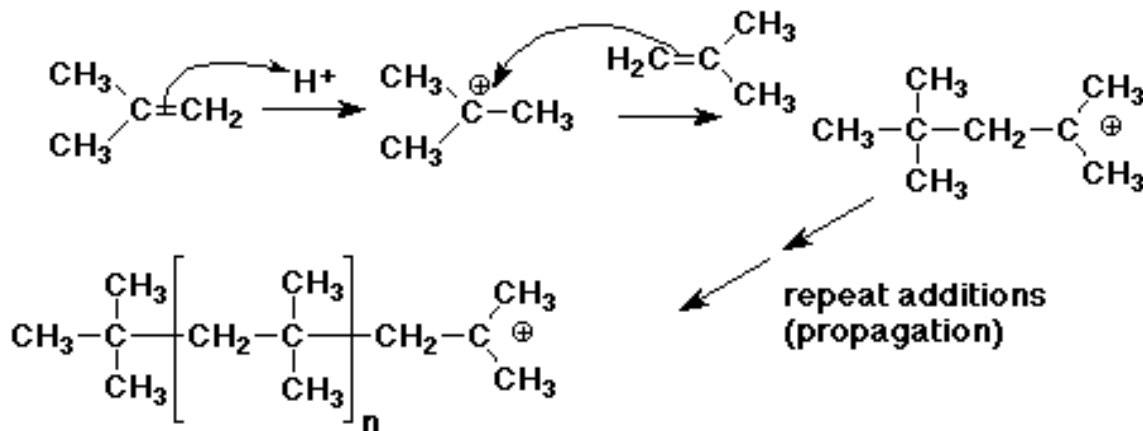
Initiator	Conditions	Kinetic Investigation	Reference
Table 1-6 (continued)			
TiCl <sub>4</sub>	Living Polymerization carried out at -80 °C, investigated effect of initial concentration of initiator, solvent quality, monomer concentration and temperature on the propagation rate.	$\ln\left(\frac{[M]_o}{[M]}\right) = K_1 k_p [TiCl_4]_0 t$	Paulo et al. (2000) [39]
Conventional tertiary alkyl chloride initiators	Dimethylaluminum chloride catalyzed living isobutylene polymerization in 60/40 v/v nonpolar/polar solvent mixtures of hexane/methylene chloride and hexane methyl chloride at -75 to -80 °C.	$\ln\left(\frac{[M]_o}{[M]}\right) = K_1 k_p [TiCl_4]_0 t$ $\frac{M_w}{M_n} = 1.2; M_n = 150 \text{ kDa}$	Bahadur et al. (2000) [40]
5-tert-butyl-1,3-bis(2-chloro-2-propyl)benzene (t-Bu-m-DCC) or 2-chloro-2,4,4-trimethylpentane (TMPCl) in conjunction with TiCl <sub>4</sub>	Living Polymerization carried out at -80 °C in hexane/methyl chloride or methylcyclohexane/methyl chloride (60:40 v/v) cosolvents, and either 2,4-dimethylpyridine (DMP) or 2,6-di-tert-butylpyridine (DTBP) was used as an electron donor (ED).	$\ln\left(\frac{[M]_o}{[M]}\right) = K_{eq} k_p [CE] [TiCl_4]^n t$ Where [CE] is the total concentration of chain ends	Storey and Donnalley (2000) [28]
2-chloro-2,4,4-trimethylpentane (TMPCl)/TiCl <sub>4</sub> and AlCl <sub>3</sub>	Carbocationic polymerization in CH <sub>2</sub> Cl <sub>2</sub> at -78 °C.	$r_p = k_p ([R^+][M] + [R^+A^-][M])$ $k_p = 10^5 \text{ Lmol}^{-1}\text{s}^{-1}$	Schlaad et al. (2000) [16]

Initiator	Conditions	Kinetic Investigation	Reference
Table 1-6 (continued)			
Proton exchanged Montmorillonite clay	Polymerization in methylene chloride/hexane solvents at -7 °C. Monomer conversion was found to be higher in non-polar (hexane) solvent when compared with the polar (methylene chloride) solvent.	No kinetic investigation	Harrane et al. (2002) [41]
TiCl <sub>4</sub> , Me <sub>2</sub> AlCl, and BCl <sub>3</sub>	Carbocationic polymerization in hexane/MeCl 60/40 v/v solvent at -80 °C.	$\ln \left( \frac{[IB]_o}{[IB]} \right) = k_p \frac{K_{D0}k_1}{k_{-1}} [LA]^n [P - Cl]t$	Sipos et al. (2003) [17]
TiCl <sub>4</sub>	<p>Living polymerization of polyisobutylenes possessing exclusively exo-olefin end groups was carried out by end-quenching TiCl<sub>4</sub>-catalyzed quasi-living isobutylene (IB) polymerizations with a hindered base at -60 to -40 °C.</p> <p>Polymerizations were initiated from either 2-chloro-2,4,4-trimethylpentane (TMPCl) or 1,3-bis(2-chloro-2-propyl)-5-tert-butylbenzene, in 60/40 hexane/methyl chloride in the presence of 2, 6-dimethylpyridine.</p>	<p>Coupling of ionized chain ends with exo-olefin terminated chains is a complicating side reaction whose severity increases as [CE] increases and/or as temperature decreases.</p> <p>Higher temperatures produce higher concentrations of free base, which suppresses coupling and enables faster proton abstraction.</p>	Simison et al. (2006) [42]

Initiator	Conditions	Kinetic Investigation	Reference
Table 1-6 (continued)			
Methylaluminum Bromide Coinitiators	Carbocationic polymerization in hexane at -80 °C.	$r_p = k_p[R^+][M]$	De and Faust (2006) [43]
AlBr <sub>3</sub>	<p>Solution polymerization of isobutylene in heptane, catalyzed by aluminum tribromide was investigated over the temperature range between -60 to +20 °C.,</p> <p>The polymerization was found to take place at a high rate even at low catalyst and monomer concentrations, without addition of water as a cocatalyst. The overall rate of polymerization was found to be of first order with respect to the monomer and of second order to the catalyst. The activation energy of the polymerization was found to be practically zero within the temperature range investigated.</p>	$-\frac{dM}{dt} = k[M][AlBr_3]^2$ $k = (1.5 \pm 0.4) \times 10^5 s^{-1} mol^{-2} l^2$	Chmelir et al. (2007) [24]
AlCl <sub>3</sub> , AlCl <sub>3</sub> OBu <sub>2</sub> , AlCl <sub>3</sub> OPh <sub>2</sub> , AlCl <sub>3</sub> 0.7EtOAc	Cationic polymerization of isobutylene using AlCl <sub>3</sub> based initiating systems at -20, -40 and -60 °C.	No kinetic expressions.	Vasilenko et al.(2010) [44]

## 1.4 LITERATURE STUDIES ON ISOBUTYLENE POLYMERIZATION REACTION MECHANISMS

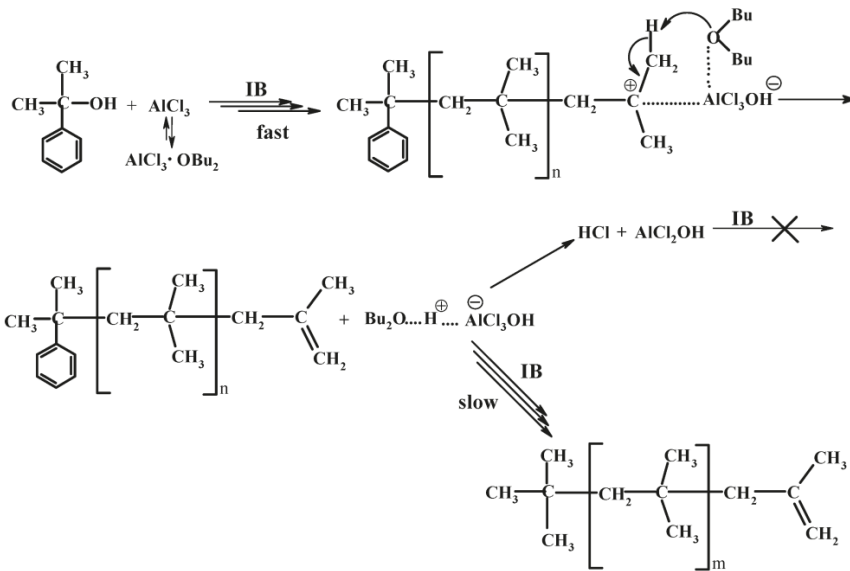
Generally, the reaction mechanism of the isobutylene polymerization is shown in Figure 3; and as can be observed, once a hydrogen ion breaks the isobutylene double bond, an isobutyl carbocation forms. The positively charged isobutyl carbocation then proceeds to add more monomers to the growing polymer chain by breaking the double bond of the isobutylene monomer. The repeated addition of the monomers continues during the propagation step of the polymer.



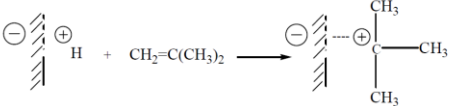
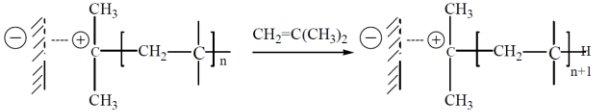
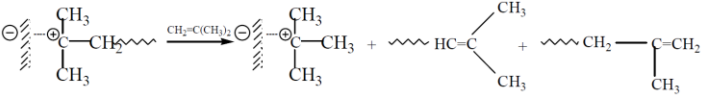
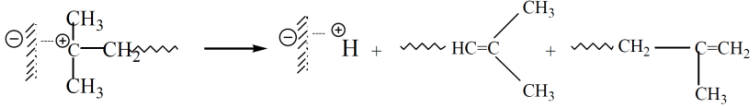
**Figure 1-3.** Isobutylene polymerization processes reaction mechanism [5]

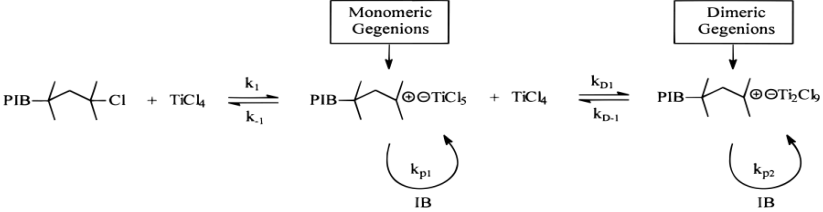
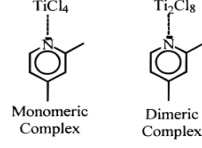
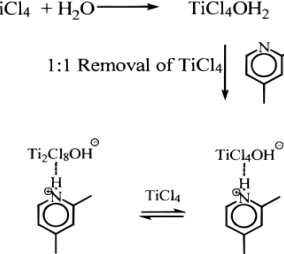
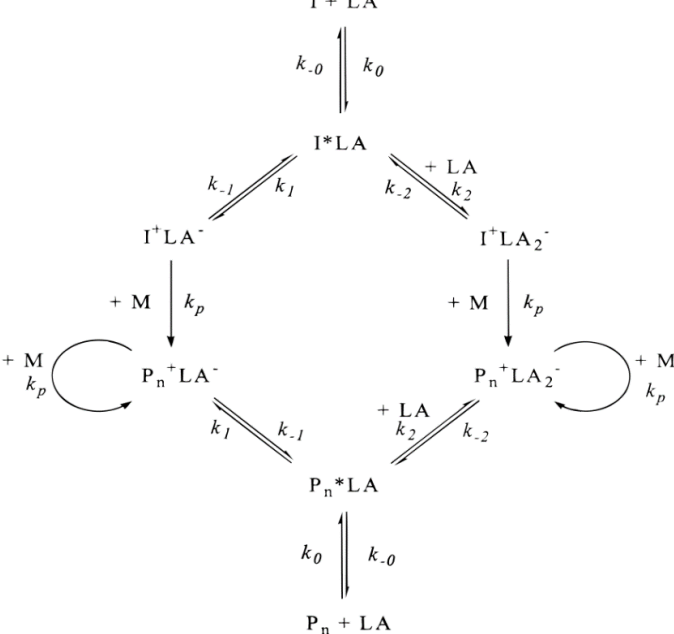
As a matter of fact, the mechanism of isobutylene polymerization has been extensively investigated in the literature, and numerous different mechanisms have been proposed depending on the type of initiators and the reaction conditions used, as given in Table 1-7.

**Table 1-7.** Proposed mechanisms for isobutylene polymerization [3-5, 19, 23, 26-29]

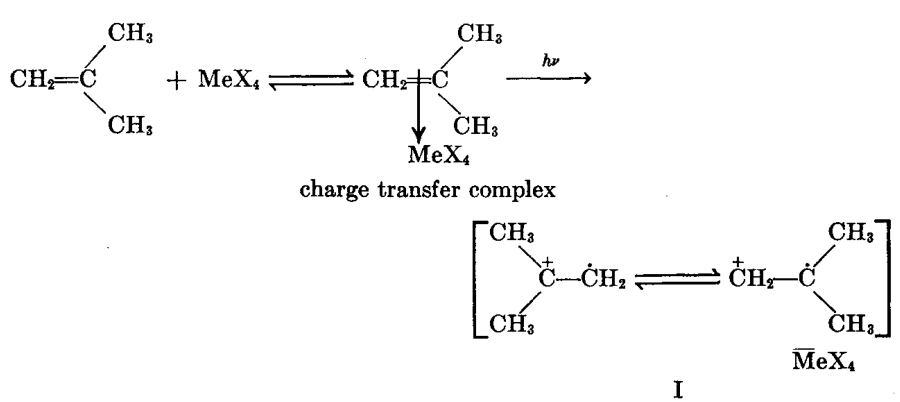
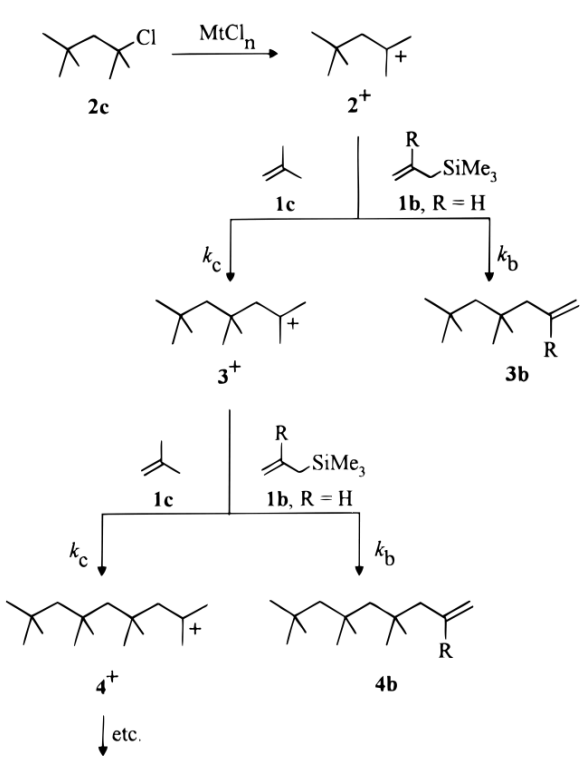
Proposed Mechanistic Scheme	Reference
<p><b><u>AlCl<sub>3</sub> based initiator</u></b></p>  <p>The scheme illustrates the proposed mechanism for isobutylene polymerization using an AlCl<sub>3</sub> based initiator. The reaction starts with isobutylene (IB) reacting with a phenyl-substituted isobutylene alcohol and AlCl<sub>3</sub>. The reaction is fast, leading to the formation of a polymer chain with a terminal carbocation. This carbocation then reacts with another IB molecule in a slow step to propagate the chain. A side reaction shows the polymer chain reacting with HCl and AlCl<sub>3</sub>OH to form a terminated chain and AlCl<sub>3</sub>OH, which is crossed out with an X.</p>	<p>Vasilenko et al. (2000) [44]</p>
<p><b><u>AlBr<sub>3</sub> catalyzed solution polymerization:</u></b></p> $2C \xrightleftharpoons[k_0']{k_0} C^+ \cdot C^-$ $C^+ \cdot C^- + M \xrightarrow{k_1} C-M^+ \cdot C^-$ $C-M^+ \cdot C^- + (n-1)M \xrightarrow{k_2} C-M_n^+ \cdot C^-$ $C-M_n^+ \cdot C^- \xrightarrow{k_3} C-M_n + H^+ \cdot C^-$ $C-M_n^+ \cdot C^- + M \xrightarrow{k_4} C-M_n + M^+ \cdot C^-$ $M_n^+ \cdot C^- + M \xrightarrow{k_4} M_n + M^+ \cdot C^-$	<p>Chmelir et al. (2007) [24]</p>

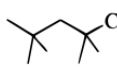
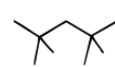
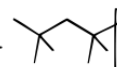
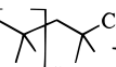
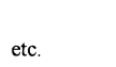
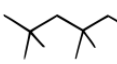
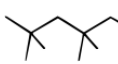
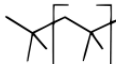
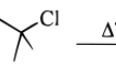

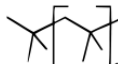
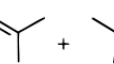
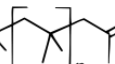
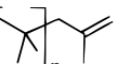


Proposed Mechanistic Scheme	Reference
Table 1-7 (continued)	
<p><b><u>C<sub>6</sub>H<sub>5</sub>C(CH<sub>3</sub>)<sub>2</sub>Cl/BCl<sub>3</sub> initiator</u></b></p> <p>Ion generation:</p> $\text{C}_6\text{H}_5\text{C}(\text{CH}_3)_2\text{Cl} + \text{BCl}_3 \rightleftharpoons \text{C}_6\text{H}_5\text{C}^+(\text{CH}_3)_2 \text{BCl}_4^-$ <p>Cationation:</p> $\text{C}_6\text{H}_5\text{C}^+(\text{CH}_3)_2 + \text{CH}_2\text{C}(\text{CH}_3)_2 \longrightarrow \text{C}_6\text{H}_5\text{C}(\text{CH}_3)-\text{CH}_2\text{C}^+(\text{CH}_3)_2$ <p>Propagation:</p> $\sim\text{CH}_2\text{C}^+(\text{CH}_3)_2 + \text{CH}_2\text{C}(\text{CH}_3)_2 \longrightarrow \sim\text{CH}_2\text{C}(\text{CH}_3)_2-\text{CH}_2\text{C}^+(\text{CH}_3)_2$ <p>Termination:</p> $\sim\text{CH}_2\text{C}^+(\text{CH}_3)_2 \text{BCl}_4^- \longrightarrow \sim\text{CH}_2\text{C}(\text{CH}_3)_2\text{Cl} + \text{BCl}_3$	<p>Guhaniyogi et al. (1982)[31]</p>
<p><b><u>Chain termination of PIB in a cumyl chloride/TiCl<sub>4</sub>/2,4-dimethylpyridine initiator</u></b></p> <p>1,2-hydride shift</p> <p>1,2-methide shift</p> <p>1,2-hydride shift</p> <p>1,2-methide shift</p>	<p>Storey et al.(1998) [21]</p>

Proposed Mechanistic Scheme	Reference
Table 1-7 (continued)	
<p><b><u>BCl<sub>3</sub> and CH<sub>3</sub>Cl initiator</u></b></p> <p><b>Initiation</b></p> <p>a) <math display="block">2\text{BCl}_3 \xrightleftharpoons{K_1} \text{BCl}_2^+ \text{BCl}_4^-</math></p> <p><math display="block">\text{BCl}_2^+ \text{BCl}_4^- + \text{CH}_2=\text{C}(\text{CH}_3)_2 \xrightarrow{k_1} \text{BCl}_2\text{-CH}_2\text{-}\overset{+}{\text{C}}(\text{CH}_3)_2 \text{BCl}_4^-</math></p> <p><math display="block">\text{BCl}_2\text{-}[\text{CH}_2\text{-C}(\text{CH}_3)_2]^+ \text{BCl}_4^- \rightleftharpoons \text{BCl}_3 + \text{BCl}_2\text{-CH}_2\text{-C}(\text{CH}_3)_2\text{-Cl}</math></p> <p>or b) <math display="block">\text{BCl}_3 + \text{CH}_2=\text{C}(\text{CH}_3)_2 \xrightarrow{k_2} \text{BCl}_2\text{-CH}_2\text{-C}(\text{CH}_3)_2\text{-Cl}</math></p> <p><math display="block">\text{BCl}_3 + \text{BCl}_2\text{-CH}_2\text{-C}(\text{CH}_3)_2\text{-Cl} \rightleftharpoons \text{BCl}_2\text{-}[\text{CH}_2\text{-C}(\text{CH}_3)_2]^+ \text{BCl}_4^-</math></p> <p><b>Propagation</b></p> <p><math display="block">\text{BCl}_2\text{-CH}_2\text{-}\overset{+}{\text{C}}(\text{CH}_3)_2 \text{BCl}_4^- + \text{M} \xrightarrow{k_p} \text{BCl}_2\text{-}[\text{CH}_2\text{-C}(\text{CH}_3)_2]_n^+ \text{BCl}_4^-</math></p> <p><b>Termination-reinitiation</b></p> <p><math display="block">\text{BCl}_2\text{-}[\text{CH}_2\text{-C}(\text{CH}_3)_2]_n^+ \text{BCl}_4^- \xrightleftharpoons{K_2} \text{BCl}_3 + \text{BCl}_2\text{-}[\text{CH}_2\text{-C}(\text{CH}_3)_2]_n\text{-Cl}</math></p>	<p>Balogh et al. (1994) [35]</p>
<p><b><u>Proton exchanged Montmorillonite clay initiator:</u></b></p> <p><b>Initiation:</b></p> <p></p> <p><b>Propagation:</b></p> <p></p> <p><b>Termination:</b></p> <p><i>Transfer to monomer:</i></p> <p></p> <p><i>Transfer to initiator:</i></p> <p></p>	<p>Harrane et al. (2002) [41]</p>

Proposed Mechanistic Scheme	Reference
Table 1-7 (continued)	
<p><b><u>5-tert-butyl-1,3-bis(2-chloro-2-propyl)benzene (t-Bu-m-DCC) or 2-chloro-2,4,4-trimethylpentane (TMPCl) in conjunction with TiCl<sub>4</sub></u></b></p>  <p><b><u>Possible Side Reactions</u></b></p> <div style="display: flex; justify-content: space-around;"> <div data-bbox="402 730 634 961"> <p>Complex Formation</p>  <p>Monomeric Complex Dimeric Complex</p> <p>1:1 Removal of TiCl<sub>4</sub> 2:1 Removal of TiCl<sub>4</sub></p> </div> <div data-bbox="695 730 1008 1066"> <p>Salt Formation</p>  <p>1:1 Removal of TiCl<sub>4</sub> 2:1 Removal of TiCl<sub>4</sub></p> </div> </div>	<p>Storey and Donnalley (2000) [28]</p>
<p><b><u>TiCl<sub>4</sub> Initiation:</u></b></p> 	<p>Paulo et al. (2000) [39]</p>



Proposed Mechanistic Scheme	Reference
Table 1-7 (continued)	
<p><b><u>Photo-initiation of isobutylene polymerization with Lewis acids</u></b></p>  <p style="text-align: center;">I</p>	<p>Marek et al. (1976) [12]</p>
<p><b><u>Initiation of the polymerization initiated by AlBr<sub>3</sub> in the presence of some Friedel-Crafts halogenides (TiCl<sub>4</sub>, TiBr<sub>4</sub>, and SnCl<sub>4</sub>)</u></b></p> $A + T \rightleftharpoons A^- T^+ \xrightarrow{M} T - M^+ A^-$ <p>where A is AlBr<sub>3</sub>, T is TiCl<sub>4</sub>, TiBr<sub>4</sub>, or SnCl<sub>4</sub>, and M is monomer</p>	<p>Marek and Chmelir (1968) [9]</p>
<p><b><u>Carbocationic polymerization of isobutylene using tertiary chloride with a Lewis acid:</u></b></p> 	<p>Roth and Mayr (1996) [15]</p>

Proposed Mechanistic Scheme	Reference
Table 1-7 (continued)	
<p><b><u>Initiating schemes of diisobutylene hydrochloride or triisobutylene hydrochloride in the presence of BCl<sub>3</sub> and benzyltriethylammonium tetrachloroborate</u></b></p> <p style="text-align: center;"><b>Scheme 1</b></p> <div><div><p>1</p></div><div><math>\xrightarrow[\text{CH}_2\text{Cl}_2, -78^\circ\text{C}]{\text{TEBA, BCl}_3}</math></div><div><p>2</p></div><div>+</div><div><p>n = 1    3</p></div><div>+</div><div><p>n = 2    4</p></div><div>+</div><div><p>n = 3    5</p></div><div>etc.</div></div> <div><div><p>2</p></div><div><math>\xrightarrow[\text{CH}_2\text{Cl}_2, -78^\circ\text{C}]{\text{TEBA, BCl}_3}</math></div><div><p>3</p></div><div>+</div><div>etc.</div></div> <p style="text-align: center;"><b>Scheme 2</b></p> <div><div><p>n = 1    2</p></div><div><p>n = 2    3</p></div><div><p>n = 3    4</p></div><div><math>\xrightarrow{\Delta T}</math></div><div><p>n = 1    2a</p></div><div><p>n = 2    3a</p></div><div><p>n = 3    4a</p></div><div>+</div><div><p>n = 1    2b</p></div><div><p>n = 2    3b</p></div><div><p>n = 3    4b</p></div><div>side product</div><div>main product</div></div>	Roth et al. (1997) [37]

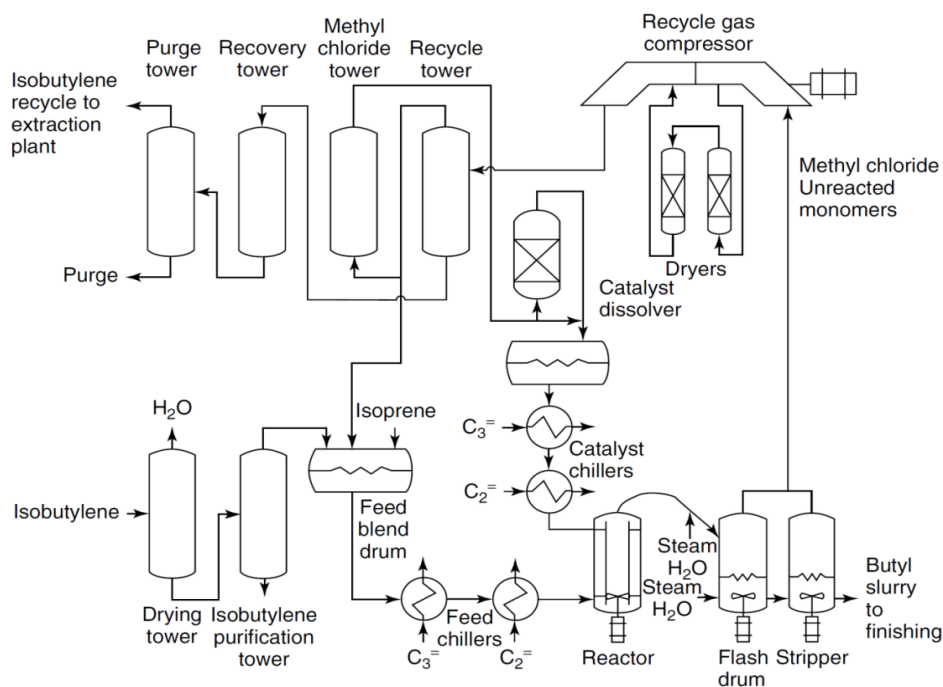
## 1.5 COMMERCIAL ISOBUTYLENE POLYMERIZATION PROCESSES

Most of the isobutyl polymers are commercially produced by copolymerization of isobutylene and isoprene in the presence of methylchloride ( $\text{CH}_2\text{Cl}_2$ ) as a solvent and an initiator consisting of a Lewis Acid and an alkyl halide. The Lewis acid used in many of the commercial butyl rubber plants is aluminum chloride, which is a low-cost solid soluble in methylchloride. Aluminum alkyls solutions are now becoming more popular because they simplify the initiator preparation and have been shown to increase the monomer conversion. The manufacture of high molecular weight polyisobutylene (PIB) requires a complex process consisting of feed purification, feed blending, polymerization, slurry stripping, and finishing.

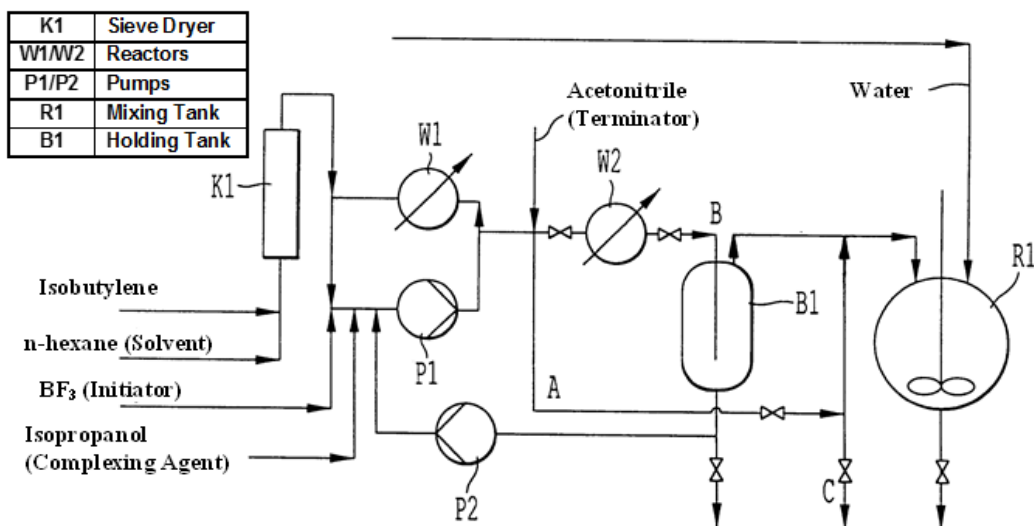
Figure 1-4 shows a schematic diagram representing the major units in a PIB plant. An alternative process, developed in Russia, uses a  $\text{C}_5\text{--C}_7$  hydrocarbon as a solvent and an aluminum alkyl halide as an initiator; and the polymerization is conducted in scraped surface reactors at  $-90$  to  $-50$  °C [19, 21, 23, 28, 29, 42, 45]. The solution process avoids the use of methylchloride, which is an advantage when producing high molecular weight PIBs. However, the energy costs of this process are greater than those of the slurry process because of the higher viscosity of the polymer solution.

Figure 1-5 shows the process for preparing low molecular weight, highly reactive PIBs developed by BASF. The process is carried out in the liquid-phase of isobutene or in hydrocarbon streams comprising isobutene, with the aid of a boron trifluoride complex initiator operating at  $-40$  to  $20$  °C and at pressures from 1 to 20 bar. The polymerization is carried out until the residual isobutene content of the reaction mixture is less than 2% by weight. Moreover, the boron trifluoride complex initiator, which is obtained in the form of dispersed droplets or coherent phase, is subsequently enriched and recycled back to the polymerization unit. This

process is claimed to produce low molecular weight, highly reactive polyisobutylene having an average molecular weight from 500 to 5000 g/mol and a terminal double bond content of more than 80 mol % [8].

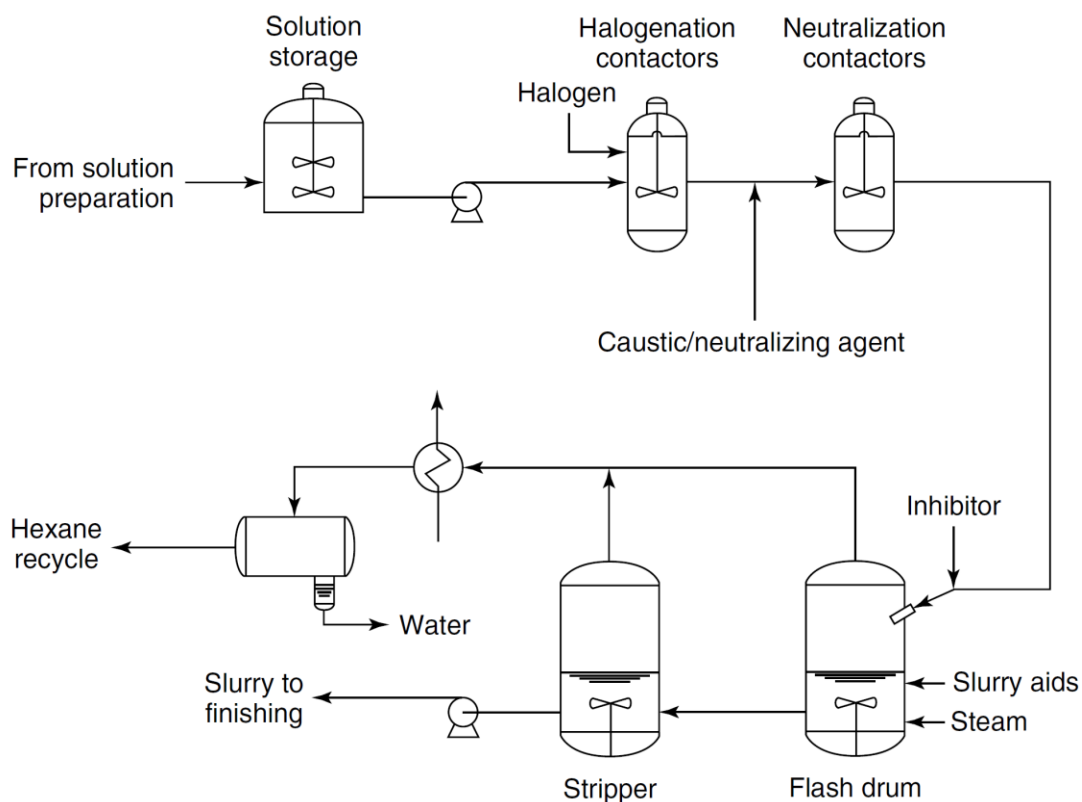


**Figure 1-4.** Schematic of the high molecular weight (butyl rubber) IB polymerization process [3, 5]



**Figure 1-5.** Schematic of the BASF low molecular weight IB polymerization process [8]

The manufacture of halopolyisobutylenes, such as bromobutyl, chlorobutyl, and exxpro [bromopoly(isobutylene-co-p-methylstyrene)] requires a second chemical reaction, which is the halogenation of the polymer backbone. This can be achieved in two ways: (1) the finished polymer produced in the butyl plant can be dissolved in a hydrocarbon solvent, such as hexane or pentane; and (2) a solvent replacement process can be used to dissolve the polymer from the slurry leaving the reactor. A schematic flow diagram of the halogenation process is shown in Figure 1-6.



**Figure 1-6.** Schematic of the halogenation process [3, 5]

### 1.5.1 Monomer purification

In order to produce high molecular weight polymers with high isobutylene conversion and a reasonable reactor service factor, the feed must be pure and dry. The process has to start with high quality isobutylene (> 99%), which must be dried, and other olefins, e.g., butene-1, butene-2, propene, and oxygenated hydrocarbons, such as dimethylether and methanol, have to be removed. A number of commercial processes are available for producing the required high purity isobutylene. An extraction process based on sulfuric acid has been developed by several companies and is being used extensively [46]. Significant quantities of isobutylene are also produced by dehydration of tert-butyl alcohol. The highest purity isobutylene is produced by MTBE (methyl-t-butyl ether [1634-04-4]) decomposition plants. This process starts with the selective reaction of dilute isobutylene in a C<sub>4</sub> stream with methanol over an acid ion-exchange resin, e.g., Amberlyst 15, to form MTBE. This ether is used mainly as a high octane blending component for low lead gasoline. Catalytic decomposition at 170-200 °C and 600 kPa (5.9 atm) over a fixed-bed of acid catalyst, e.g., SiO<sub>2</sub>Al<sub>2</sub>O<sub>3</sub> or Amberlyst 15, produces high purity isobutylene. The isobutylene is then dried by azeotropic distillation and purified in a super-fractionating distillation column to reduce the butenes to < 1000 ppm. It is important to note that if water is not removed, it will cause icing in the feed chillers, leading to a poor reactor service factor. The purified isobutylene is then blended with a recycled methylchloride stream containing a low level of isobutylene (~5%). Finally, the co-monomer, isoprene or p-methylstyrene, is added. In this blending process, the control of the ratio of the co-monomer to the isobutylene is very important. This is because it has a significant impact on the composition

of the polymer produced, the monomer conversion, and the stability of the reactor operation. For these reasons, a combination of both an analyzer and a mass balance control are often used to maintain the composition of the feed blend. The feed blend contains 20-40 wt% of isobutylene and 0.4-1.4 wt% of isoprene or 1-2 wt% of p-methylstyrene, depending on the grade of butyl rubber to be produced; and the remainder is methyl chloride.

### **1.5.2 Polymerization**

An initiator solution is produced by passing pure methylchloride through packed beds of granular aluminum chloride at 45 °C. The concentrated solution formed is diluted with additional methylchloride to which an initiator activator is added and the solution is later stored. Before entering the reactor, the feed blend and initiator solutions are chilled to -100 to -90 °C in a series of heat exchangers. The cold feed and initiator are introduced continuously into the reactor including a central vertical draft tube surrounded by concentric rows of cooling tubes. The reactor is constructed with 3.5% or 9 wt% nickel steel, or alloys, which have adequate impact strength at the low temperature of the polymerization reaction. The production of high molecular weight butyl requires a polymerization temperature below -90 °C and the reaction is exothermic, generating 0.82 MJ/kg (350 Btu/lb) of heat. This requires a two-stage refrigeration system which uses boiling propylene or propane and ethylene as refrigerants. In some plants ammonia is used in the first stage of the refrigeration process.

The reactor is the main unit of all butyl plant and the operation of the other units of the plant is dictated by the reactor. In the reactor, polymer chains are produced by the initiator and propagate in solution. The chain propagation occurs in microseconds, but the overall reaction rate is controlled by the slower initiation sequence. As individual polymer, formed molecules

precipitate to produce a fine milky slurry of submicron-sized particles. These particles grow in the reactor by agglomeration.

The molecular weight of the polymer produced is set by the ratio of the chain-making to chain-terminating processes. In commercial plants, the molecular weight and composition of the polymer formed are controlled by the concentration of the monomer in the reactor liquid-phase and the amount of the terminating or transfer species present to interrupt the chain growth. The slurry composition depends on the monomer content of the feed stream and the extent of the monomer conversion. In practice, the flow rate of the monomer and initiator to the reactor are the principal operating variables, where their residence time is often in the range 30-60 min. The original reactor design, known as the draft tube reactor, has been used commercially since the initial development of butyl in the 1940's. An improved design, in which the draft tube is replaced by additional tubes and the circulation pump is redesigned, has recently been proposed [44]. In addition to these changes of the mechanical design of the reactor, improvements of the polymerization chemistry and solvent have been investigated in the last decade, such as the use of supercritical carbon dioxide and the aluminum alkyls.

## **1.6 EFFECT OF MIXING**

Polymer properties are significantly affected by the uneven distribution of some intermediate or transitional species, which make up the bulk of the polymers. Polymer size distribution can mainly be controlled through mixing strategies during the polymerization reaction. Cationic polymerization is typically sensitive to mixing [47]. In order to set up a proper model to mimic the real conditions, one must take mixing effects into consideration so that the derived polymer



properties (Conversion, Mn, PDI (Polydispersity Index)) do not deviate from the expectation. According to Tosun [47], however, one challenge in modeling the effects of mixing is related to the fact that the viscosity of the polymer steadily changes during the polymerization process, which requires the adjustment of the assumptions regarding the degree and homogeneity of the turbulence created, which governs the micro- and macro- mixing in the process. Moreover, incorporating detailed polymerization with a mixing model will result in a mathematical complexity.

Despite the difficulty of building a comprehensive model which combines reaction kinetics and mixing, extensive efforts have been made in the past decades to explain the interaction in these complex systems. Marini and Georgakis [48] developed a compartmental model to investigate the effect of imperfect mixing on the production of low density polyethylene (LDPE) in stirred tank reactors, by accounting for the effects of mixing limitations at the initiator feed point. Their model showed that imperfect mixing in the reactor leads to significant variations in the molecular weight distribution of the polymer.

Villermaux [49] developed a mixing model using segregated zones with bulk convection and mass diffusion across the zone interfaces in stirred tank reactors with the aim of highlighting the effects of micro- and macro- mixing scales on the reactor performance. Tosun [47] extended Villermaux's mixing model to the radical polymerization in a stirred tank reactor with 3 segregated zones, which include two feeding zones for the initiator and the monomer, and one cumulative zone, exchanging mass with the other two feeding zones. In these models, the Damkohler number ( $Da_M$ ) is used in order to describe the speeds of mixing and reaction. It is defined as a ratio of the characteristic mixing time constant ( $\tau_M$ ) to the reaction time constant ( $\tau_R$ ).

$$D_{aM} = \frac{\tau_M}{\tau_R} \quad (9)$$

In this equation,  $\tau_R$  is defined mathematically as the inverse of the kinetic rate constant as given in Equation (10) for an  $n^{\text{th}}$  order reaction. Thus, for a first order reaction ( $n = 1$ ),  $\tau_R$  is a fixed value.

$$\tau_R = \frac{1}{kC^{n-1}} \quad (10)$$

Also,  $\tau_M$  is defined as a local mixing time constant, which counted from the initial contact of the reactants molecules until the homogenous presence at micro-level. From industrial application perspective,  $\tau_M$  is referred to as the blend time, which is the time required to achieve a certain degree of homogeneity, defined at any a given time  $t$  as:

$$M(t) = \frac{C_o - C(t)}{C_o - C_\infty} \quad (11)$$

Where  $C_\infty$  is the concentration of a tracer after an infinite period of time.

A standard target homogeneity of 95% is typically considered sufficient for many industrial applications [50]. An alternative method to calculate  $\tau_M$  at 99% homogeneity, which also accounts for the geometric characteristics of the mixing vessel and impeller is Equation (12), proposed Fasano and Penney [51].

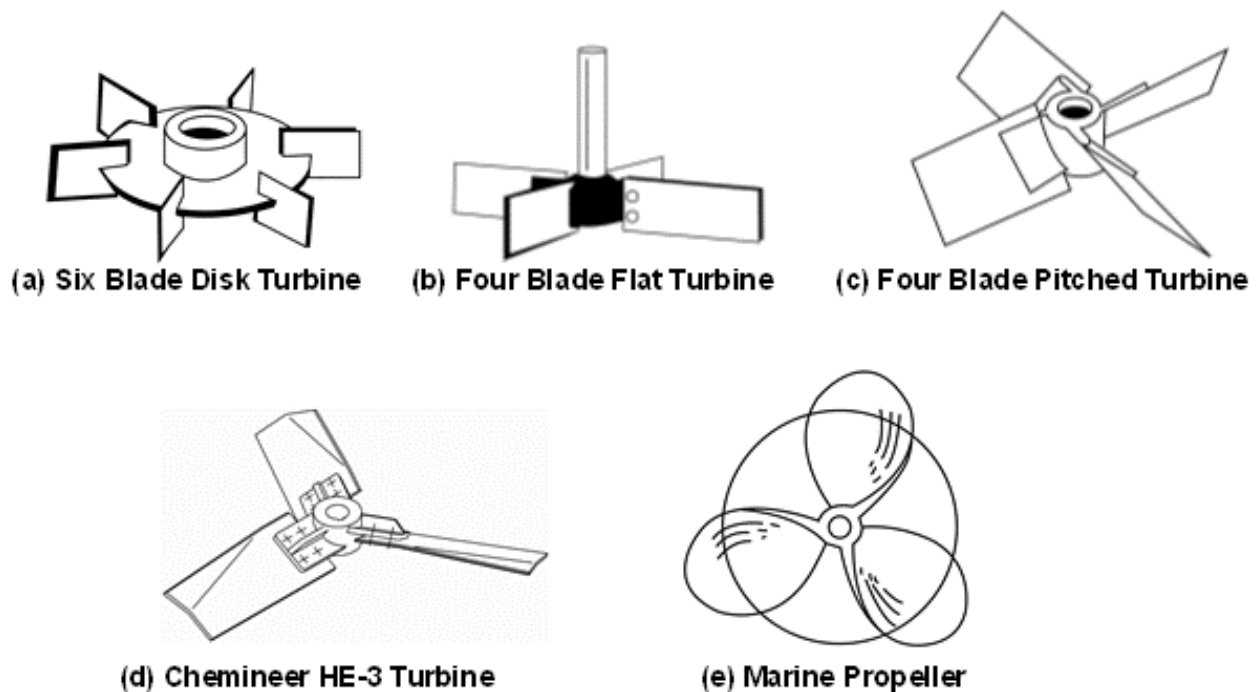
$$N = \frac{\alpha}{\tau_M} \left( \frac{D_r}{D_{imp}} \right)^\beta \left( \frac{H_r}{D_r} \right)^{0.5} \quad (12)$$

In this equation,  $N$  is the impeller speed in revolution per second (rps),  $D_{imp}$  and  $D_r$  are the impeller and reactor diameters, respectively, and  $H_r$  is the fluid height inside the reactor. Also,  $\alpha$

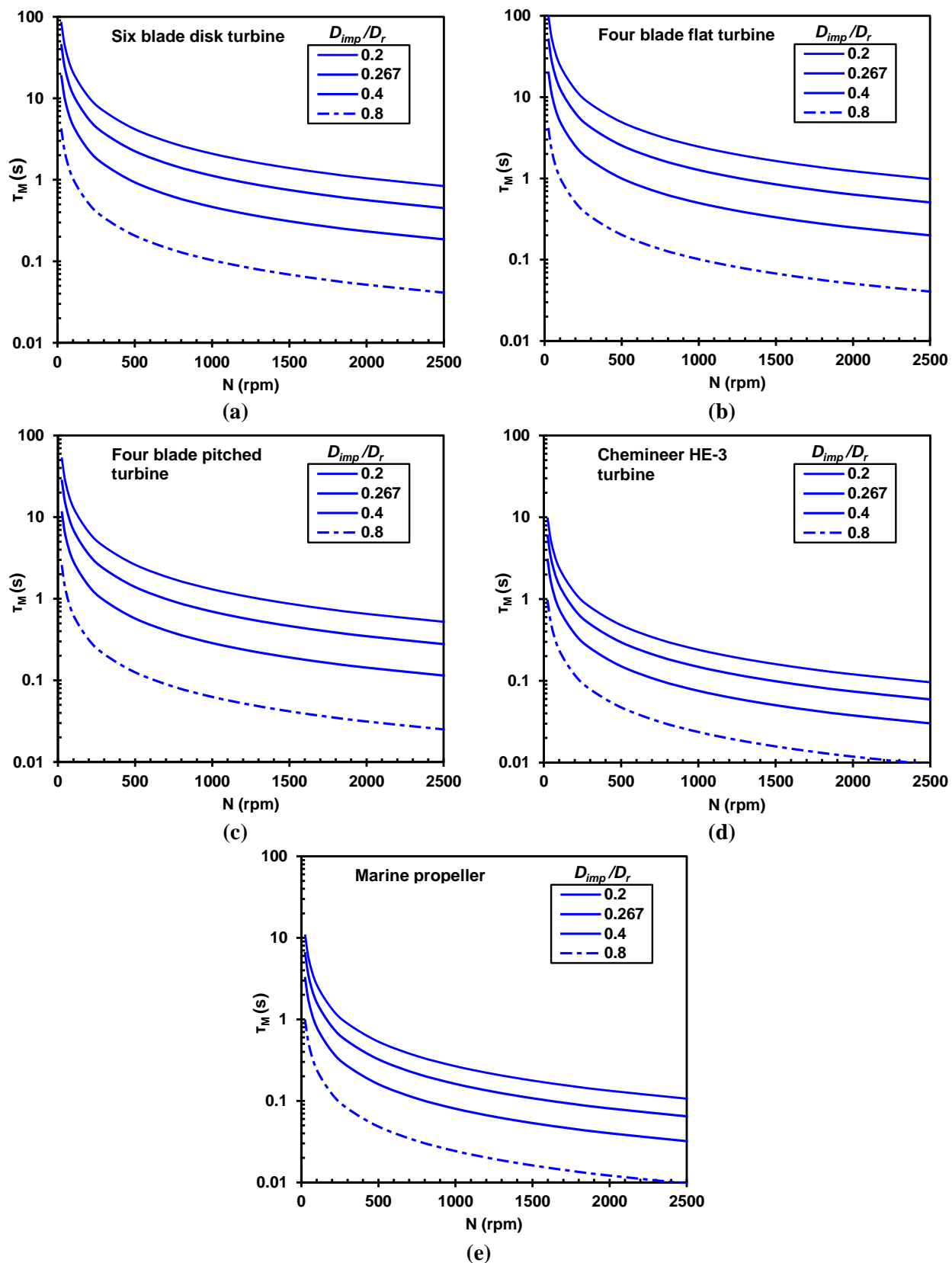
and  $\beta$  are empirical coefficients, which are specific for each impeller type, as given in Table 1-8. The impeller types of interest are shown in Figure 1-7. Also, Figure 1-8 illustrates the effect of mixing speed on the mixing time constant ( $\tau_M$ ) calculated using Equation (12) for the different impellers types and sizes ( $D_{imp}/D_r$ ) at  $H_r/D_r = 1$ .

**Table 1-8.** Empirical coefficients for Equation (12) for different impeller types [51]

<b>Impeller type</b>	<b><math>\alpha</math></b>	<b><math>\beta</math></b>
Six blade disk turbine	1.06	2.17
Four blade flat turbine	1.01	2.30
Four blade pitched turbine	0.641	2.19
Chemineer HE-3 turbine	0.272	1.67
Marine propeller	0.274	1.73



**Figure 1-7.** Schematic of the different impeller types shown in Table 1-8



**Figure 1-8.** Effect of mixing speed on the mixing time constant for different impellers at  $H_r/D_r = 1$

It should be noted that in Equation (10), if the mixing time constant ( $\tau_M$ ) is much greater than the reaction time constant ( $\tau_R$ ), i.e., at high  $Da_M$  value, the reactants molecules have limited contact time due to the poor mixing condition. Thus the apparent reaction kinetic rate is strongly affected by the mixing rate.

### **1.7 NUMBER AVERAGE MOLECULAR WEIGHT ( $M_N$ ), WEIGHT AVERAGE MOLECULAR WEIGHT ( $M_w$ ), AND POLYDISPERSITY INDEX (PDI)**

The most commonly used definitions to describe polymer molecular weight are: Number average molecular weight  $M_n$ , and weight average molecular weight  $M_w$ . The number average molecular weight is defined as the arithmetic mean of the molecular weight distribution of a polymer:

$$M_n = \frac{\sum N_i M_i}{\sum N_i} \quad (13)$$

Where  $M_i$  is the molecular weight of polymer  $i$  chain and  $N_i$  is the number of polymers with molecular weight  $M_i$ . In some cases,  $M_n$  could be predicted by the polymerization reaction mechanism, but in most circumstances it is measured through experimental methods such as end-group analysis, ebullioscopy, osmometry and cryoscopy [3].

The weight average molecular weight ( $M_w$ ) denotes ‘how much’ polymer  $i$  contribute to the total average molecular weight as defined in Equation (14). A growing  $M_w$  can reliably tell the general propagation of most polymers, whereas same phenomenon cannot represent the overall behavior of a polymer when its  $M_n$  increases.

$$M_w = \frac{\sum N_i M_i^2}{\sum N_i M_i} \quad (14)$$

Molecular weight distribution is also called polydispersity index (PDI). It is defined as the ratio of the weight average to the number average molecular weight.

$$PDI = M_w/M_n \quad (15)$$

In the ideal case where  $PDI = 1$ , the polymer chains are monodispersed. As the polymer distribution broadens, PDI increases, and therefore PDI is used to measure the broadness of a polymer distribution.

It should be mentioned that polydispersity in cationic polymerization varies considerably due to the competitive rate of initiation, termination and chain transfer reactions. Typically, a rapid initiation usually narrows PDI, similarly, inhibited termination and chain transfer reactions can also effectively drive PDI closer to the unity [3]. In living cationic polymerization, where chain breaking reactions are almost nonexistent, the polydispersity is ideally one.

## 1.8 MODELING ISOBUTYLENE POLYMERIZATION USING ASPENPLUS

Basha et al. [52] developed a kinetic model in AspenPlus v. 7.2 for the IBP process carried out in a size of 4.5 m<sup>3</sup> using Aluminum Chloride (AlCl<sub>3</sub>) as initiator in hexane as a solvent. The feed to the reactor was set to 1000 kg/hr (95% isobutylene monomer and 5% AlCl<sub>3</sub> initiator). The reactions were assumed to follow the cationic polymerization and were set at - 80 °C and 1 atm. Since there were no available literature data for AlCl<sub>3</sub>, the model predictions could not be validated. However, the model was used to predict the experimental data by Zhao et al. [53, 54],

obtained for IBP using a different initiator ( $\text{TiCl}_4$ ) at different temperature -  $95\text{ }^\circ\text{C}$  in a 2-gallon pilot plant reactor. Details of this model can be found in Appendix A.

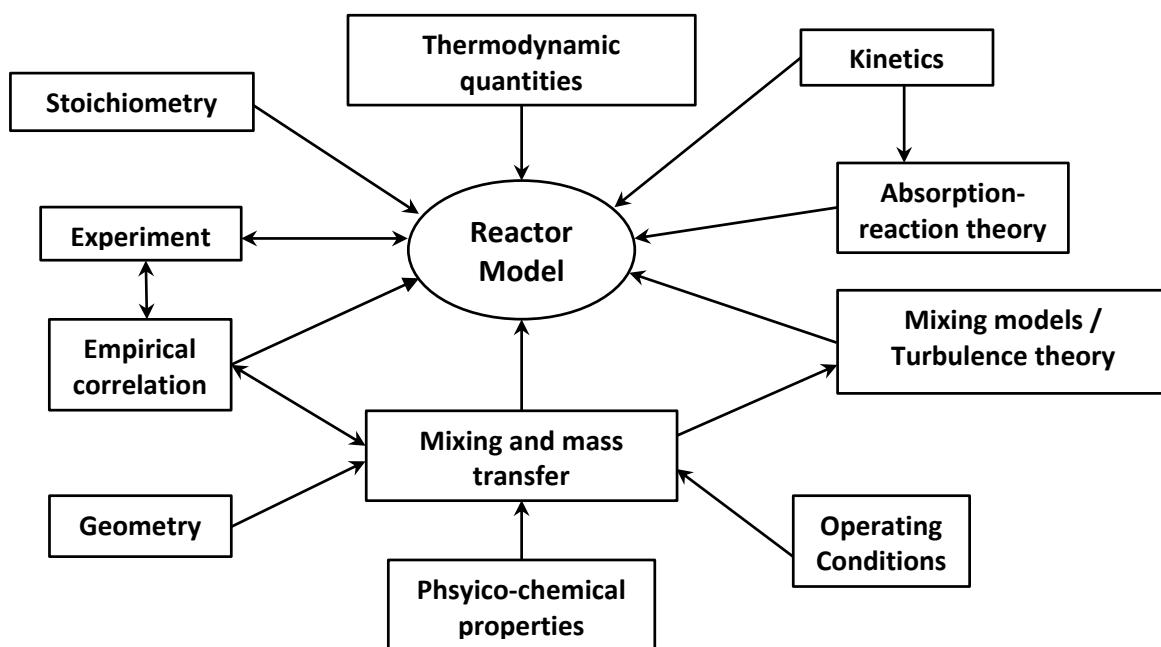
The problems associated with this Aspen model are (1) it is over simplified and limited only to the  $\text{AlCl}_3$  initiator; (2) the reaction rate constants for each step could not be found in the literature and therefore they were estimated; (3) validation of the model predictions was impossible due to the lack of experimental data; and (4) the effect of mixing was not included. Thus, there is a great need to develop a comprehensive model capable of predicting the performance of the isobutylene polymerization process under actual industrial conditions.

## **2.0 RESEARCH OBJECTIVE**

The preceding section demonstrated that reaction kinetics and mechanisms of the isobutylene polymerization are widely different/complex and the process could be carried out in agitated reactors under different operating conditions. The overall performance of these reactors is governed by the reaction kinetics, which are independent of the reactor type and size, and by the mixing and transport parameters, which are strongly dependent, not only on the reactor type and size, but also on the operating conditions.

The overall objective of this study is to develop a comprehensive reactor model to predict the performance of the isobutylene polymerization process in agitated vessels, which can be easily fine-tuned and ultimately used to optimize process. The model should account for the isobutylene polymerization reaction kinetics as well as mixing characteristics. The basic reactor model equations are material balance for all phases, energy balance and momentum balance. These model equations include many parameters, which are related to the reaction kinetics, mixing, heat and mass transfer. These parameters are required in order to solve the model equations. The interplay among these parameters shows that they are dependent on the reaction and mixing time scales which are directly related to the operating conditions as well as reactor type and size as illustrated in Figure 2-1.





**Figure 2-1.** Interplay among the equation parameters required for the reactor model

In order to achieve this objective, the following two tasks were carried out:

**Task 1:** A kinetics-based model for the isobutylene polymerization process in agitated reactors was developed in Matlab. The model incorporated four main reaction steps, initiation, propagation, chain transfer and termination. A sensitivity analysis investigating the effect of different kinetic reaction rate constants on three main performance metrics, monomer conversion, number average molecular weight and polydispersity index, was performed.

**Task 2:** The effect of mixing was incorporated into the model and implemented into Matlab. The model was subsequently used to investigate the effects of mixing on the isobutylene polymerization process performance.

### 3.0 RESEARCH APPROACH

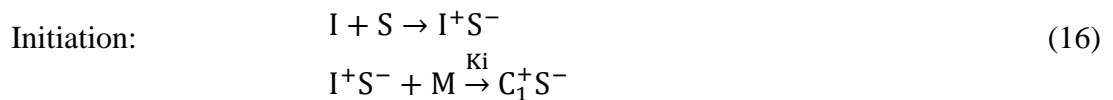
#### 3.1 KINETIC MODEL AND NOTATIONS

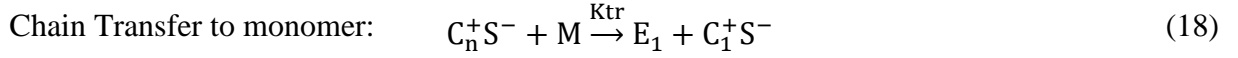
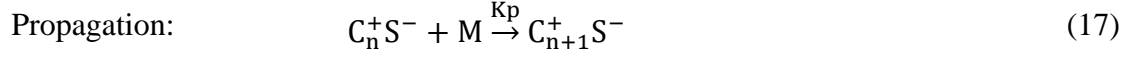
In this study, the reactor model developed was based on the reactive system by Vasilenko et al. [44, 55] for the cationic polymerization of isobutylene using  $AlCl_3/H_2O$  as initiator. The notations used in the model to represent the different species involved are provided in Table 3-1.

**Table 3-1.** Notations used in the model

Notation	Species
[I]: Concentration of initiator	$AlCl_3$
[S]: Concentration of Solvent	<i>Hexane</i>
[M]: Concentration of monomer	$(CH_3)_2C = CH_2$
[A]: Concentration of active unit	$H[CH_2C(CH_3)_2]_nCH_2C^+(CH_3)_2$
[C]: Concentration of structural unit	$-H[CH_2C(CH_3)_2]_nCH_2C^+(CH_3)_2 -$
[E1]: Concentration of polymer with chain end E1 (chain transfer to monomer)	$H[CH_2C(CH_3)_2]_nCH_2C(CH_3) = CH_2$ Or $H[CH_2C(CH_3)_2]_nCH = C(CH_3)_2$
[E2]: Concentration of polymer with chain end E2 (chain termination)	$H[CH_2C(CH_3)_2]_nCH_2C(CH_3)ClCH_2$

In the model, the reaction steps used are:





### 3.2 ASSUMPTIONS

The following assumptions were made:

1. Uniform reaction activity: The reaction activity for all species begins at the same time, without any reaction starting earlier or dominating within any time period. This allows all of the growing chains with different lengths to actively participate in the process. The only sign which can distinguish polymers from others is the end group produced through chain transfer or termination.
2. Linear chain: Polymer chains or actively propagating monomers/initiators with any end group are assumed to have straight structure, without any branching. The linear chain assumption enables the mass transfer model to accurately estimate the molecular weight based on the reaction progress regardless of the disruptive chain growth with other shapes, which could occur in actual cases.
3. Equal chain growth: The length of polymer chain with various end group is identical in all cases. This assumption is based on the derivation of  $M_n$ , which is dependent on the concentration of species  $[A]$ ,  $[C]$ ,  $[E_1]$ , and  $[E_2]$ .

4. Constant reaction rate for every propagating polymer chain length. Although in cationic polymerization, this has not been reported, it is necessary to assume reaction rates would by no means vary when other peripheral conditions change. For example, propagating chains with different length should have the same reaction rate constant; and all the polymerization reaction rates constants are not impacted by a temperature change or a variation of concentration.
5. Irreversible reactions: no reaction is reversible so that the consumed reactants and produced products can be accumulated and accounted for independently of the process.

### 3.3 MASS BALANCE

The mass balance equations for each reaction step are given in Table 3-2. The transient concentration of each species can be determined, and a kinetic sensitivity analysis is conducted by varying the kinetic constants.

**Table 3-2.** Mass balance equations for the different reaction steps

Step	Mass Balance Equation
Initiation	$\frac{d[M]}{dt} = -k_i[I][M] - k_p[A][M] - k_{tr}[A][M]$ $\frac{d[I]}{dt} = -k_i[I][M]$
Propagation	$\frac{d[A]}{dt} = k_i[I][M] - k_t[A]; \quad \frac{d[C]}{dt} = k_p[A][M]$
Chain Transfer	$\frac{d[E1]}{dt} = k_{tr}[A][M]$

Table 3-2 (continued)	
Termination	$\frac{d[E_2]}{dt} = k_t[A]$

The number average molecular weight ( $M_n$ ) was calculated using the correlation by Chen et al. [56] for the linear chain assumption of chain analysis according to Equation (20).

$$M_n = \frac{W}{n} = \frac{\sum_i n_i M_i}{\sum_i n_i} = 2 \times \left( \frac{[C]M_{wC} + \sum_i [E_i]M_{wEi} + [A]M_{wA}}{[A] + \sum_i [E_i]} \right) \quad (20)$$

The polydispersity index (PDI) was calculated using the correlation by Puskas et al. [18] given in Equations (21) and (22).

$$PDI = \frac{DP_w}{DP_n} = 1 + \frac{1}{\beta} \left[ \frac{2}{X} - 1 \right] \quad (21)$$

$$\beta = \frac{k_t}{k_p[I]_0} \quad (22)$$

Where X is the conversion, defined as follows:

$$X = 1 - \frac{M}{M_T} \quad (23)$$

### 3.4 MIXING INCORPORATION INTO THE MODEL

During isobutylene polymerization, the reaction and the mixing rates have competing effects on the overall yield. In the case of a reaction containing two reactants, the chemical reaction starts when the two reactants are brought in contact at the molecular level, until one or both of them

are completely consumed and then the reaction stops. In the case where the mixing time constant is much smaller than the reaction time constant, the reaction is slow and the species are sufficiently mixed such that the effect of mixing on the reaction can be safely ignored. However, in the case of cationic polymerization, the reaction time constant is much smaller than the mixing time constant, the reaction is intrinsically rapid and the species are not sufficiently mixed such that the effect of mixing on the reaction cannot be ignored. In other words, the overall performance of polymer yield is strongly dependent on the mixing.

In small-scale applications, mixing effect is insignificant, since small amounts of reactants are able to achieve ideal mixing within significantly small time constant, so the measured reaction rate is close to the real rate. In industrial-scale applications, however, mixing effect is significant since poor mixing, especially during reaction early stages, prolongs the time for the molecules to be brought into contact for the reaction to proceed.

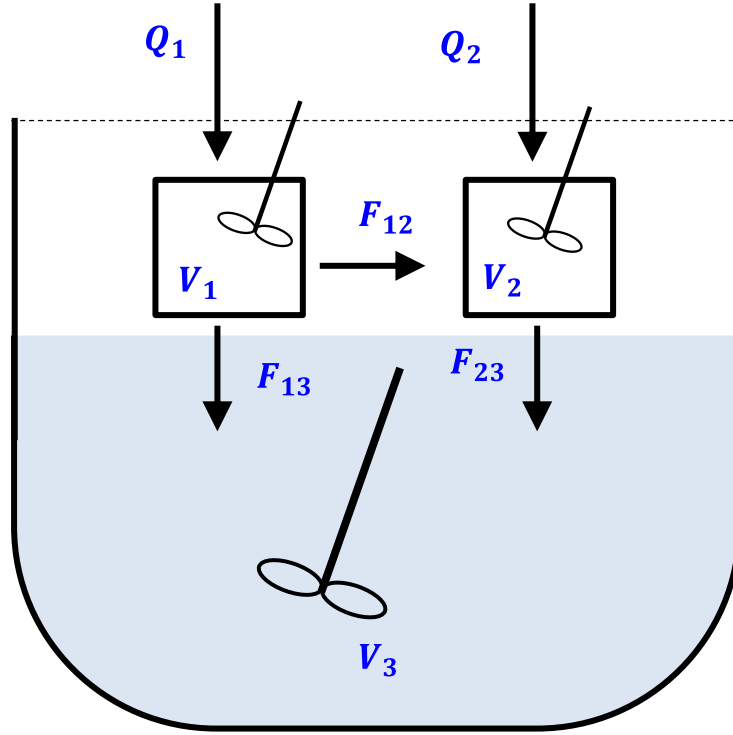
### **3.4.1 The Theory of Segregation**

This theory was initially proposed by Baldyga and Bourne [57-59] and further developed by Villiermaux [49] to provide a more accurate representation of the turbulent mixing and chemical reaction. The theory is based on defining the difference between the purest substance and its surrounding fluid concentration [47], based on three scales: (1) macro-mixing; (2) meso-mixing; and (3) micro-mixing. Macro-mixing scale refers to the distribution of large ‘blobs’ of different species over the reaction zone and is typically prevail during the early stages of mixing. Meso-mixing scale refers to the movement and breakup of these ‘blobs’ due to inertial forces, resulting in independent movement of the species and the development of a uniform distribution of the species within the reactor. Micro-mixing scale refers to the size reduction of these ‘blobs’ due to

velocity gradients (such as near the tip of the impeller) which results in higher interfacial area for contact.

This theory was further developed by Tosun [47] when modeling a semi-batch reactor with three major segregation zones for free radical polymerization. In his model, a segregating zone was introduced to mimic the condition that channels of mass transfer among each zone are governed by dimensionless mixing time scale ( $\theta_M$ ), which represents the lifetime of various turbulent eddies (macro-mixing, meso-mixing, and micro-mixing); and the dimensionless molecular diffusion time scale ( $\theta_X$ ). Also, the segregated feed zone model was built on the semi-batch stirred reactor with two separated inlet streams which contain isobutylene monomer and initiator.

In this study, our mixing model is composed of three segregated zones as shown in Figure 10. Zone 1 is the initiator, Zone 2 is the monomer and Zone 3 is the polymer. The initiator with an initial concentration  $C_{0j1}$  is fed into zone  $V_1$  at a flow rate  $Q_1$ . Likewise, the monomer with the concentration  $C_{0j2}$  is fed into zone  $V_2$  at a flow rate  $Q_2$ .  $V_1$  and  $V_2$  exchange mass with the larger zone  $V_3$  through convection, which is physically done by reactor agitator.



**Figure 3-1.** Scheme of mixing model with segregation zones

The bulk flow movement inside the reactor will determine the mixing time scale ( $t_M$ ), which refers to the time required to achieve mixing homogeneity starting from the point of complete segregation, and expresses the combined effects of macro- and micro-mixing.  $t_M$  was also reported to be proportional to the internal mean eddy life time [49]. Thus, the segregation model incorporates the volume balance and mass balance to predict the yield of the produced polymers when accounting for the influence of mixing.

The volume balance Equations (24) to (28) are used in this model:

$$\frac{dV_1}{dt} = Q_1 - \frac{V_1}{t_M} \quad (24)$$

$$\frac{dV_2}{dt} = Q_2 - \frac{V_2}{t_M} \quad (25)$$



$$\frac{dV_3}{dt} = \frac{V_1 + V_2}{t_M} \quad (26)$$

$$V_T = V_1 + V_2 + V_3 \quad (27)$$

$$\frac{dV_T}{dt} = Q_1 + Q_2 \quad (28)$$

$V_T$  is the total volume of fluid in the reactor.

The mass balance Equations (29) to (32) for the  $j^{\text{th}}$  species in each zone and in the whole reactor are written as:

$$\text{Zone 1: } \frac{d(V_1 C_{j1})}{dt} = R_{j1} V_1 + Q_1 C_{j1}^0 - F_{j13} - F_{j12} \quad (29)$$

$$\text{Zone 2: } \frac{d(V_2 C_{j2})}{dt} = R_{j2} V_2 + Q_2 C_{j2}^0 - F_{j23} + F_{j12} \quad (30)$$

$$\text{Zone 3: } \frac{d(V_3 C_{j3})}{dt} = R_{j3} V_3 + F_{j13} + F_{j23} \quad (31)$$

$$\frac{d(V_T C_j)}{dt} = R_j V_T + Q_1 C_{j1}^0 + Q_2 C_{j2}^0 \quad (32)$$

$R_j$  represents the kinetic reaction rate of each species, as given in Equations (33) to (38):

$$R_{M_j} = -ki[I]_j[M]_j - kp[A]_j[M]_j - ktr[A]_j[M]_j \quad (33)$$

$$R_{I_j} = -ki[I]_j[M]_j \quad (34)$$

$$R_{A_j} = ki[I]_j[M]_j - kt[A]_j \quad (35)$$

$$R_{C_j} = kp[A]_j[M]_j \quad (36)$$

$$R_{E1_j} = ktr[A]_j[M]_j \quad (37)$$

$$R_{E2_j} = kt[A]_j \quad (38)$$

It should be noted that the units of each of the reaction rate constants are different as follows:

$$\begin{aligned}
k_i &: [\text{mol}/\text{m}^3]^{-1}\text{s}^{-1} \\
k_p &: [\text{mol}/\text{m}^3]^{-1}\text{s}^{-1} \\
k_{tr} &: [\text{mol}/\text{m}^3]^{-1}\text{s}^{-1} \\
k_t &: \text{s}^{-1}
\end{aligned}$$

Also,  $F_j$  represents the mass transfer between the zones according to Equations (39) to (41).

$$F_{j13} = \frac{V_1 C_{j1}}{t_M} + \frac{V_1 (C_{j1} - C_{j3})}{t_{13}} \quad (39)$$

$$F_{j23} = \frac{V_2 C_{j2}}{t_M} + \frac{V_2 (C_{j2} - C_{j3})}{t_{23}} \quad (40)$$

$$F_{j12} = \frac{(V_1 + V_2)(C_{j1} - C_{j2})}{t_{12}} = 0 \quad (41)$$

In the above equations,  $t_{13}$ ,  $t_{23}$  and  $t_{12}$  (or  $t_x$  where  $x = 13, 23$  and  $12$ ) refer to the time related to mass diffusion across the interface, driven by the concentration gradient at the boundary of two segregated zones. Also,  $t_{13}$  and  $t_{23}$  are linked with the natural mass diffusion time, however  $t_{12}$  is considered to be infinite because the two feed zones 1 and 2 are almost completely segregated [57-59] and therefore this term is analogous to the mass diffusivity for each species.

In the case of ideal mixing, the mixing ( $t_M$ ) and diffusion time ( $t_x$ ) are close to zero, which means that mixing in the three zones reaches completion once the monomer and initiator enter the reactor. On the other hand, if  $t_M$  and  $t_x$  are infinite, it means that the zones are completely segregated and no reactions take place.

In our model, since the initiator dissociates readily in the solvent and the initiation step occurs instantaneously when compared with the propagation step, it is assumed that there is no mass exchange between Zones 1 and 2, and that the initiator and monomer are completely

mixed upon entering the reactor, therefore the term  $F_{j12}$  is set to zero in the Equation (41).

Equation (29) was rearranged to separate the variables and yield Equation (42).

$$\frac{d(V_1 C_{j1})}{dt} = V_1 \frac{dC_{j1}}{dt} + C_{j1} \frac{dV_1}{dt} \quad (42)$$

Subsequently the terms  $\frac{dV_1}{dt}$  and  $F_{j13}$  were replaced with Equations (24) and (39), respectively,

to give Equation (43).

$$(Q_1 - \frac{V_1}{t_M})C_{j1} + \frac{dC_{j1}}{dt}V_1 = R_{j1}V_1 + Q_1C_{j1}^o - \frac{V_1C_{j1}}{t_M} + \frac{V_1(C_{j1} - C_{j3})}{t_{13}} \quad (43)$$

Equation (43)(42) can be rearranged into the following:

$$\frac{dC_{j1}}{dt} = R_{j1} - \frac{C_{j1}}{t_{13}} + \frac{C_{j3}}{t_{13}} - \frac{C_{j1}Q_1}{V_1} + \frac{Q_1C_{j1}^o}{V_1} \quad (44)$$

Similarly, Equations (45) and (46) can be obtained for zones 2 and 3, respectively:

$$\frac{dC_{j2}}{dt} = R_{j2} - \frac{C_{j2}}{t_{23}} + \frac{C_{j3}}{t_{23}} - \frac{C_{j2}Q_2}{V_2} + \frac{Q_2C_{j2}^o}{V_2} \quad (45)$$

$$\frac{dC_{j3}}{dt} = R_{j3} + \frac{V_1C_{j1}}{V_3t_M} + \frac{V_1(C_{j1}-C_{j3})}{V_3t_{13}} + \frac{V_2C_{j2}}{V_3t_M} + \frac{V_2(C_{j2}-C_{j3})}{V_3t_{23}} - \frac{C_{j3}V_1}{V_3t_M} - \frac{C_{j3}V_2}{V_3t_M} \quad (46)$$

Every species involved in the equations is then listed in Table 3-3 below, where the  $j^{\text{th}}$  species is represented with a first number denoting the species and a second number denoting the zone. For instance,  $C_{12}$  indicate species 1 in zone 2.

**Table 3-3.** Species concentration variables in this model

<b>Species</b>	<b>Zone 1</b>	<b>Zone 2</b>	<b>Zone 3</b>
Initiator: [I]	C <sub>11</sub>	C <sub>12</sub>	C <sub>13</sub>
Monomer: [M]	C <sub>21</sub>	C <sub>22</sub>	C <sub>23</sub>
Active Monomer: [A]	C <sub>31</sub>	C <sub>32</sub>	C <sub>33</sub>
Polymer Chain: [C]	C <sub>41</sub>	C <sub>42</sub>	C <sub>43</sub>
Polymer undergoing chain transfer: [E1]	C <sub>51</sub>	C <sub>52</sub>	C <sub>53</sub>
Polymer undergoing chain termination: [E2]	C <sub>61</sub>	C <sub>62</sub>	C <sub>63</sub>
V	V <sub>1</sub>	V <sub>2</sub>	V <sub>3</sub>

### 3.5 NORMALIZATION OF THE MODEL EQUATIONS

Reference variables are introduced to normalize each variable appearing in the above equations, such that the numerically derived solutions would not be impacted by the units, but rather indicate the behavior of model variables. Three referencing values were introduced,  $T_0$ ,  $V_0$  and  $C_0$ , representing the time, volume and concentration, respectively.  $T_0$  represents the reaction half-life time, which is considered as the time when the concentration of the monomer [M] drops to half of  $[M]_0$ , and is represented using Equation (47).

$$T_0 = \frac{\ln\left(\frac{[M]_0}{[M]_{1/2}}\right)}{k_o} = \frac{\ln 2}{k_o} \quad (47)$$

Where  $k_0$  is the pseudo first order kinetic constant for the monomer consumption, which was approximated to be equal to the termination rate constant ( $k_t$ ) [60].

The reference concentration  $C_0$  is taken to be  $[M]_0$ , which is the concentration of the monomer feed stream. In addition,  $V_0$  is chosen as the initial volume of solvent in the reactor. Hence, all of the variables could be redefined as shown in Equations (47) to (53).

$$\hat{V} = V/V_0 = V/V_T(o) \quad (48)$$

$$\theta = t/T_o \quad (49)$$

$$\hat{Q} = T_o Q/V_0 \quad (50)$$

$$\hat{C}_j = C_j/C_o \quad (50)$$

$$\theta_M = t_M/T_o \quad (51)$$

$$\theta_X = t_X/T_o \quad (X = 13, 23) \quad (52)$$

$$\theta_{12} = t_{12}/T_o \quad (\text{infinite}) \quad (53)$$

Subsequently, the normalized volume balance and mass transfer equations can be rewritten as Equations (54) to (60).

$$\frac{d(\hat{V}_1 \hat{C}_{j1})}{d\theta} = \hat{R}_{j1} \hat{V}_1 + \hat{Q}_1 \hat{C}_{j1}^o - \hat{F}_{j13} - \hat{F}_{j12} \quad (54)$$

$$\frac{d(\hat{V}_2 \hat{C}_{j2})}{d\theta} = \hat{R}_{j2} \hat{V}_2 + \hat{Q}_2 \hat{C}_{j2}^o - \hat{F}_{j23} - \hat{F}_{j12} \quad (55)$$

$$\frac{d(\hat{V}_3 \hat{C}_{j3})}{d\theta} = \hat{R}_{j3} \hat{V}_3 + \hat{F}_{j13} + \hat{F}_{j23} \quad (56)$$

$$\frac{d(\hat{V}_T \hat{C}_j)}{d\theta} = \hat{R}_j \hat{V}_T + \hat{Q}_1 \hat{C}_{j1}^o + \hat{Q}_2 \hat{C}_{j2}^o \quad (57)$$

$$\hat{F}_{j13} = \frac{\hat{V}_1 \hat{C}_{j1}}{\theta_M} + \frac{\hat{V}_1 (\hat{C}_{j1} - \hat{C}_{j3})}{\theta_{13}} \quad (58)$$

$$\hat{F}_{j23} = \frac{\hat{V}_2 \hat{C}_{j2}}{\theta_M} + \frac{\hat{V}_2 (\hat{C}_{j2} - \hat{C}_{j3})}{\theta_{23}} \quad (59)$$

$$\hat{F}_{j12} = \frac{(\hat{V}_1 + \hat{V}_2)(\hat{C}_{j1} - \hat{C}_{j2})}{\theta_{12}} \approx 0 \quad (60)$$

Equations from (54) to (60) were solved numerically by Matlab using a fourth order Runge-Kutta method, represented using the ODE45 function [61, 62] in order to calculate the monomer conversion, number and weight average molecular weights, and polymer polydispersity index of the IBP process. The times frame set for ODE45 to solve the group of differential equations is denoted Tspan.

## **4.0 RESULTS AND DISCUSSIONS**

### **4.1 EFFECTS OF REACTION RATE CONSTANTS ON THE MODEL PREDICTIONS IN THE ABSENCE OF MIXING**

A sensitivity analysis was conducted to investigate the effect of kinetic rate constants for initiation, propagation, chain transfer and termination on the model prediction of the monomer conversion, number average molecular weight and the polydispersity index, was conducted. The simulation was based on only pure reaction kinetics, which was borrowed from the method of chain analysis [18, 39, 53, 63]. In this method, the macro-molecules with various chain lengths and structures can be simplified as polymers possessing several types of end groups. It is important to note that the effect of mixing was ignored in these sensitivity analysis calculations.

The following assumptions were made for the sensitivity analysis:

1. The average length of each polymer chain ( $M_n$ ) is composed of 50 monomers and 1 end group structure;
2. The reactor has a dimensionless volume of 30 and the two inlet streams having dimensionless flow rates were at 1 for each. These values were arbitrarily selected to allow for sufficient representation of the reactor performance.

3. The dimensionless batch time ( $\theta_B$ ) was set to 15, which was enough to complete all required calculations.

The values of the parameters set in Matlab for solving the differential equations are given in Table 4-1.

**Table 4-1.** Model parameters used in Matlab to investigate the effects of reaction rate constants

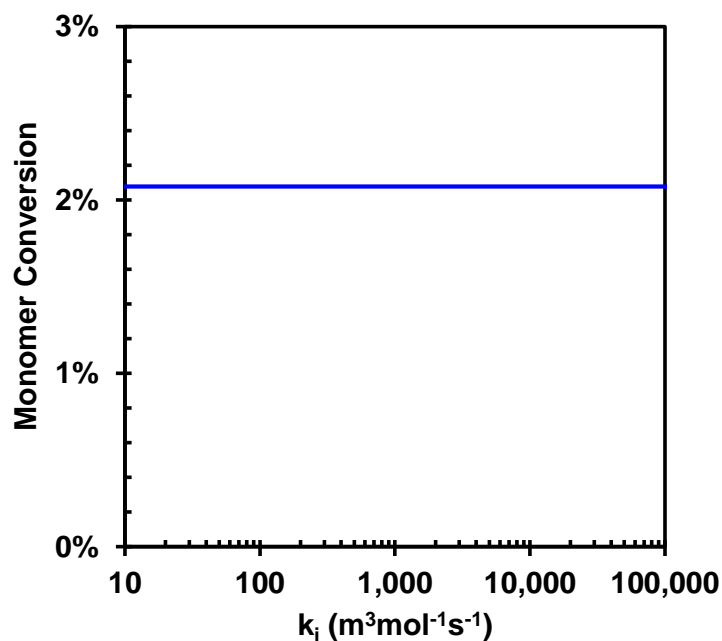
Parameter	Value	Comments
Tspan	[0 ,15]	Running time boundaries
Initial conditions	[1,0,0.01,0,0,0]	[[M],[A],[I],[E1],[C],[E2]]
$k_i$	10 to $10^5$ mol/m <sup>3</sup> ·s	Range investigated
$k_p$	10 to $10^5$ mol/m <sup>3</sup> ·s	Range investigated
$k_{tr}$	0.1 to $10^5$ mol/m <sup>3</sup> ·s	Range investigated
$k_t$	0.1 to $10^5$ s <sup>-1</sup>	Range investigated
Mw [C]	2750	50 monomeric units
Mw [E1]	55	End group
Mw [E2]	92	End group
Mw [A]	232	Active species
$\beta$	20	

As can be observed in this table, the Tspan set for ODE45 to solve the group of differential equations is set to 0-15. The monomer inlet concentration is set to 1 and the initiator concentration is set to 0.01, a ratio of 1000/1 in order to account for a wide range of experimental conditions. It should be noted that all the input and output data in the simulation are dimensionless.



#### 4.1.1 Effect of the initiation rate constant ( $k_i$ )

The effect of the initiation reaction rate constant on the monomer conversion, the number average molecular weight ( $M_n$ ) and polydispersity index (PDI) are shown in Figures 11, 12 and 13, respectively. As shown in these figures, the initiation rate constant ( $k_i$ ) has no effect on any of these parameters. This behavior is in agreement with other findings in the literature [7, 44, 55, 64] and can be attributed to the ionic dissociation of the initiator resulting in  $k_i$  values, which are significantly greater than those of the propagation and termination rate constants, leading to insignificant effects on the polymerization process. It should be noted that since the value of  $k_i$  has no effect on the intermediate products, it was decided to assign  $k_i$  a moderate rate suitable for reducing the calculation time and complexity [18, 47, 65, 66] and accordingly  $k_i$  was set to the same value as  $k_p$ .



**Figure 4-1.** Effect of  $k_i$  on Monomer Conversion

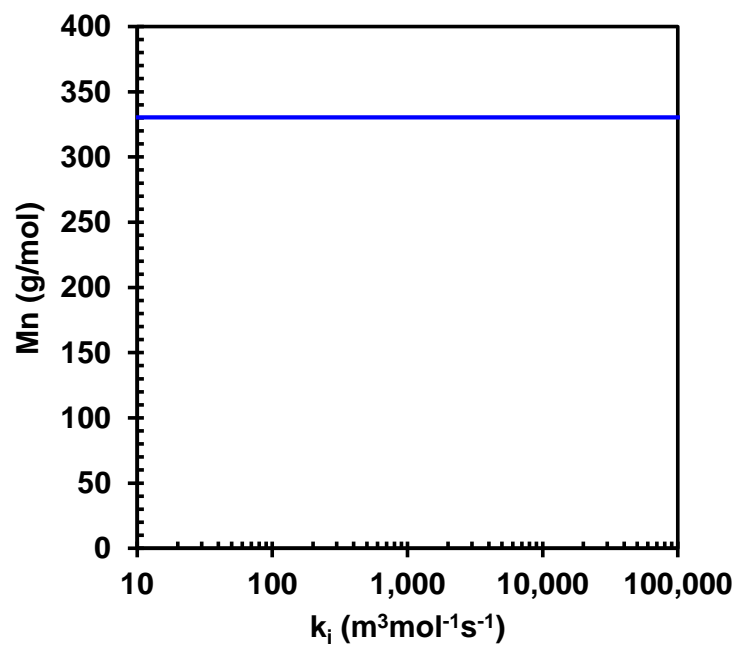


Figure 4-2. Effect of  $k_i$  on the Number Average Molecular Weight

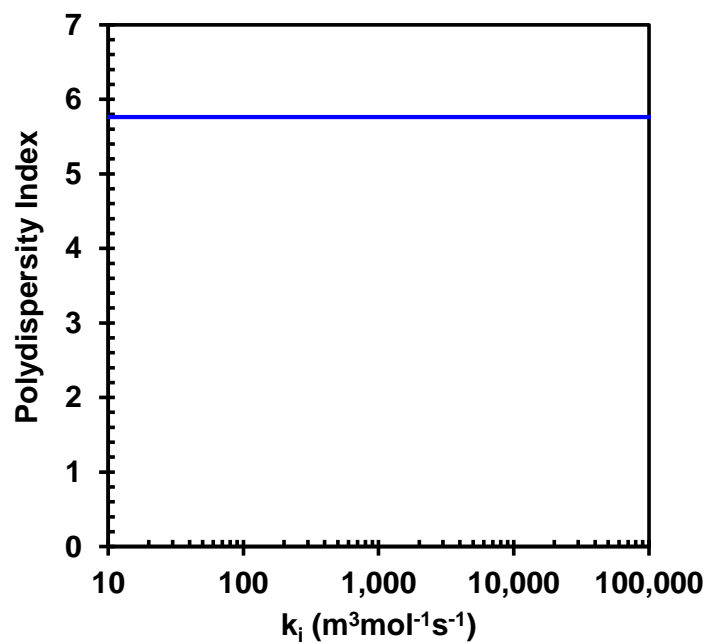


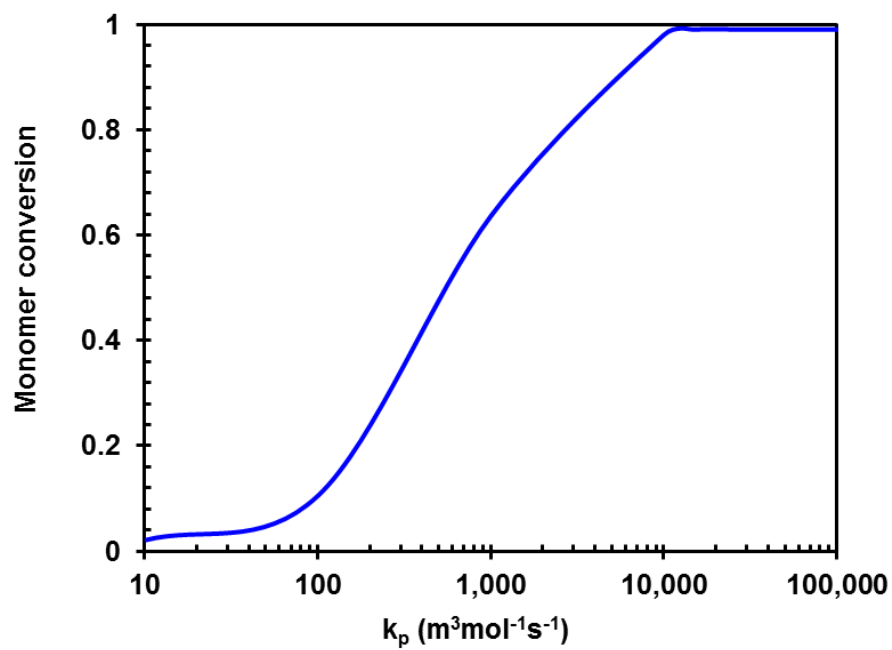
Figure 4-3. Effect of  $k_i$  on the Polydispersity Index

#### 4.1.2 Effect of the propagation rate constant ( $k_p$ )

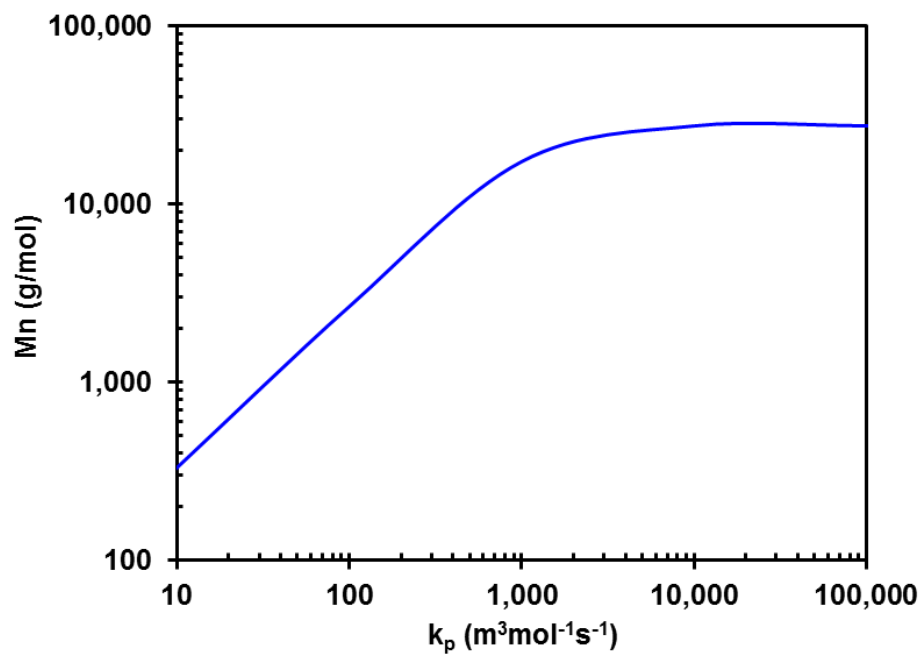
The role of  $k_p$  in the propagation step is mathematically described as the coefficient for polymers to grow by adding monomers sequentially to the chain. Figure 4-4 shows the effect of  $k_p$  on the monomer conversion; and as can be seen, the monomer conversion is low at  $k_p = 10$  ( $\text{m}^3\text{mol}^{-1}\text{s}^{-1}$ ) and then it increases to 100% at  $k_p = 10^4$  ( $\text{m}^3\text{mol}^{-1}\text{s}^{-1}$ ). Figure 4-5 shows the effect of  $k_p$  on the  $M_n$ ; and as can be seen  $M_n$  value increases almost linearly with  $k_p$  in the range of  $10^2$  and  $10^4$  ( $\text{m}^3\text{mol}^{-1}\text{s}^{-1}$ ), and then it flattens out. This behavior is online with the assumption that the propagation step is where a single monomer is added sequentially to the polymer.

On the other hand, Figure 4-6 shows the effect of  $k_p$  on the polydispersity index and as can be observed, the polydispersity index drops at first and then almost levels off at  $k_p$  about  $10^3$  ( $\text{m}^3\text{mol}^{-1}\text{s}^{-1}$ ).

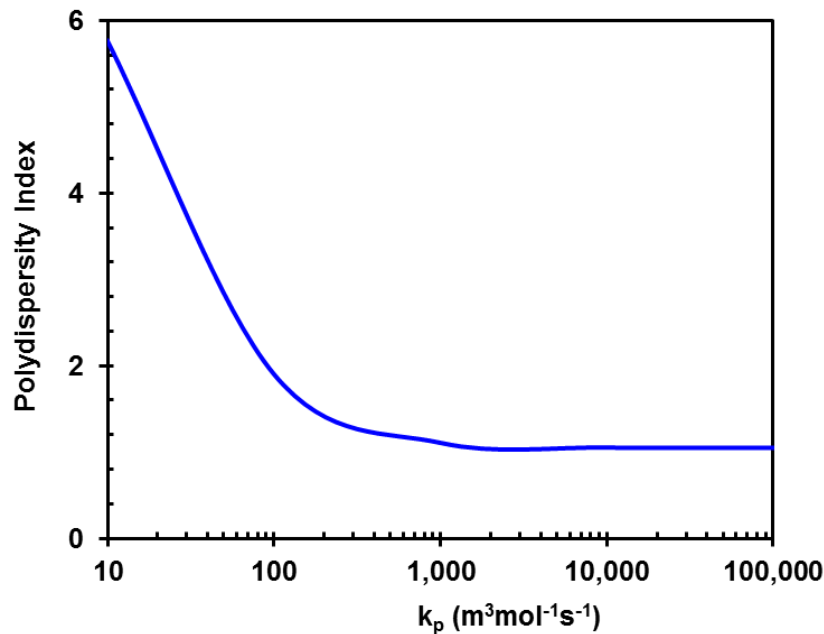
Thus, if the low polydispersity index is the target for the IBP process, then  $k_p$  in the order of  $10^3$  ( $\text{m}^3\text{mol}^{-1}\text{s}^{-1}$ ) would be preferred. At such a value, the monomer conversion would be about 62% and  $M_n$  would be about 20,000 g/mol as can be deduced from Figures 4-4 and 4-5, respectively.



**Figure 4-4.** Effect of  $k_p$  on the Monomer Conversion



**Figure 4-5.** Effect of  $k_p$  on the Number Average Molecular Weight



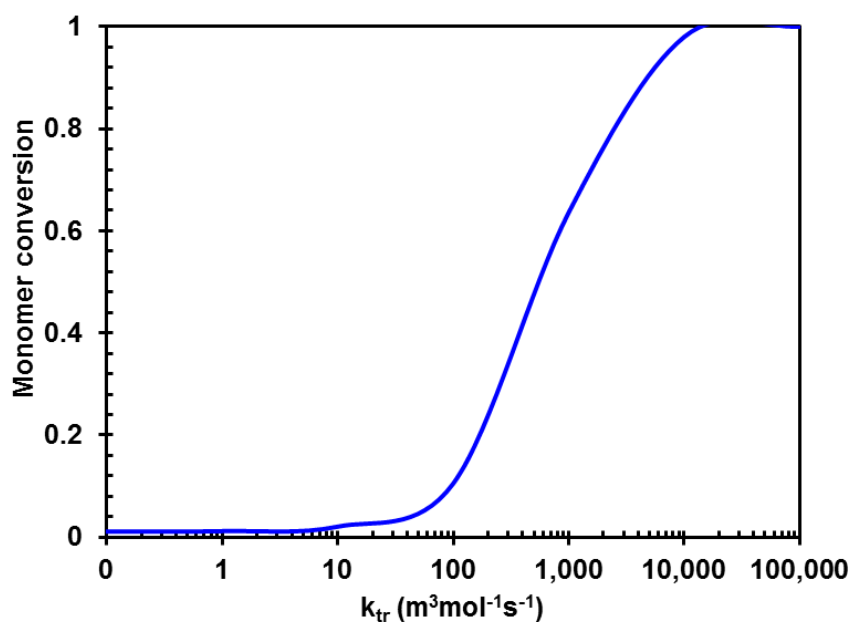
**Figure 4-6.** Effect of  $k_p$  on the Polydispersity Index

#### 4.1.3 Effect of the chain transfer rate constant ( $k_{tr}$ )

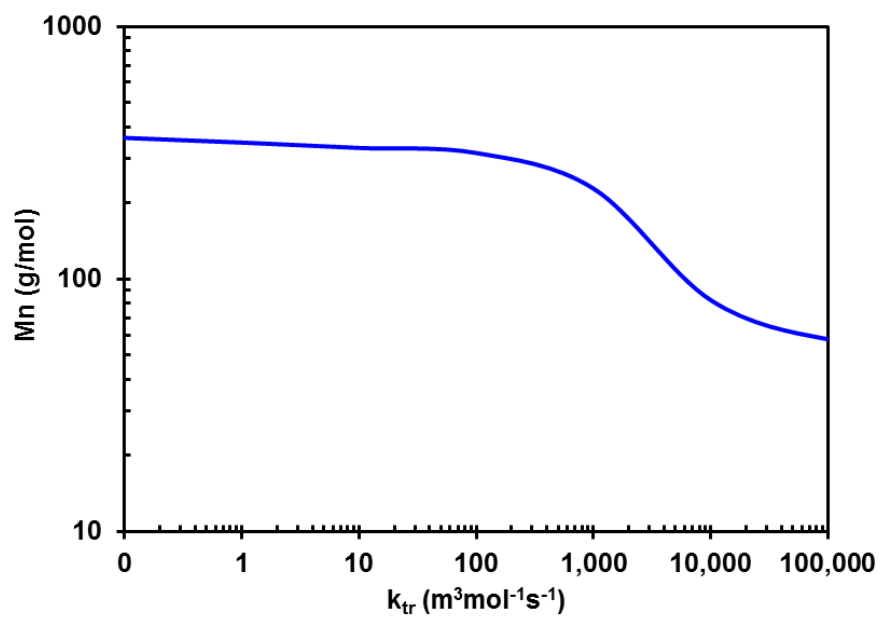
The chain transfer rate constant  $k_{tr}$  has two opposite effects on the monomer conversion and the number average molecular weight ( $M_n$ ), as shown in Figures 4-7 and 4-8, respectively. The Monomer conversion increases exponentially at  $k_{tr}$  values greater than 10 ( $\text{m}^3\text{mol}^{-1}\text{s}^{-1}$ ), whereas  $M_n$  declines rapidly at  $k_{tr}$  values greater than  $10^3$  ( $\text{m}^3\text{mol}^{-1}\text{s}^{-1}$ ), which shows that high  $k_{tr}$  rate suppresses  $M_n$ .

Moreover, Figure 4-9 shows the effect of  $k_{tr}$  on the polydispersity index; and as can be seen the polydispersity index rapidly decreases at  $k_{tr}$  values greater than 1 ( $\text{m}^3\text{mol}^{-1}\text{s}^{-1}$ ), which indicates that higher chain transfer rate constants promotes homogeneity in the polymer molecular weight distribution. This behavior is in agreement with experimental finding reported in the literature [21, 23, 29].

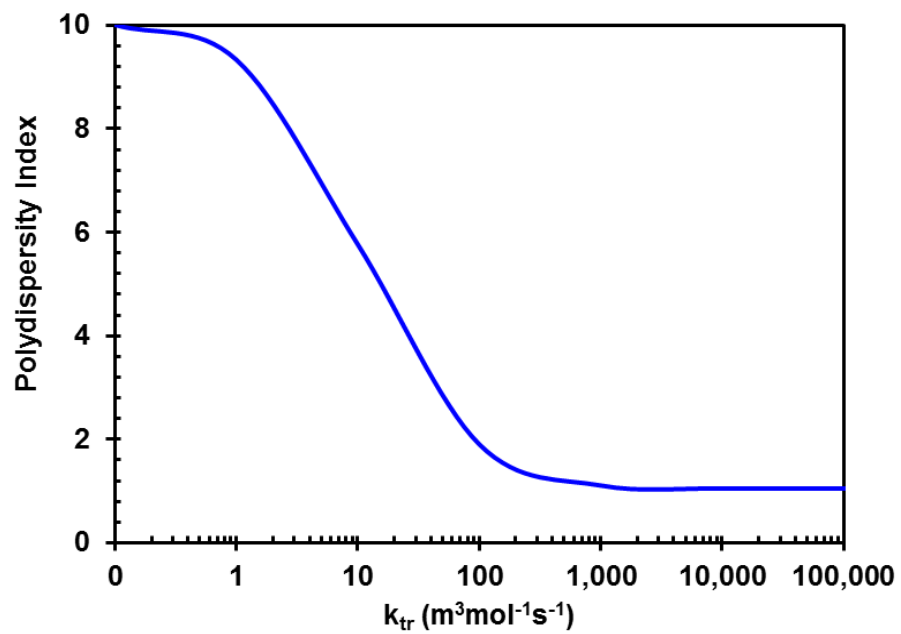
This behavior is because the chain transfer inhibits the growth of polymer chain by adding an unsaturated monomer as end group. Such chain breaking reaction largely controls the chain growth, which means the cationic polymerization is extremely sensitive to the change of  $k_{tr}$ . Moreover, transferring to monomer produces polymers with unsaturated end groups, which consume monomers but generate active species, and therefore the polydispersity index would decrease at high values of  $k_{tr}$ . It should be noted that the values of  $M_n$  varied in the range from 60 to 370 g/mol, which is strikingly small when  $k_{tr}$  values vary from 0 to  $10^5$  ( $\text{m}^3\text{mol}^{-1}\text{s}^{-1}$ ).



**Figure 4-7.** Effect of  $k_{tr}$  on the Monomer Conversion



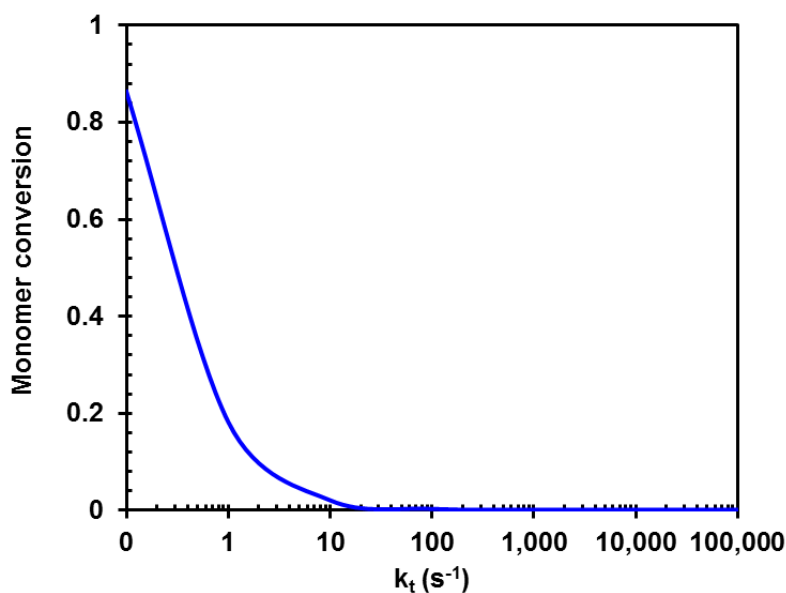
**Figure 4-8.** Effect of  $k_{tr}$  on the Number Average Molecular Weight



**Figure 4-9.** Effect of  $k_{tr}$  on the Polydispersity Index

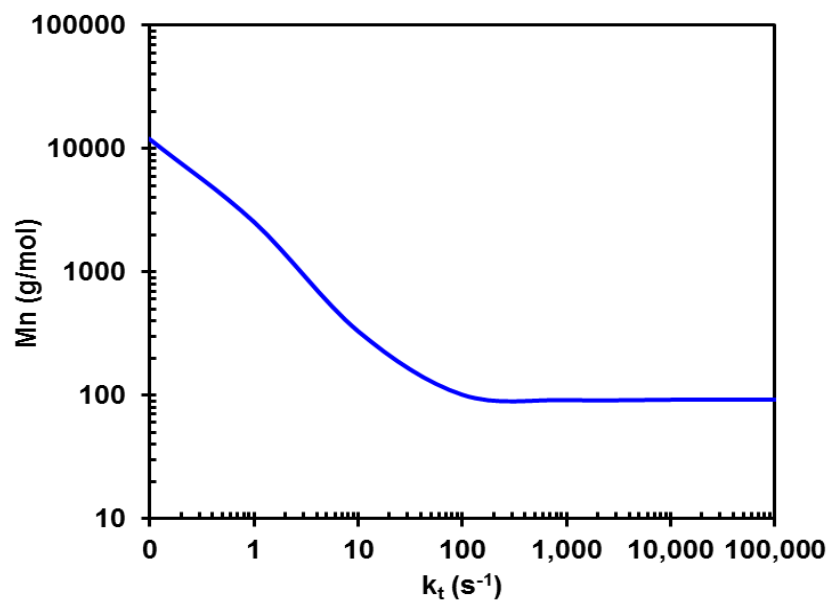
#### 4.1.4 Effect of the termination rate constant ( $k_t$ )

A higher termination rate constant ( $k_t$ ) clearly decreases the performance of the polymerization process, as shown in Figures 4-10 and 4-11, which present the effect of  $k_t$  on the monomer conversion and the number average molecular weight, respectively. It is obvious that a larger termination rate constant should be avoided when long polymer chains are desired. Unlike  $k_{tr}$ , which decreases  $M_n$  and promotes polydispersity, increasing  $k_t$ , decreases the monomer conversion and the number average molecular weight. Actually, most industrial cation polymerization plants tend to minimize the effect of the termination step by using highly purified solvents and raw materials. Thus, in order to obtain high monomer conversion and number average molecular weight at a polydispersity index close to the unity,  $k_t$  value has to be small.

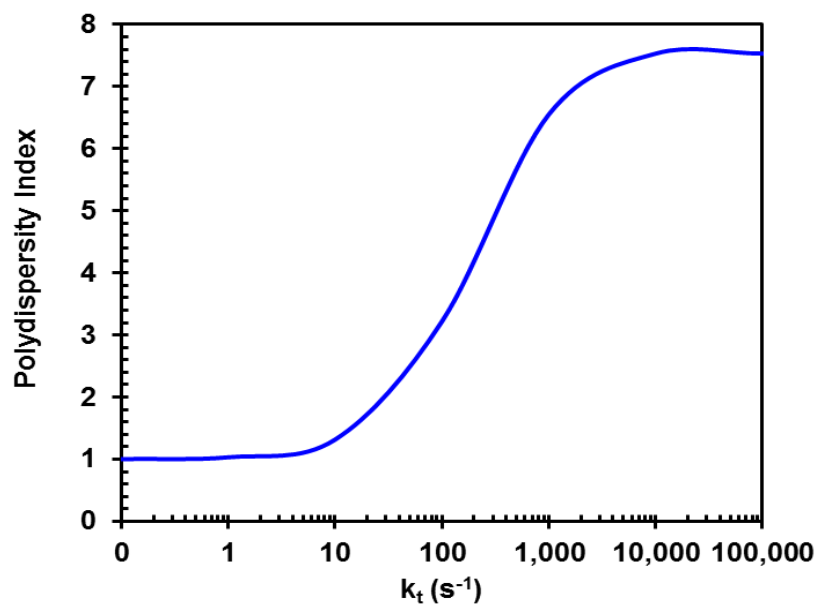


**Figure 4-10.** Effect of  $k_t$  on the Monomer Conversion





**Figure 4-11.** Effect of  $k_t$  on the Number Average Molecular Weight



**Figure 4-12.** Effect of varying  $k_t$  on the Polydispersity Index

## 4.2 EFFECT OF MIXING

The effect of mixing on the polymerization process performance was subsequently investigated under the following assumptions:

1. Throughout the simulation, the viscosity was taken as a constant so that  $\theta_M$  was a controlled variable in the sensitivity analysis. In his paper, Baldyga [57-59] reported  $\theta_M$  to approximately equal the average eddy life time linked to bulk convection and turbulent diffusion.
2. The dimensionless mixing time ( $\theta_M$ ) was varied between 0.01 and 100 for the sensitivity analysis calculations. This is approximately equal to the average eddy life time linked to bulk convection and turbulent diffusion, as reported by Baldyga [57-59].
3. In our model, all reaction kinetic rate constants were constant at any time during the polymerization process. This assumption greatly eliminates the complexity of modeling although in real cases, most of the kinetic rate constants are affected by the change in concentration, solvent polarity and temperature. The values for  $k_i$ ,  $k_p$ ,  $k_{tr}$  and  $k_t$  were set to  $10^3 \text{ (m}^3\text{mol}^{-1}\text{s}^{-1}\text{)}$ ,  $10^3 \text{ (m}^3\text{mol}^{-1}\text{s}^{-1}\text{)}$ ,  $10^3 \text{ (m}^3\text{mol}^{-1}\text{s}^{-1}\text{)}$  and  $10 \text{ s}^{-1}$ , respectively.

The effect of mixing on the conversion, number average molecular weight and polydispersity index was investigated by varying the dimensionless mixing time scale ( $\theta_M$ ) and mass diffusion

time scale ( $\theta_X$ ). Seven separate cases, as shown in Table 4-2, corresponding to various degrees of mixing were considered.

**Table 4-2.** Summary of Mixing effects for all mixing time constants

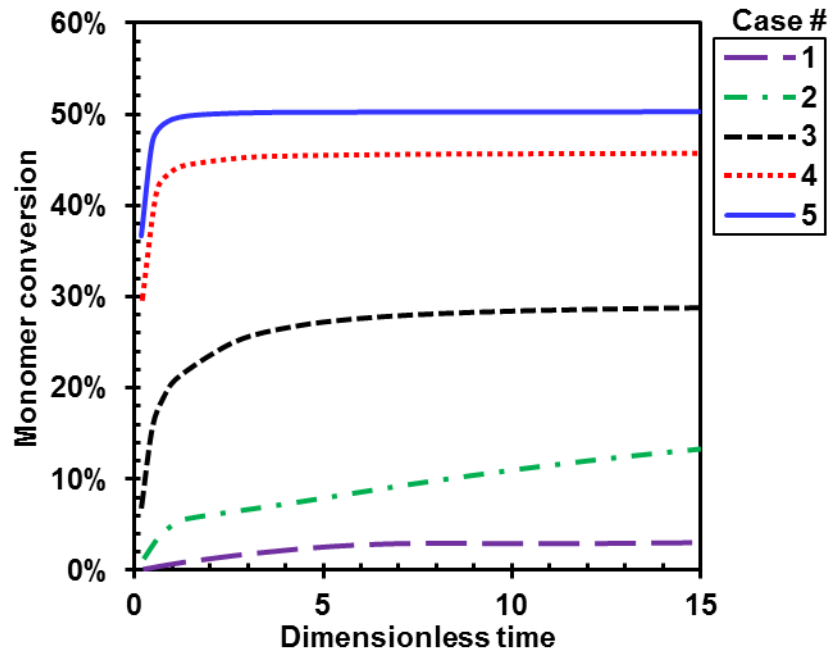
Case #	$\theta_X (\theta_{13} = \theta_{23})$	$\theta_M$	Comment on Mixing behavior
1	100	100	Negligible mixing
2	10	10	Poor
3	1	1	Sufficient
4	0.1	0.1	Good
5	0.01	0.01	Perfect
6	10	0.1	Good bulk mixing and poor mass diffusivity (Solvent Effect)
7	0.1	10	Poor bulk mixing and good mass diffusivity (Solvent Effect)

Figures 4-13 and 4-14 show the change in the monomer conversion with the dimensionless mixing time for the seven cases mentioned above. As shown in

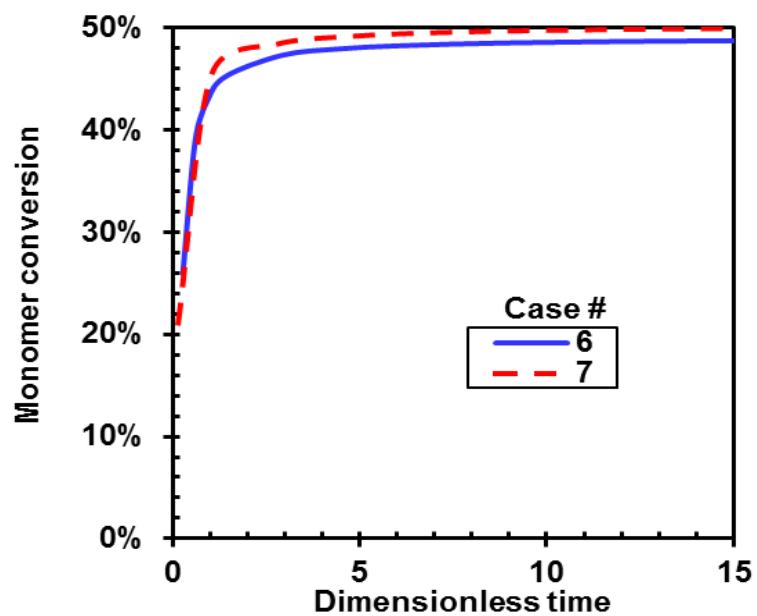
Figure 4-13, the monomer conversion increases with increasing mixing time scale, which corresponds to better mixing. Whereas Figure 4-14 shows that the monomer conversion for Case 7, which corresponds to poor bulk mixing, but good mass diffusivity, is slightly higher than that for Case 6, which corresponds to good bulk mixing, but poor mass diffusivity. These results indicate that, theoretically, a solvent which promotes very high mass diffusivities may offset the effect of poor mixing; however, it should be noted that this is not practically attainable.

Figures 4-15 and 4-16 show the change in the number average molecular weight with dimensionless mixing time for the seven cases. As can be observed the effect of mixing on the monomer concentration is identical to that of monomer conversion.

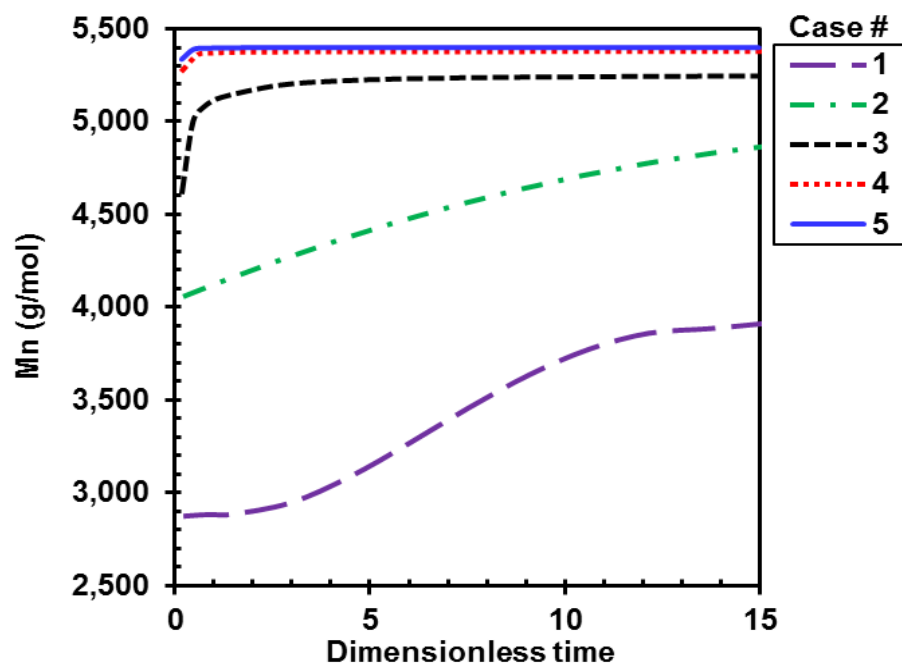
Moreover, Figures 4-17 and 4-18 show the effect of dimensionless mixing time on the polydispersity index; and as can be observed increasing the mixing time results in a lower polydispersity index, and thus a more uniform product distribution, whereas poor mixing results in higher polydispersity indices, which in turn would have a significant effect on the product physical properties.



**Figure 4-13.** Effect of dimensionless mixing time on the monomer conversion (Cases 1-5)



**Figure 4-14.** Effect of dimensionless mixing time on the monomer conversion (Cases 6-7)



**Figure 4-15.** Effect of dimensionless mixing time on the Mn (Cases 1-5)

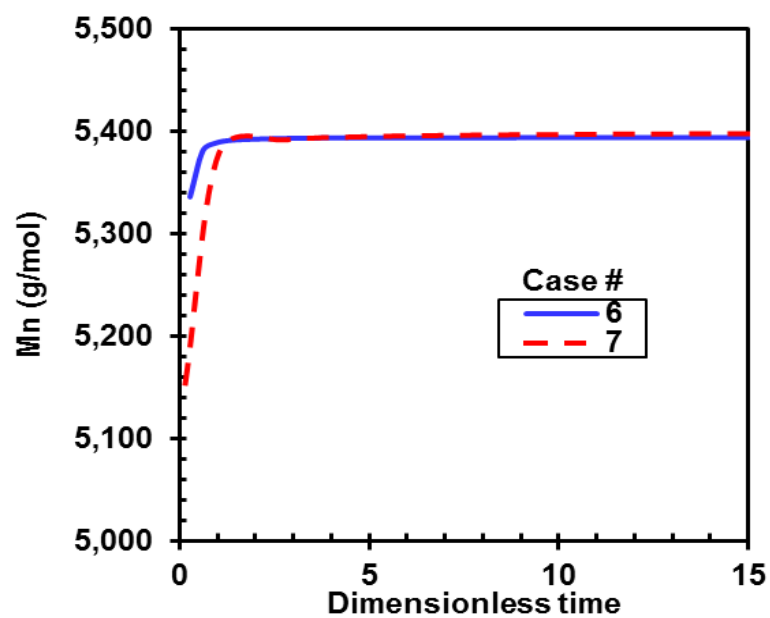


Figure 4-16. Effect of dimensionless mixing time on the Mn (Cases 6-7)

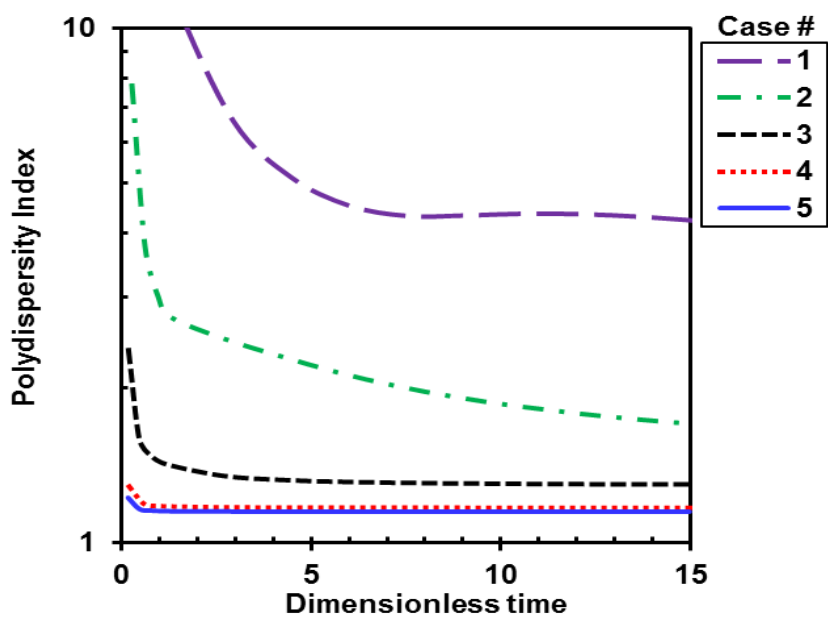


Figure 4-17. Effect of dimensionless mixing time on the Polydispersity index (Cases 1-5)

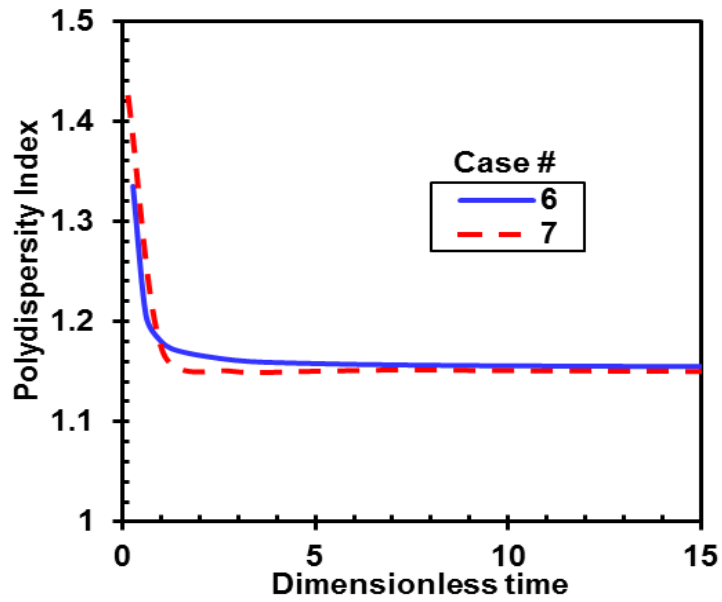


Figure 4-18. Effect of dimensionless mixing time on the Polydispersity index (Cases 6-7)

### 4.3 MODEL PREDICTION OF THE OVERALL REACTOR PERFORMANCE

In order to determine the effect of mixing on the overall reactor performance, eight different cases were investigated as shown in Table 4-3.

Table 4-3. Summary of sensitivity analysis cases

Case No.	$\hat{Q}_T (\hat{Q}_1 + \hat{Q}_2)$	$\Phi = C_m/C_{ini}$	kp	$\theta_M$	$\theta_X(\theta_{13} = \theta_{23})$
P-1	2	100	1000	10	10
P-2	2	100	100	10	10
P-3	2	1000	1000	10	10
P-4	6	100	1000	10	10
G-1	2	100	1000	0.1	0.1
G-2	2	100	100	0.1	0.1
G-3	2	1000	1000	0.1	0.1
G-4	6	100	1000	0.1	0.1

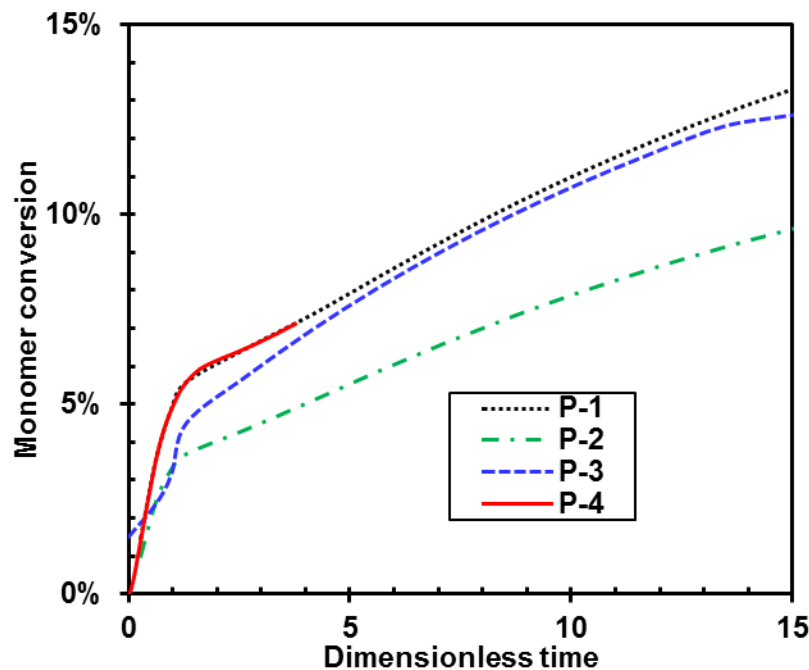
As shown in this table, the three main operating conditions considered are: (1) Total monomer flow  $\hat{Q}_T$ ; (2) Ratio of monomer to initiator in the feed ( $\phi$ ); and (3) Propagation rate constant  $k_p$ . Moreover, the cases were classified into two sets, P and G, referring to poor and good mixing, respectively. The poor mixing cases (P-1 to P-4) were set by setting  $\theta_X = \theta_M = 10$ , whereas the good mixing (G-1 to G-4) were set by inputting  $\theta_X = \theta_M = 0.1$ . The eight cases are as follows:

1. Cases P-1 and G-1 are regarded as the reference for the other cases as poor and good mixing.
2. Cases P-2 and G-2: The value of  $k_p$  is set to 100, which is 0.1 of the value used in Cases P-1 and G-1. This is used to gauge the relative importance of the propagation rate on the overall performance.
3. Cases P-3 and G-3: The ratio of the monomer to the initiator in the inlet stream ( $\phi$ ) is set to 1000, which is ten times the values used in cases P-1 and G-1.
4. Cases P-4 and G-4: The value which is the total flow rate to the reactor  $[\hat{Q}_T]$  is set to 6, up to 3 times the value used in Cases P-1 and G-1. This is used to investigate the effect of reactor size on the performance of the polymerization process model.

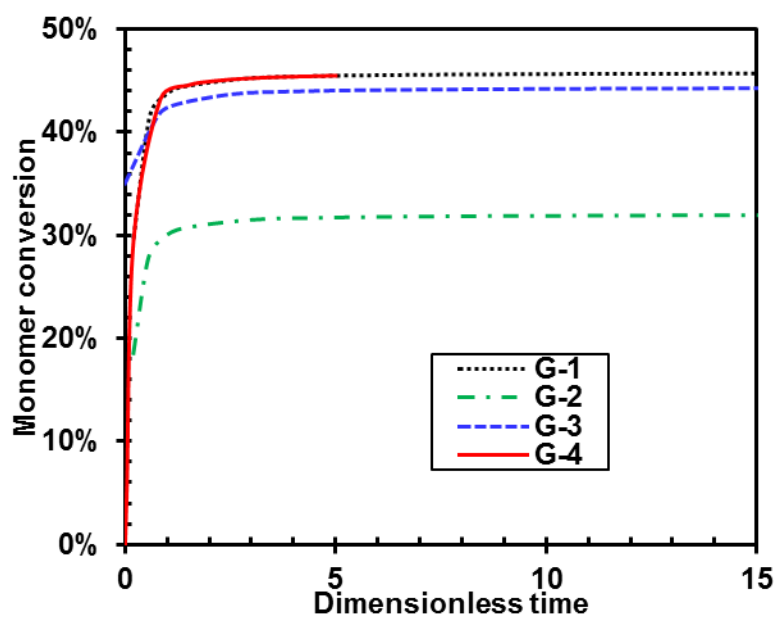
Figures 4-19 and 4-20 show the effect of dimensionless time on the monomer conversion for all the case mentioned above. As can be seen in these figures, cases P-1 to P-4, which correspond to poor mixing have significantly lower conversions when compared with those of cases G-1 to G-4, which correspond to good mixing. A similar behavior can be observed for the number average molecular weight as shown in Figures 4-21 and 4-22, for the poor and good mixing cases, respectively. On the other hand, the polydispersity index appear to decrease with better mixing as shown in Figure 4-24 when compared with that shown in Figure 4-23.



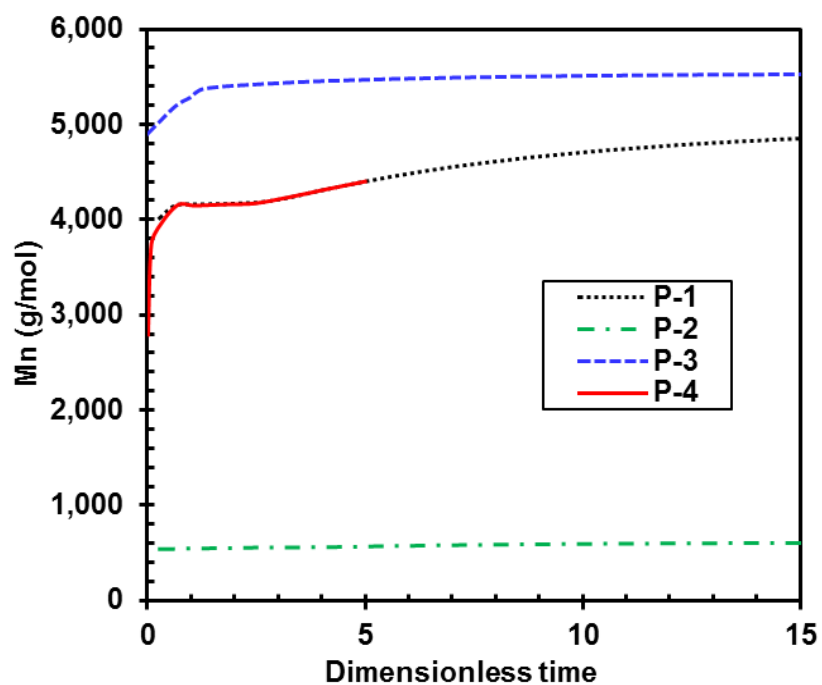
Moreover, Figures 4-25 to 4-28 show the mixing performance values for the different reactor geometries and impeller designs, the exact mixing values are provided in Table B-1 in Appendix B. As can be seen in these figures, both the mixing time and the impeller type have a significant effect on the required rotation speed of the impeller. Thus, the model developed in this study could be used to provide a detailed analysis of the reactor performance, geometry and mixing.



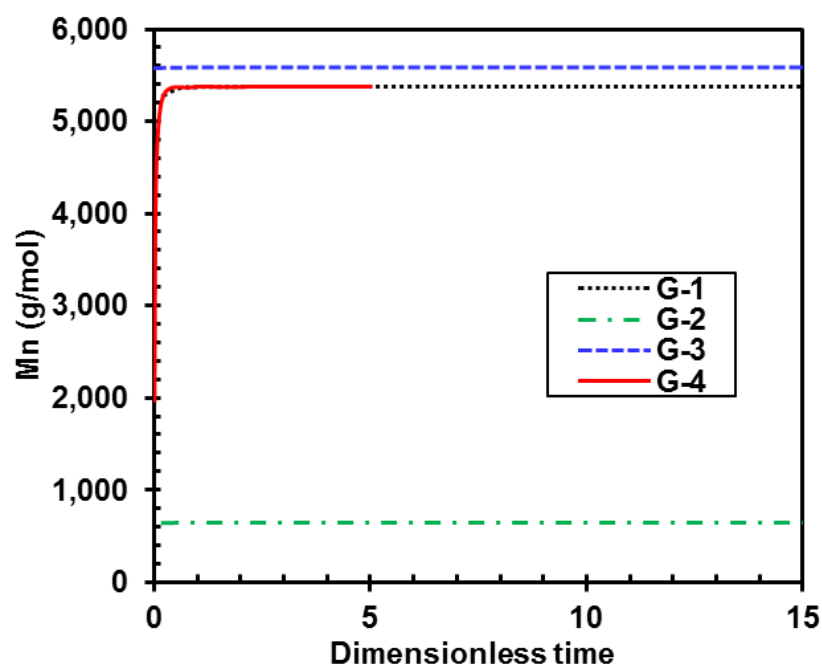
**Figure 4-19.** Effect of dimensionless mixing time on the monomer conversion (Case P1 - P4 in poor mixing)



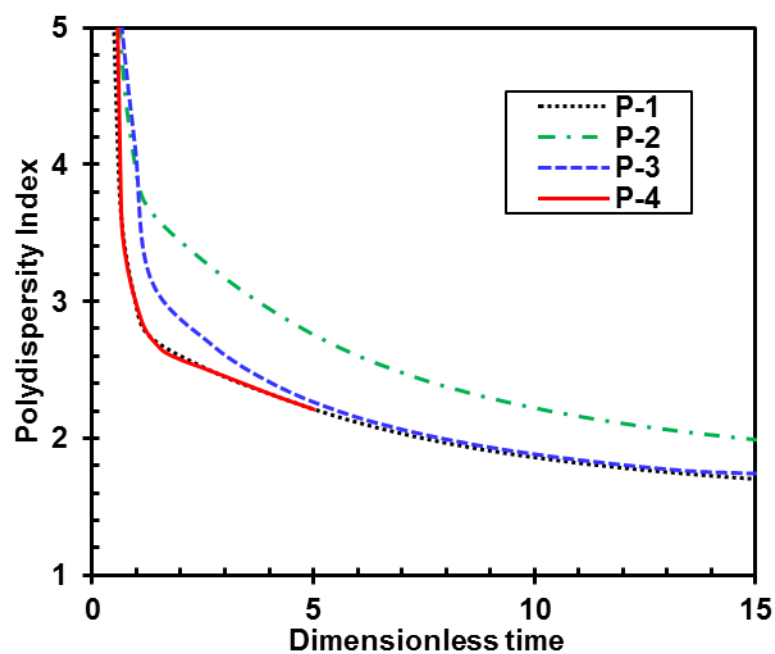
**Figure 4-20.** Effect of dimensionless mixing time on the monomer conversion  
(Case G1 - G4 in good mixing)



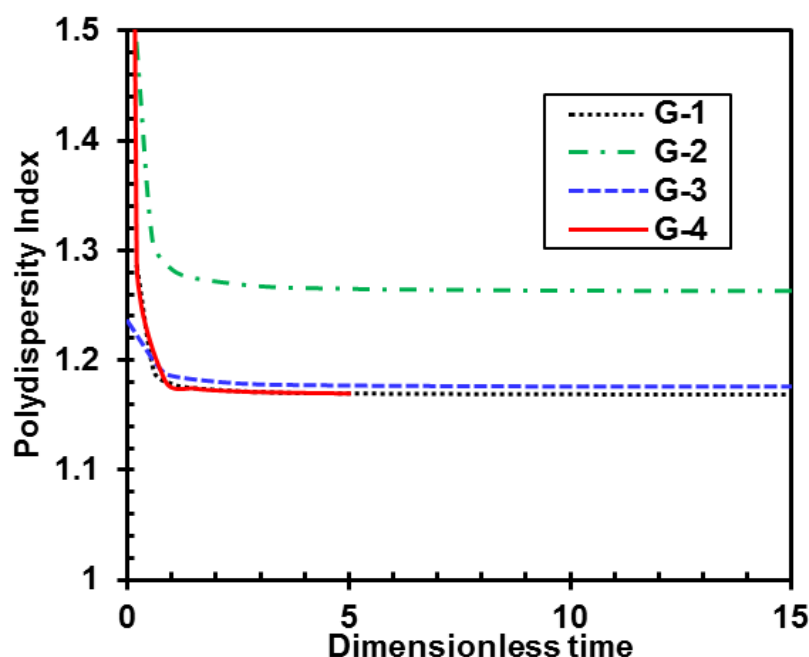
**Figure 4-21.** Effect of dimensionless mixing time on the Mn  
(Case P1 - P4 in poor mixing)



**Figure 4-22.** Effect of dimensionless mixing time on the Mn  
(Case G1 - G4 in good mixing)



**Figure 4-23.** Effect of dimensionless mixing time on the Polydispersity Index  
(Case P1 - P4 in poor mixing)



**Figure 4-24.** Effect of dimensionless mixing time on the Polydispersity Index  
(Case G1 - G4 in good mixing)

Figures 4-25 to 4-28 show the mixing performance for the different reactor geometries and impeller designs; and the mixing speed values are provided in Table B-1 in Appendix B. As can be seen in these figures, the mixing time and the impeller type have a significant effect on the required rotation speed of the impeller. Thus, the model developed in this study could be used to provide a detailed analysis of the reactor performance, geometry and required mixing speed under different mixing scenarios for the isobutylene polymerization process in agitated reactors.

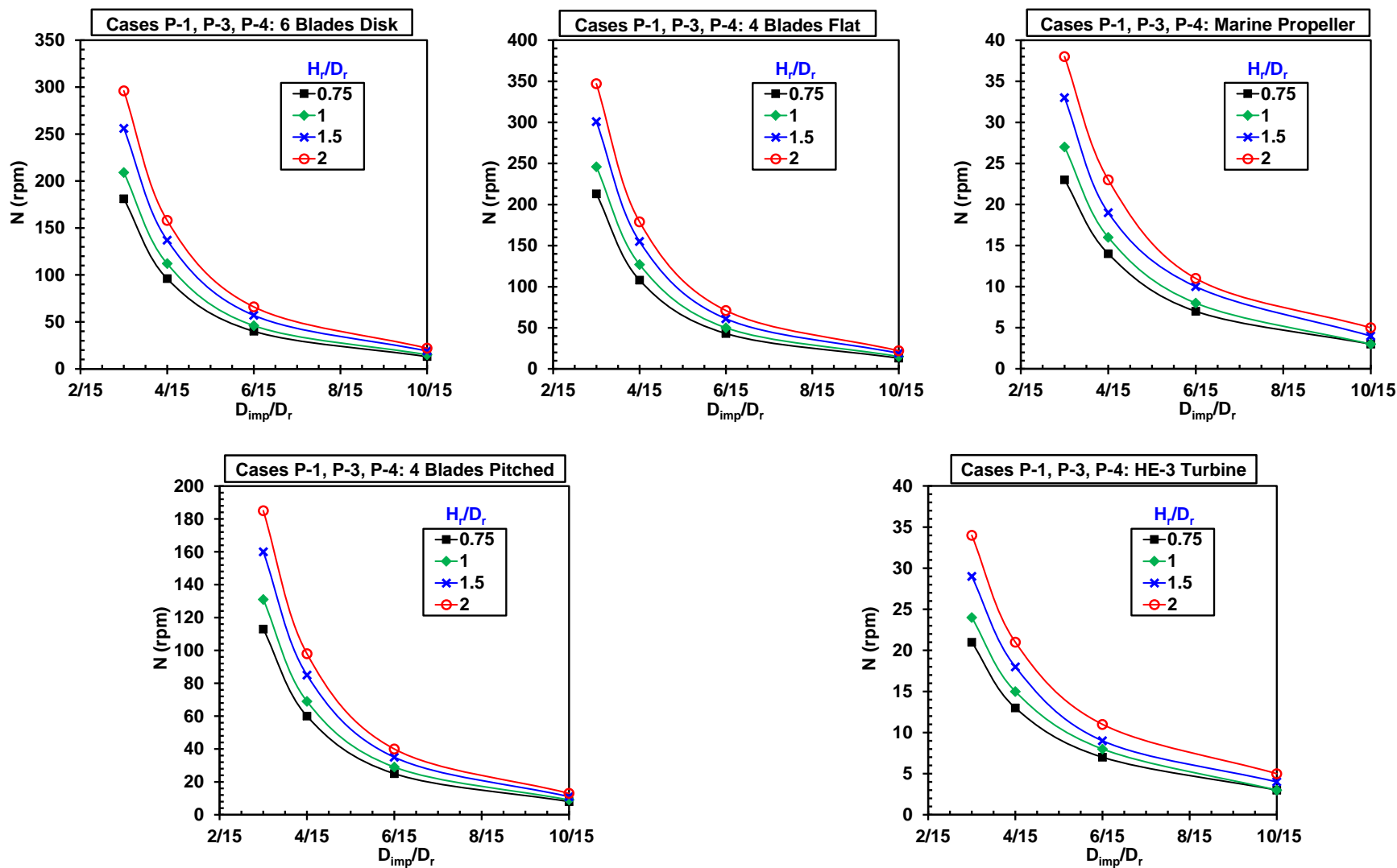


Figure 4-25. Effect of reactor type and impeller type/size on the mixing speed (Cases P-1, P-3 and P-4)

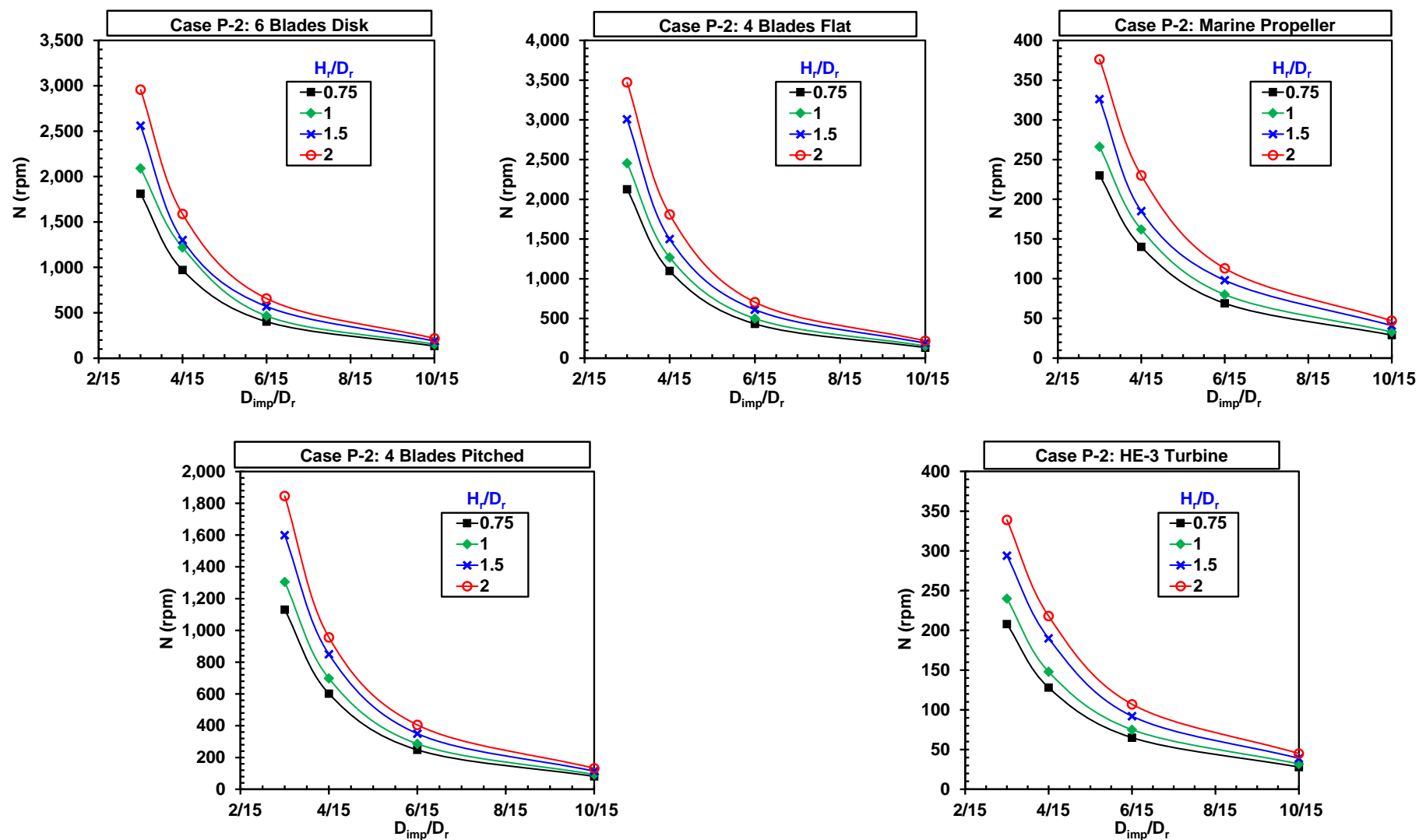


Figure 4-26. Effect of reactor type and impeller type/size on the mixing speed (Case P-2)

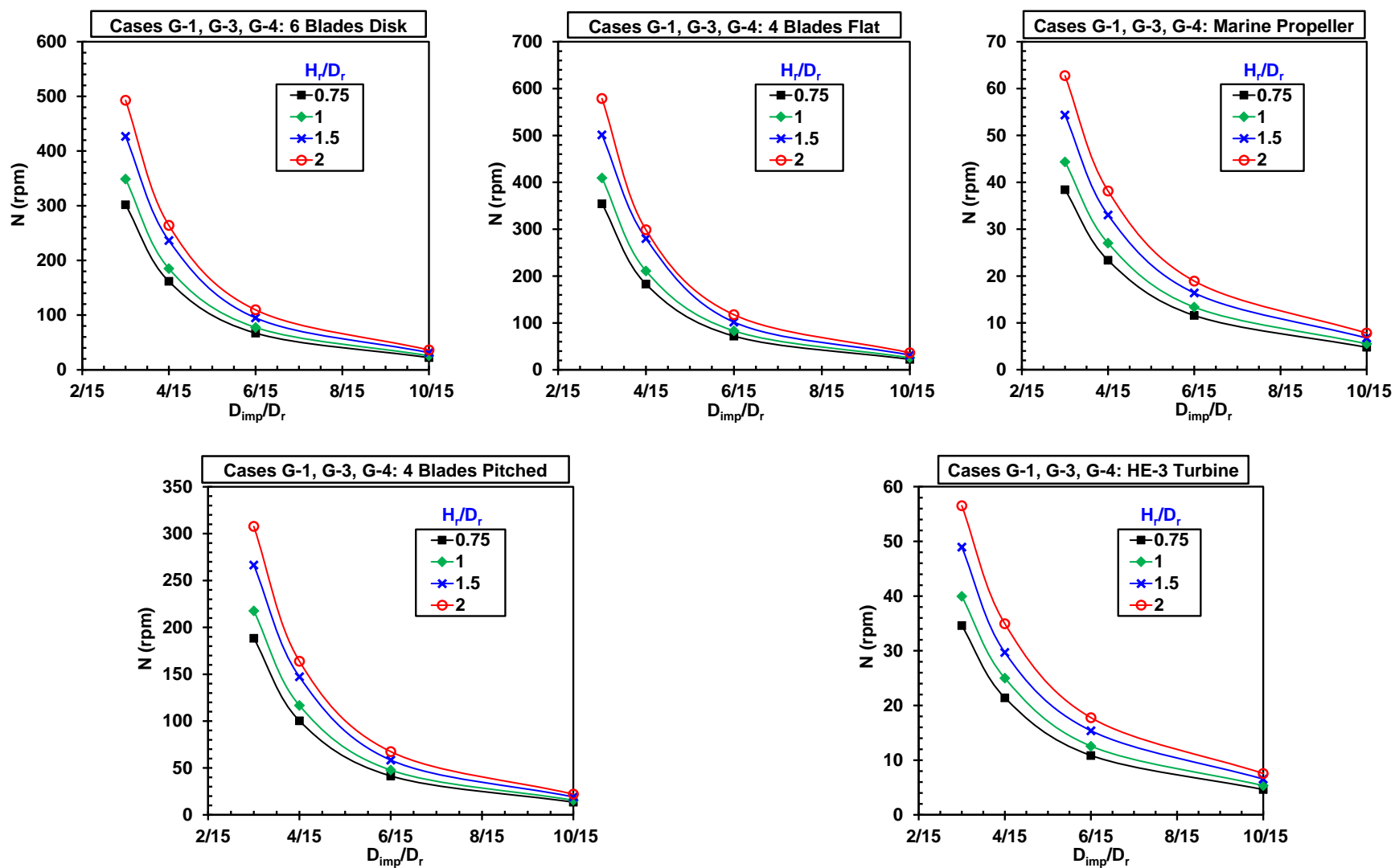


Figure 4-27. Effect of reactor type and impeller type/size on the mixing speed  
(Cases G-1, G-3 and G-4)

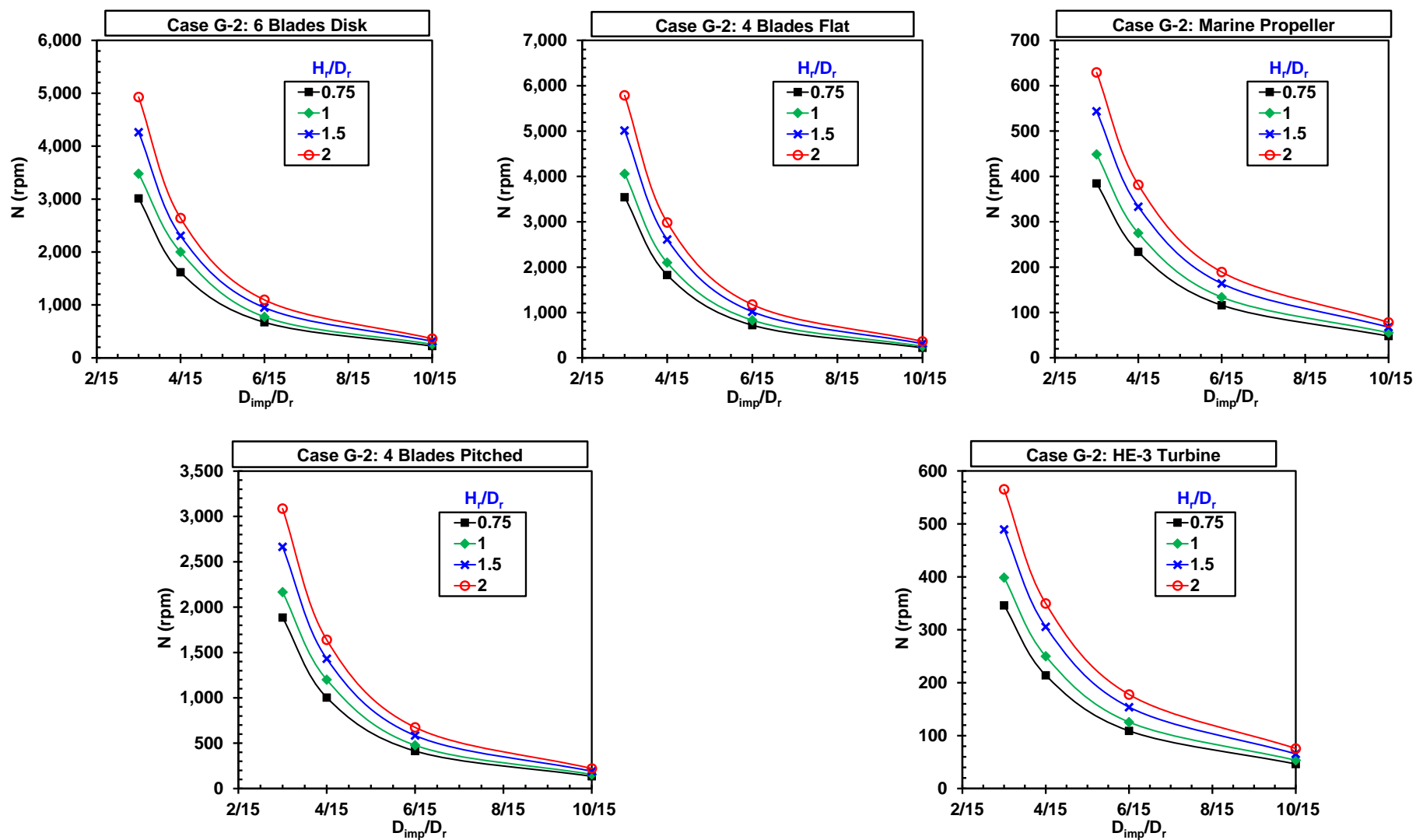


Figure 4-28. Effect of reactor type and impeller type/size on the mixing speed (Case G-2)



## 5.0 CONCLUSIONS

In this study, a comprehensive model for isobutylene polymerization (IBP) in agitated reactors, which takes into account the polymerization reaction kinetics and mixing effects, was developed in Matlab. In the absence of mixing, the model was used to carry out sensitivity analyses to quantify the effects of the reaction rate constants of the initiation ( $k_i$ ), propagation ( $k_p$ ), chain transfer ( $k_{tr}$ ) and chain termination ( $k_t$ ) steps, occurring in the IBP, on the three main performance metrics, the monomer conversion, the number average molecular weight and the polydispersity index. In the presence of mixing, the model was used to conduct a parametric study in order to predict the effect of mixing, reactor type, and impeller type as well as design on the three main IBP process performance metrics. The model in the absence and presence of mixing predictions led to the following conclusions:

1. Increasing the initiation reaction rate constant ( $k_i$ ) was found to have negligible effect on the monomer conversion, number average molecular weight and polydispersity index.
2. Increasing the propagation reaction rate constant ( $k_p$ ) appeared to have significant effect on the overall process performance since it increased the monomer conversion and the number average molecular weight and decreased the polydispersity index.
3. Increasing the chain transfer reaction rate constant ( $k_{tr}$ ) increased the monomer conversion, but decreased the number average molecular weight and polydispersity index.

4. Increasing the chain termination reaction rate constant ( $k_t$ ) decreased monomer conversion and the number average molecular weight, but increased the polydispersity index.
5. Eight different cases with various propagation reaction rate constants under poor as well as good mixing conditions were implemented in the model to study their effects on the IBP process' three main performance metrics: the monomer conversion, the number average molecular weight and the polydispersity index. The effect of mixing was found to dominate the IBP process due to its inherent fast reaction kinetics. Mixing time and the impeller type appeared to have a significant effect on the required mixing speed of the impeller. Also, all model predictions underscored the importance of good mixing in the cationic IBP process.
6. Thus, the model developed in this study could be used to provide a detailed analysis of the reactor performance, geometry and required mixing speed under different mixing scenarios for the isobutylene polymerization process in agitated reactors.

## APPENDIX A

### MODELING ISOBUTYLENE POLYMERIZATION IN ASPEN PLUS

AspenPlus v. 7.2 was used to model the IBP process carried out in an overall reactor size of 4.5 m<sup>3</sup> using Aluminum Chloride (AlCl<sub>3</sub>) as initiator in hexane solvent. The feed to the reactor was set to 1000 kg/hr (95% isobutylene monomer and 5% AlCl<sub>3</sub> initiator). The reaction conditions were set to - 80 °C and 1 atm. The reactions were assumed to follow the cationic polymerization, which includes five steps:

1. Initiator dissociation: AlCl<sub>3</sub> becomes ionized in the hexane solvent and dissociates into free ions or ion pairs;
2. Chain initiation: begins by the combination of isobutylene monomer and the ionized Lewis acid, which forms active species for the reaction
3. Propagation: The structural units linearly add monomers to the polymer chain;
4. Chain transfer: the propagating chain ends by transferring with a monomer, leaving an unsaturated carbon-carbon double bond, which is still highly reactive;
5. Termination: the propagating chain breaks by combining with a counter-ion, which is usually a negative halide ion.

It should be mentioned that the chain transfer and termination steps occur in parallel rather than sequential. This is because in actual cases, both polymers are found in the product although their concentrations can vary greatly depending on the operating conditions.

The IBP reaction kinetics were represented using the Flory-Huggins method for the 5-step polymerization reaction mechanism shown in Table 1 [67]. Different data from the literature [17, 18, 42-44, 55] were used to fit the kinetic parameters for each reaction step using  $\text{AlCl}_3$  as initiator. The kinetic constants for the polymerization process were assumed to follow an Arrhenius-type equation:

$$k = k_0 \exp \left[ -\frac{E_a}{R} \left( \frac{1}{T} - \frac{1}{T_{ref}} \right) \right] \quad (61)$$

The values for the kinetic constants for each reaction step are also shown in Table 1.

**Table A-1.** Kinetic parameters for each reaction step used in the model [67]

Step	Reaction	$k_n$ (1/hr)	$E_a$ (J/kmol)	$T_{ref}$ (K)
1. Initiator dissociation	$\text{I} \rightarrow \text{I} (\text{sol})$	$10^{10}$ (instantaneous)	5	283.15
2. Initiation	$\text{I} + \text{M} \rightarrow \text{A}_1^*$	100	5	283.15
3. Propagation	$\text{A}_1^* + \text{M} \rightarrow \text{A}_2^*$ $\text{A}_{n-1}^* + \text{M} \rightarrow \text{A}_n^*$	50	50	283.15
4. Chain transfer	$\text{A}_n^* + \text{M} \rightarrow \text{A}_1^* + \text{P}$	$10^{-5}$	50	283.15
5. Chain termination	$\text{A}_n^* \rightarrow \text{P}$	$10^{-5}$	50	283.15

The RBatch process unit in AspenPlus was used to represent the IBP reactor model. This model was selected since it allows for transient analysis of certain polymer related parameters, such as number and weight average molecular weights and polydispersity index. The basic governing equations in this model involve the material balance of the species in a control volume, which is the reactor. The material balance equation of the  $i^{\text{th}}$  species is:

$$\frac{d(C_i V_{reactor})}{dt} = Q_{feed} C_{i-feed} - Q_{out} C_{i-out} + R_i V_{reactor} \quad (62)$$

The equations for all species are solved by integration as a function of time.

The model was then used to predict the transient composition of all the species involved in the reaction, as shown in Figure 1. The model was also used to determine the weight average molecular weight (Equation (3)) and the number average molecular weight (Equation (4)), as shown in Figure 2.

$$M_w = \frac{\sum N_i M_i^2}{\sum N_i M_i} \quad (63)$$

$$M_n = \frac{\sum N_i M_i}{\sum N_i} \quad (64)$$

Moreover, the model was used to track the degree of polymerization (DOP) during the IBP process, as shown in Figure 3. The DOP is a measure of the average number of monomer units in the polymer and as such, it can be expressed based on either the number average (Equation (5)) or the weight average (Equation (6)).

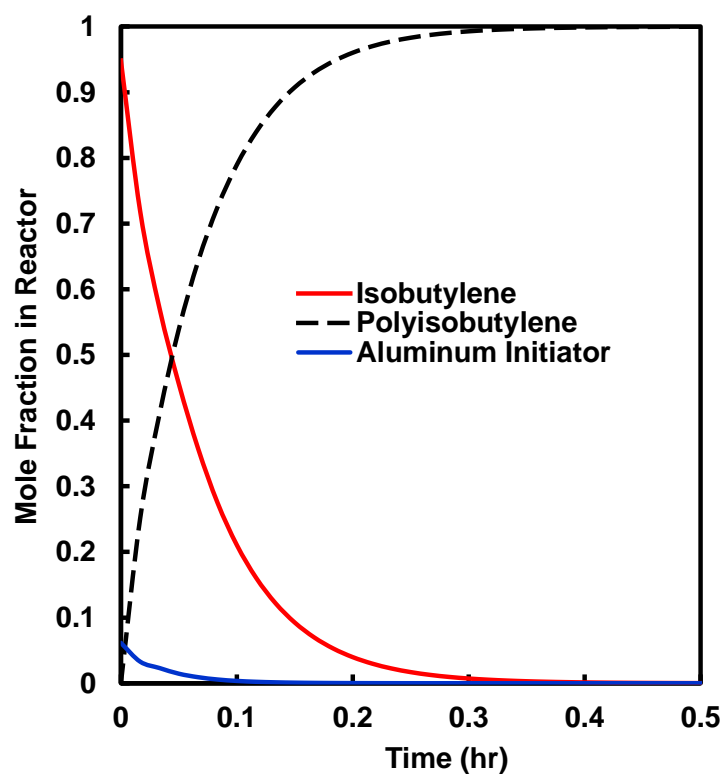
$$n_n = \frac{M_n}{m_o} \quad (65)$$

$$n_w = \frac{M_w}{m_o} \quad (66)$$

Our model was also used to investigate the effect of operating temperature on the overall conversion and the polydispersity index of the IBP process, as shown in Figure 4. The polydispersity index is a measure of the spread of molecular weight distributions (Equation (6)), and is typically used as an indicator of the desired product quality.

$$PDI = \frac{M_w}{M_n} \geq 1 \quad (67)$$

Furthermore, the effect of the initiator concentration in the feed on Isobutylene conversion was investigated, as shown in Figure 5 and as can be seen there is no effect on the conversion at initiator concentrations in the feed > 15 wt%.



**Figure A-1.** Compositions of Isobutylene, Polyisobutylene and  $\text{AlCl}_3$  Initiator during IBP

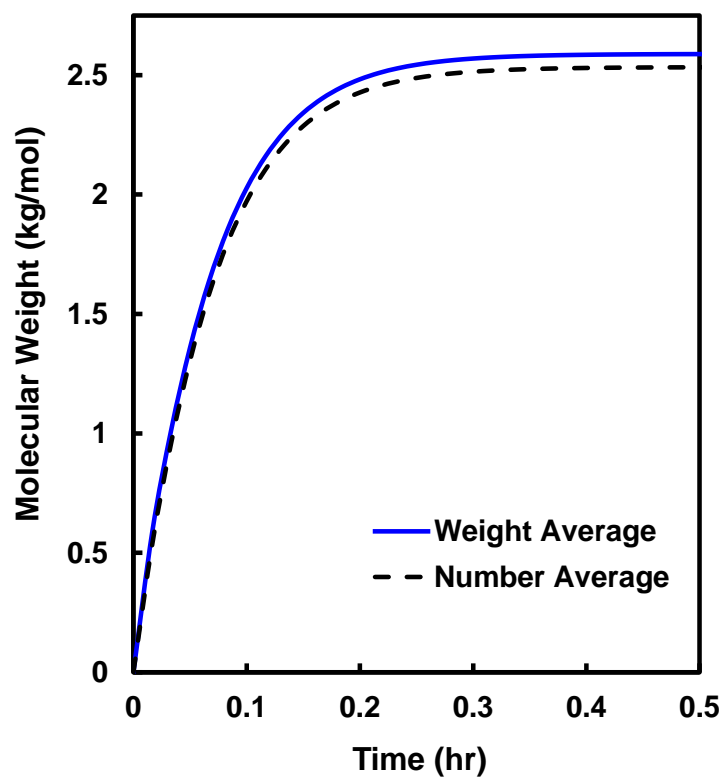


Figure A-2. Weight average and Number average molecular weights during IBP

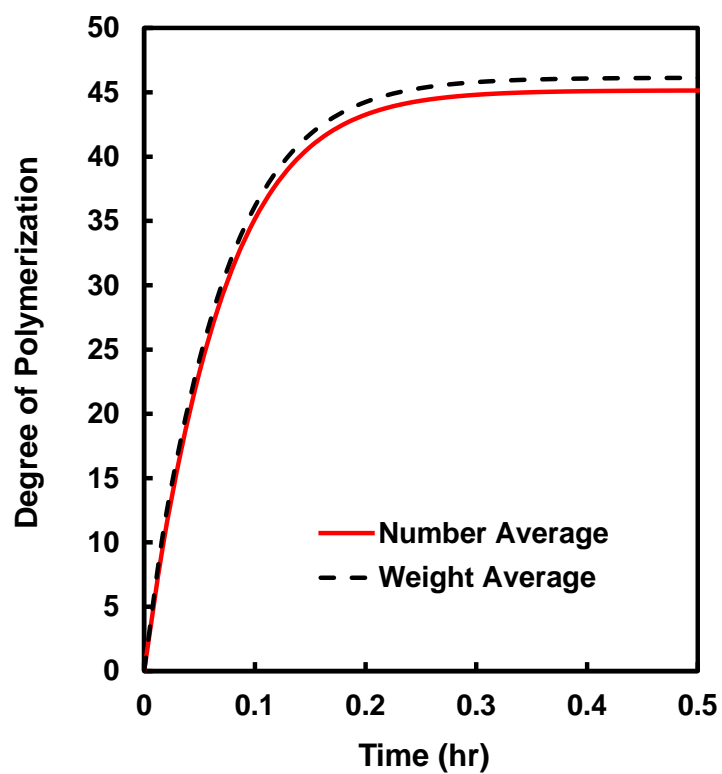


Figure A-3. Weight average and number average during IBP

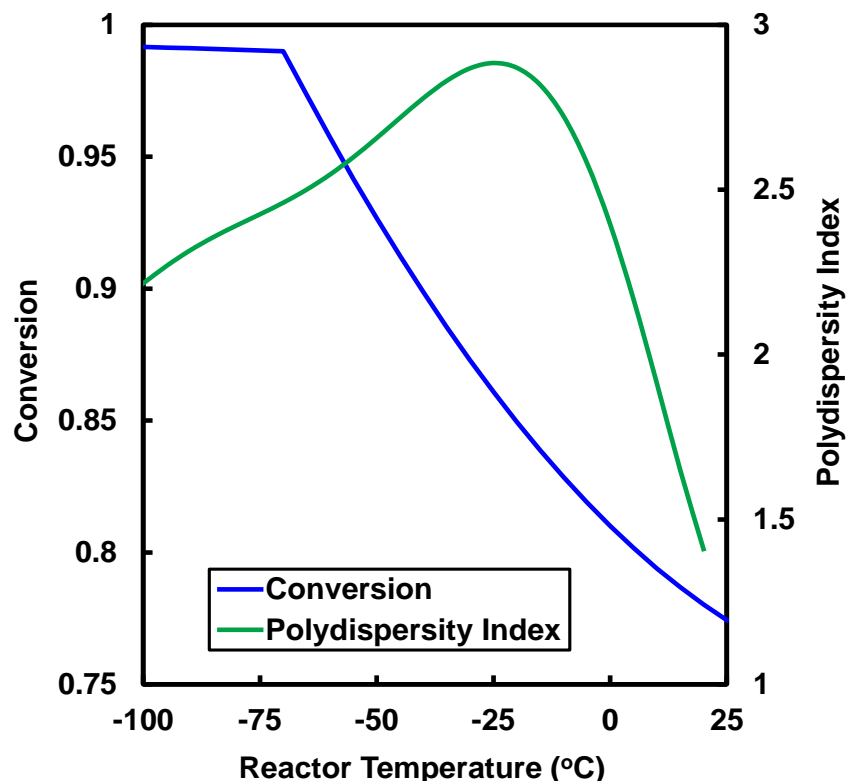


Figure A-4. Effect if temperature on the conversion and polydispersity index of the IBP process

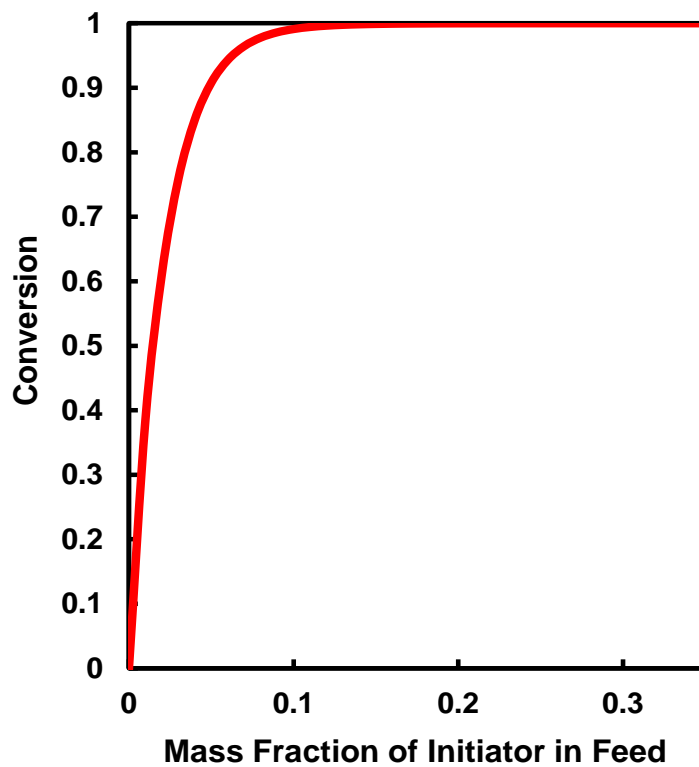
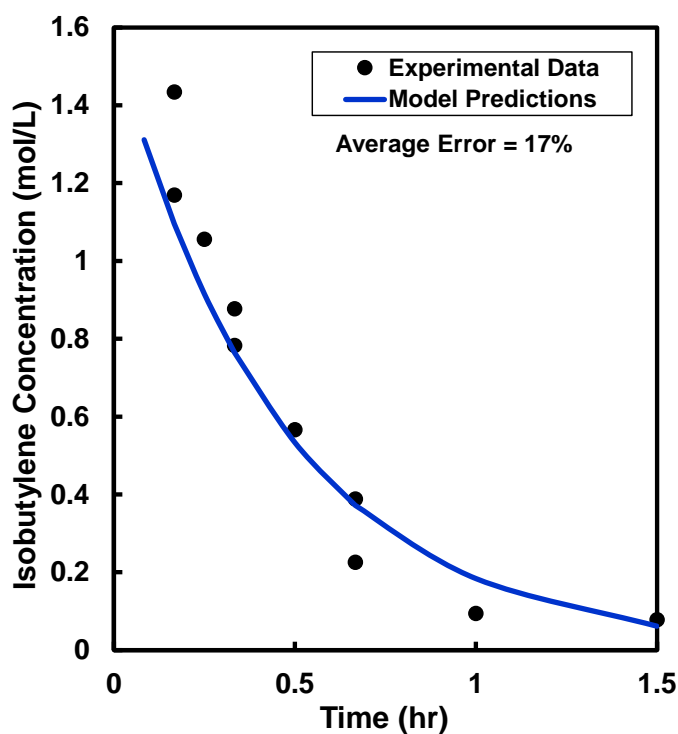


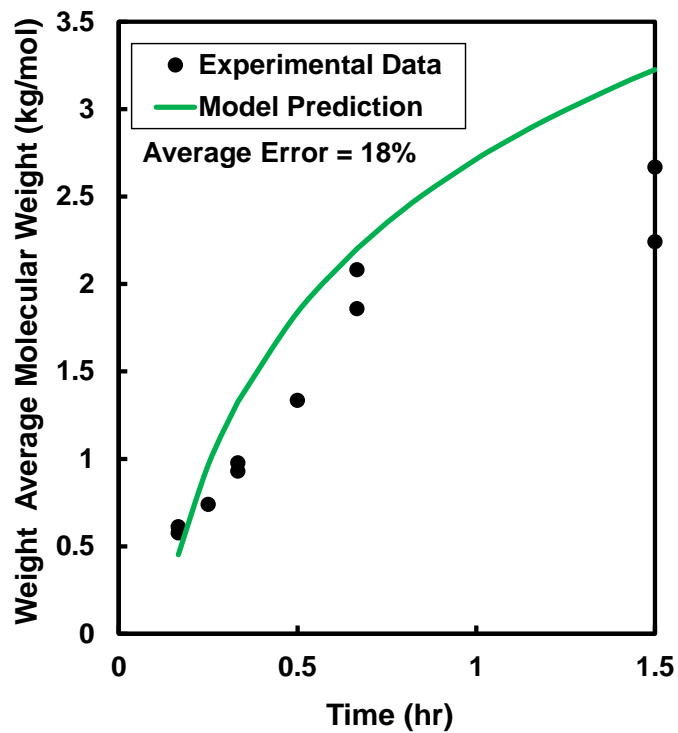
Figure A-5. Effect of initiator concentration on isobutylene conversion



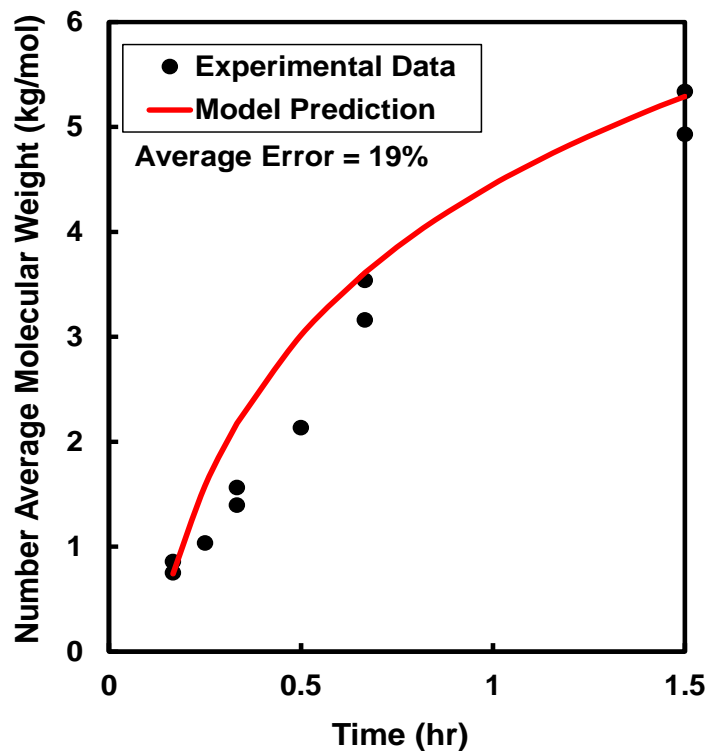
The Aspen model was used to predict the experimental data by Zhao et al. [53, 54], obtained for IBP using a different initiator ( $\text{TiCl}_4$ ) at different temperature -  $95^\circ\text{C}$  in a 2-gallon pilot plant reactor. A comparison between the model predictions and the experimental data is shown in Figures 6, 7 and 8. As can be seen in these figures, even though our model was developed using different initiator, the model is capable of predicting the isobutylene concentration, the number average molecular weight and the weight average molecular weight of the experimental with average errors of these predictions are 17%, 18% and 19%, respectively.



**Figure A-6.** Model predictions of the IB concentration experimental data by Zhao et al. [53, 54]



**Figure A-7.** Model predictions of the weight average molecular weight experimental data by Zhao et al. [53, 54]



**Figure A-8.** Model validation of the number average molecular weight against the experimental data by Zhao et al. [53, 54]

## APPENDIX B

### EFFECT OF REACTOR TYPE AND IMPELLER TYPE/SIZE ON THE MIXIN SPEED

**Table B-1.** Effect of reactor type and impeller type/size on the mixing speed

Case #	$H_r/D_r$	$D_{imp}/D_r$	N (rpm)				
			6 blades disk turbine	4 blades flat turbine	4 blades pitched turbine	Chemineer HE-3 turbine	Marine propeller
<b>P-1</b>	0.75	0.667	13	13	8	3	3
	0.75	0.400	40	43	25	7	7
	0.75	0.267	96	108	60	13	14
	0.75	0.200	181	213	113	21	23
	1	0.667	15	15	9	3	3
	1	0.400	46	50	29	8	8
	1	0.267	112	127	69	15	16
	1	0.200	209	246	131	24	27
	1.5	0.667	19	19	11	4	4
	1.5	0.400	57	61	35	9	10
	1.5	0.267	137	155	85	18	19
	1.5	0.200	256	301	160	29	33
	2	0.667	22	22	13	5	5
	2	0.400	66	71	40	11	11
	2	0.267	158	179	98	21	23
	2	0.200	296	347	185	34	38
<b>P-2</b>	0.75	0.667	133	133	81	28	29
	0.75	0.400	402	432	248	65	69
	0.75	0.267	970	1,098	602	128	140
	0.75	0.200	1,810	2,126	1,131	208	230
	1	0.667	153	154	93	32	33
	1	0.400	465	499	286	75	80
	1	0.267	1,218	1,268	698	148	162

Case #	H <sub>r</sub> /D <sub>r</sub>	D <sub>imp</sub> /D <sub>r</sub>	N (rpm)				
			6 blades disk turbine	4 blades flat turbine	4 blades pitched turbine	Chemineer HE-3 turbine	Marine propeller
	Table B-1 (continued)						
	1	0.200	2,090	2,455	1,305	240	266
	1.5	0.667	188	189	114	39	41
	1.5	0.400	569	611	350	92	98
	1.5	0.267	1,300	1,500	850	190	185
	1.5	0.200	2,560	3,007	1,599	294	326
	2	0.667	217	218	132	45	47
	2	0.400	657	705	405	107	113
	2	0.267	1,587	1,810	956	218	230
	2	0.200	2,956	3,472	1,846	339	376
P-3	0.75	0.667	13	13	8	3	3
	0.75	0.400	40	43	25	7	7
	0.75	0.267	96	108	60	13	14
	0.75	0.200	181	213	113	21	23
	1	0.667	15	15	9	3	3
	1	0.400	46	50	29	8	8
	1	0.267	112	127	69	15	16
	1	0.200	209	246	131	24	27
	1.5	0.667	19	19	11	4	4
	1.5	0.400	57	61	35	9	10
	1.5	0.267	137	155	85	18	19
	1.5	0.200	256	301	160	29	33
	2	0.667	22	22	13	5	5
	2	0.400	66	71	40	11	11
	2	0.267	158	179	98	21	23
	2	0.200	296	347	185	34	38
P-4	0.75	0.667	13	13	8	3	3
	0.75	0.400	40	43	25	7	7
	0.75	0.267	96	108	60	13	14
	0.75	0.200	181	213	113	21	23
	1	0.667	15	15	9	3	3
	1	0.400	46	50	29	8	8
	1	0.267	112	127	69	15	16
	1	0.200	209	246	131	24	27
	1.5	0.667	19	19	11	4	4
	1.5	0.400	57	61	35	9	10
	1.5	0.267	137	155	85	18	19
	1.5	0.200	256	301	160	29	33

Case #	$H_r/D_r$	$D_{imp}/D_r$	N (rpm)				
			6 blades disk turbine	4 blades flat turbine	4 blades pitched turbine	Chemineer HE-3 turbine	Marine propeller
			Table B-1 (continued)				
	2	0.667	22	22	13	5	5
	2	0.400	66	71	40	11	11
	2	0.267	158	179	98	21	23
	2	0.200	296	347	185	34	38
G-1	0.75	0.667	22	22	13	5	5
	0.75	0.400	67	72	41	11	12
	0.75	0.267	162	183	100	21	23
	0.75	0.200	302	354	188	35	38
	1	0.667	26	26	16	5	6
	1	0.400	77	83	48	13	13
	1	0.267	185	211	117	25	27
	1	0.200	349	409	218	40	44
	1.5	0.667	31	31	19	7	7
	1.5	0.400	95	102	58	15	16
	1.5	0.267	236	280	147	30	33
	1.5	0.200	427	501	266	49	54
	2	0.667	36	36	22	8	8
	2	0.400	109	118	67	18	19
	2	0.267	264	299	164	35	38
	2	0.200	493	579	308	57	63
G-2	0.75	0.667	221	222	135	46	48
	0.75	0.400	671	721	414	109	116
	0.75	0.267	1,616	1,828	1,003	214	233
	0.75	0.200	3,013	3,544	1,885	346	384
	1	0.667	256	256	156	54	55
	1	0.400	774	831	477	126	134
	1	0.267	2000	2,100	1200	250	275
	1	0.200	3,480	4,060	2,166	399	449
	1.5	0.667	313	314	191	66	68
	1.5	0.400	948	1,018	584	154	164
	1.5	0.267	2,305	2,609	1,431	306	333
	1.5	0.200	4,263	5,011	2,665	490	543
	2	0.667	361	363	220	76	78
	2	0.400	1,095	1,175	674	178	189
	2	0.267	2,639	2,986	1,639	350	381
	2	0.200	4,929	5,787	3,086	565	629
G-3	0.75	0.667	22	22	13	5	5

Case #	H <sub>r</sub> /D <sub>r</sub>	D <sub>imp</sub> /D <sub>r</sub>	N (rpm)				
			6 blades disk turbine	4 blades flat turbine	4 blades pitched turbine	Chemineer HE-3 turbine	Marine propeller
	Table B-1 (continued)						
	0.75	0.400	67	72	41	11	12
	0.75	0.267	162	183	100	21	23
	0.75	0.200	302	354	188	35	38
	1	0.667	26	26	16	5	6
	1	0.400	77	83	48	13	13
	1	0.267	185	211	117	25	27
	1	0.200	349	409	218	40	44
	1.5	0.667	31	31	19	7	7
	1.5	0.400	95	102	58	15	16
	1.5	0.267	236	280	147	30	33
	1.5	0.200	427	501	266	49	54
	2	0.667	36	36	22	8	8
	2	0.400	109	118	67	18	19
	2	0.267	264	299	164	35	38
	2	0.200	493	579	308	57	63
G-4	0.75	0.667	22	22	13	5	5
	0.75	0.400	67	72	41	11	12
	0.75	0.267	162	183	100	21	23
	0.75	0.200	302	354	188	35	38
	1	0.667	26	26	16	5	6
	1	0.400	77	83	48	13	13
	1	0.267	185	211	117	25	27
	1	0.200	349	409	218	40	44
	1.5	0.667	31	31	19	7	7
	1.5	0.400	95	102	58	15	16
	1.5	0.267	236	280	147	30	33
	1.5	0.200	427	501	266	49	54
	2	0.667	36	36	22	8	8
	2	0.400	109	118	67	18	19
	2	0.267	264	299	164	35	38
	2	0.200	493	579	308	57	63

## BIBLIOGRAPHY

- [1] J. P. Kennedy and E. Maréchal, *Carbocationic polymerization*: Wiley, 1982.
- [2] S. Rach and F. Kühn, "On the Way to Improve the Environmental Benignity of Chemical Processes: Novel Catalysts for a Polymerization Process," *Sustainability*, vol. 1, pp. 35-42, 2009.
- [3] H. F. Mark and J. I. Kroschwitz, *Encyclopedia of Polymer Science and Technology*: John Wiley & Sons, 2003.
- [4] J. A. Brydson, *Plastics Materials*: Butterworth-Heinemann, 1999.
- [5] I. U. A. Sangalov, K. S. Minsker, and G. E. Zaikov, *Polymers Derived from Isobutylene: Synthesis, Properties, Application*: Taylor & Francis, 2001.
- [6] J. J. Harrison, C. M. Mijares, M. T. Cheng, and J. Hudson, "Negative Ion Electrospray Ionization Mass Spectrum of Polyisobutenylsuccinic Anhydride: Implications for Isobutylene Polymerization Mechanism," *Macromolecules*, vol. 35, pp. 2494-2500, 2002/03/01 2002.
- [7] J. Burrington, J. Johnson, and J. Pudelski, "Cationic Polymerization Using Heteropolyacid Salt Catalysts," *Topics in Catalysis*, vol. 23, pp. 175-181, 2003/08/01 2003.
- [8] H. P. Rath, "Preparation of highly reactive polyisobutenes," ed: Google Patents, 1994.
- [9] M. Marek and M. Chmelíř, "Influence of some friedel-crafts halides on the polymerization of isobutylene catalyzed by aluminum bromide," *Journal of Polymer Science Part C: Polymer Symposia*, vol. 23, pp. 223-229, 1968.
- [10] H. Mayr, H. Schimmel, S. Kobayashi, M. Kotani, T. Prabakaran, L. Sipos, *et al.*, "Influence of chain length on the electrophilic reactivity of carbocations," *Macromolecules*, vol. 35, pp. 4611-4615, 2002.
- [11] R. B. Taylor and F. Williams, "Kinetics of ionic processes in the radiolysis of liquids. V. Cationic polymerization of isobutylene under anhydrous conditions," *Journal of the American Chemical Society*, vol. 91, pp. 3728-3732, 1969.

- [12] M. Marek, L. Toman, and J. Pilař, "Photoinitiation by radical-cationic mechanism in the polymerization of isobutylene with lewis acids," *Journal of Polymer Science: Polymer Chemistry Edition*, vol. 13, pp. 1565-1573, 1975.
- [13] P. L. Magagnini, S. Cesca, P. Giusti, A. Priola, and M. D. Maina, "Studies on polymerizations initiated by syncatalytic systems based on aluminium organic compounds, 7. Reaction mechanisms," *Die Makromolekulare Chemie*, vol. 178, pp. 2235-2248, 1977.
- [14] !!! INVALID CITATION !!! {}.
- [15] M. Roth and H. Mayr, "A novel method for the determination of propagation rate constants: carbocationic oligomerization of isobutylene," *Macromolecules*, vol. 29, pp. 6104-6109, 1996.
- [16] H. Schlaad, Y. Kwon, L. Sipos, R. Faust, and B. Charleux, "Determination of Propagation Rate Constants in Carbocationic Polymerization of Olefins. 1. Isobutylene," *Macromolecules*, vol. 33, pp. 8225-8232, 2000/10/01 2000.
- [17] L. Sipos, P. De, and R. Faust, "Effect of temperature, solvent polarity, and nature of Lewis acid on the rate constants in the carbocationic polymerization of isobutylene," *Macromolecules*, vol. 36, pp. 8282-8290, 2003.
- [18] J. E. Puskas, S. Shaikh, K. Z. Yao, K. B. McAuley, and G. Kaszas, "Kinetic simulation of living carbocationic polymerizations. II. Simulation of living isobutylene polymerization using a mechanistic model," *European polymer journal*, vol. 41, pp. 1-14, 2005.
- [19] R. F. Storey, B. J. Chisholm, and L. B. Brister, "Kinetic study of the living cationic polymerization of isobutylene using a dicumyl chloride/TiCl<sub>4</sub>/pyridine initiating system," *Macromolecules*, vol. 28, pp. 4055-4061, 1995.
- [20] K. Ueno, H. Yamaoka, K. Hayashi, and S. Okamura, "Studies on radiation-induced ionic polymerization—II. Effect of solvent on the polymerization of isobutene at low temperature," *The International Journal of Applied Radiation and Isotopes*, vol. 17, pp. 595-602, 1966.
- [21] R. F. Storey, C. L. Curry, and L. B. Brister, "Carbocation rearrangement in controlled/living isobutylene polymerization," *Macromolecules*, vol. 31, pp. 1058-1063, 1998.
- [22] B. Ivan and J. P. Kennedy, "Living carbocationic polymerization. 31. A comprehensive view of the inifer and living mechanisms in isobutylene polymerization," *Macromolecules*, vol. 23, pp. 2880-2885, 1990/05/01 1990.
- [23] R. F. Storey and K. R. Choate, "Kinetic Investigation of the Living Cationic Polymerization of Isobutylene Using *at*-Bu-m-DCC/TiCl<sub>4</sub>/2, 4-DMP Initiating System," *Macromolecules*, vol. 30, pp. 4799-4806, 1997.



- [24] M. Chmeliř, M. Marek, and O. Wichterle, "Polymerization of isobutylene catalyzed by aluminum tribromide," *Journal of Polymer Science Part C: Polymer Symposia*, vol. 16, pp. 833-839, 1967.
- [25] O. Wichterle, M. Marek, and I. Trekoval, "Heterogeneous catalysis of isobutylene polymerization," *Journal of Polymer Science*, vol. 53, pp. 281-287, 1961.
- [26] A. A. Berlin, K. S. Minsker, Y. A. Sangalov, V. G. Oshmyan, A. G. Svinukhov, A. P. Kirillov, *et al.*, "Calculation and simulation of the polymerization of isobutylene as a fast reaction," *Polymer Science U.S.S.R.*, vol. 22, pp. 625-634, 1980.
- [27] A. Mehra, A. Pandit, and M. M. Sharma, "Intensification of multiphase reactions through the use of a microphase—II. experimental," *Chemical Engineering Science*, vol. 43, pp. 913-927, 1988.
- [28] R. F. Storey and A. B. Donnalley, "TiCl<sub>4</sub> reaction order in living isobutylene polymerization at low [TiCl<sub>4</sub>]:[chain end] ratios," *Macromolecules*, vol. 33, pp. 53-59, 2000.
- [29] R. F. Storey, A. B. Donnalley, and T. L. Maggio, "Real-time monitoring of carbocationic polymerization of isobutylene using in situ FTIR-ATR spectroscopy with conduit and diamond-composite sensor technology," *Macromolecules*, vol. 31, pp. 1523-1526, 1998.
- [30] R. Norrish and K. Russell, "Polymerization of isobutene by stannic chloride," *Transactions of the Faraday Society*, vol. 48, pp. 91-98, 1952.
- [31] S. C. Guhaniyogi, J. P. Kennedy, and W. M. Ferry, "Carbocationic Polymerization in the Presence of Sterically Hindered Bases. III. The Polymerization of Isobutylene by the Cumyl Chloride/BCl<sub>3</sub> System," *Journal of Macromolecular Science: Part A - Chemistry*, vol. 18, pp. 25-37, 1982/07/01 1982.
- [32] M. Gyor, H.-C. Wang, and R. Faust, "Living Carbocationic Polymerization of Isobutylene with Blocked Bifunctional Initiators in the Presence of Di-tert-butylpyridine as a Proton Trap," *Journal of Macromolecular Science, Part A*, vol. 29, pp. 639-653, 1992/08/01 1992.
- [33] G. Pratap, S. A. Mustafa, and J. P. Heller, "Role of triethylamine in living carbocationic polymerization of isobutylene with 1,4-dicumyl alcohol/BCl<sub>3</sub> initiating system," *Journal of Applied Polymer Science*, vol. 46, pp. 559-561, 1992.
- [34] G. Pratap, S. A. Mustafa, W. K. Hollis, and J. P. Heller, "Living carbocationic polymerization of isobutylene by tert-amyl alcohol/BCl<sub>3</sub>/1-methyl-2-pyrrolidinone initiating system," *Journal of Applied Polymer Science*, vol. 44, pp. 1069-1074, 1992.
- [35] L. Balogh, Z. Fodor, T. Kelen, and R. Faust, "Initiation via haloboration in living cationic polymerization. 2. Kinetic and mechanistic studies of isobutylene polymerization," *Macromolecules*, vol. 27, pp. 4648-4651, 1994.
- [36] F. Barsan and M. C. Baird, "The first example of polymerization of isobutylene induced by a metallocene-like initiator, [(small eta)5-C<sub>5</sub>Me<sub>5</sub>)TiMe<sub>2</sub>[(small micro]-

- Me)B(C<sub>6</sub>F<sub>5</sub>)<sub>3</sub>]," *Journal of the Chemical Society, Chemical Communications*, pp. 1065-1066, 1995.
- [37] M. Roth, M. Patz, H. Freter, and H. Mayr, "Living Oligomerization of Isobutylene Using Di- and Triisobutylene Hydrochlorides as Initiators," *Macromolecules*, vol. 30, pp. 722-725, 1997/02/01 1997.
- [38] T. D. Shaffer and J. R. Ashbaugh, "Noncoordinating anions in carbocationic polymerization," *Journal of Polymer Science Part A: Polymer Chemistry*, vol. 35, pp. 329-344, 1997.
- [39] C. Paulo, J. E. Puskas, and S. Angepat, "Effect of Reaction Conditions on the Kinetics of Living Isobutylene Polymerization at High Initiator/TiCl<sub>4</sub> Ratios," *Macromolecules*, vol. 33, pp. 4634-4638, 2000/06/01 2000.
- [40] M. Bahadur, T. D. Shaffer, and J. R. Ashbaugh, "Dimethylaluminum Chloride Catalyzed Living Isobutylene Polymerization," *Macromolecules*, vol. 33, pp. 9548-9552, 2000/12/01 2000.
- [41] A. Harrane, R. Meghabar, and M. Belbachir, "A Protons Exchanged Montmorillonite Clay as an Efficient Catalyst for the Reaction of Isobutylene Polymerization," *International Journal of Molecular Sciences*, vol. 3, pp. 790-800, 2002.
- [42] K. L. Simison, C. D. Stokes, J. J. Harrison, and R. F. Storey, "End-Quenching of Quasiliving Carbocationic Isobutylene Polymerization with Hindered Bases: Quantitative Formation of exo-Olefin-Terminated Polyisobutylene," *Macromolecules*, vol. 39, pp. 2481-2487, 2006/04/01 2006.
- [43] P. De and R. Faust, "Carbocationic Polymerization of Isobutylene Using Methylaluminum Bromide Coinitiators: Synthesis of Bromoallyl Functional Polyisobutylene," *Macromolecules*, vol. 39, pp. 7527-7533, 2006/10/01 2006.
- [44] I. V. Vasilenko, A. N. Frolov, and S. V. Kostjuk, "Cationic Polymerization of Isobutylene Using AlCl<sub>3</sub>OBu<sub>2</sub> as a Coinitiator: Synthesis of Highly Reactive Polyisobutylene," *Macromolecules*, vol. 43, pp. 5503-5507, 2010/07/13 2010.
- [45] R. F. Storey and A. B. Donnalley, "TiCl<sub>4</sub> Reaction Order in Living Isobutylene Polymerization at Low [TiCl<sub>4</sub>]:[Chain End] Ratios," *Macromolecules*, vol. 33, pp. 53-59, 2000/01/01 1999.
- [46] R. N. Webb, T. D. Shaffer, and A. H. Tsou, "Butyl Rubber," in *Encyclopedia of Polymer Science and Technology*, ed: John Wiley & Sons, Inc., 2002.
- [47] G. Tosun, "A mathematical model of mixing and polymerization in a semibatch stirred-tank reactor," *AIChE journal*, vol. 38, pp. 425-437, 1992.
- [48] L. Marini and C. Georgakis, "The effect of imperfect mixing on polymer quality in low density polyethylene vessel reactors," *Chemical engineering communications*, vol. 30, pp. 361-375, 1984.

- [49] J. Villermaux, "A simple model for partial segregation in a semibatch reactor," in *American Institute of Chemical Engineers Annual Meeting*, 1989.
- [50] A. Cybulski, M. Sharma, R. Sheldon, and J. Moulijn, *Fine Chemicals Manufacture: Technology and Engineering*: Gulf Professional Publishing, 2001.
- [51] J. Fasano and W. Penney, "Avoid blending mix-ups," *Chemical engineering progress*, vol. 87, pp. 56-63, 1991.
- [52] O. M. Basha, Y. Li, and B. I. Morsi, "Progress Report to Lubrizol Corp.: Development of a rigorous kinetic reactor model for the isobutylene polymerization (IBP) process," Department of Chemical and Petroleum Engineering, University of Pittsburgh 2016.
- [53] Y. R. Zhao, K. B. McAuley, J. E. Puskas, L. M. Dos Santos, and A. Alvarez, "Mathematical modeling of arborescent polyisobutylene production in batch reactors," *Macromolecular Theory and Simulations*, vol. 22, pp. 155-173, 2013.
- [54] L. Dos Santos, "Synthesis of arborescent model polymer structures by living carbocationic polymerization for structure property studies," *Akron, OH: University of Akron*, 2009.
- [55] I. V. Vasilenko, D. I. Shiman, and S. V. Kostjuk, "Highly reactive polyisobutylenes via  $\text{AlCl}_3\text{OBu}_2$ -coinitiated cationic polymerization of isobutylene: Effect of solvent polarity, temperature, and initiator," *Journal of Polymer Science Part A: Polymer Chemistry*, vol. 50, pp. 750-758, 2012.
- [56] J. F. Chen, H. Gao, H. K. Zou, G. W. Chu, L. Zhang, L. Shao, *et al.*, "Cationic polymerization in rotating packed bed reactor: experimental and modeling," *AIChE journal*, vol. 56, pp. 1053-1062, 2010.
- [57] J. Baldyga and J. Bourne, "A fluid mechanical approach to turbulent mixing and chemical reaction part II Micromixing in the light of turbulence theory," *Chemical Engineering Communications*, vol. 28, pp. 243-258, 1984.
- [58] J. Baldyga and J. Bourne, "A Fluid Mechanical Approach to Turbulent Mixing and Chemical Reaction Part III Computational and Experimental Results for the New Micromixing Model," *Chemical Engineering Communications*, vol. 28, pp. 259-281, 1984.
- [59] J. Baldyga and J. Bourne, "A Fluid Mechanical Approach to Turbulent Mixing and Chemical Reaction. Part I Inadequacies of Available Methods.," *Chemical Engineering Communications*, vol. 28, pp. 231-241, 1984.
- [60] F. G. Helfferich, *Kinetics of Multistep Reactions*: Elsevier Science, 2004.
- [61] J. R. Dormand and P. J. Prince, "A family of embedded Runge-Kutta formulae," *Journal of Computational and Applied Mathematics*, vol. 6, pp. 19-26, 1980/03/01 1980.
- [62] L. F. Shampine and M. W. Reichelt, "The MATLAB ODE Suite," *SIAM Journal on Scientific Computing*, vol. 18, pp. 1-22, 1997.

- [63] C. Paulo, J. Puskas, and S. Angepat, "Effect of reaction conditions on the kinetics of living isobutylene polymerization at high initiator/TiCl<sub>4</sub> ratios," *Macromolecules*, vol. 33, pp. 4634-4638, 2000.
- [64] E. Walch and R. J. Gaymans, "Synthesis of low-molecular-weight telechelic polyisobutylene," *Polymer*, vol. 34, pp. 412-417, // 1993.
- [65] P. A. Mueller, J. R. Richards, and J. P. Congalidis, "Polymerization Reactor Modeling in Industry," *Macromolecular Reaction Engineering*, vol. 5, pp. 261-277, 2011.
- [66] C. Kiparissides, "Polymerization reactor modeling: A review of recent developments and future directions," *Chemical Engineering Science*, vol. 51, pp. 1637-1659, 5// 1996.
- [67] S. Sandler, *Polymer syntheses* vol. 1: Elsevier, 2012.